NTNU – Trondheim
Norwegian University of
Science and Technology

Offshore Rankine Cycles

Jo Brandsar

NTNU

Norwegian University
of Science and Technology

Department of Energy
and Process Engineering

EPT-M-2012-24

MASTER THESIS

for

student Jo Brandsar

Spring 2012

Offshore Rankine Cycles

Offshore Rankine sykluser

Background and objective

Utilization of surpus heat from different processes connected to the offshore production of oil and gas is an increasing area of interest. This is due to the fact that all electricity utilized onboard on plaforms are produced from oil and gas and the environmental aspects with this is raised as an issure. To reduce the emissions of CO_2 from electricity production, the introduction of thermal machinery to prduce electricity is introduced.One of the technolois is the Rancine cysle. Actual areas for implementation of the compact offshore Rancine cycles are:

- Production platforms
- Production ships
- Exploration and drilling platforms
- Exploration and drilling ships

The master thesis will focus on Rankine and steam cycles used in energy recovery at offshore installations.

This work is in colaboration with SINTEF Energy Research were there is a larger project, EFFORT, with focus on electricity production offshore.

The following tasks are to be considered:

1. Scientific evaluation including technical aspects when comparing a steam cycle versus ORC for a high temperature operating conditions
2. Study of heat exchanger parameters on total cycle perfromance.
3. Development of an Excel based performance map for various expanders
4. Discussion and summary of the findings
5. Make a draft paper (10-15 pages) from the result of the work
6. Make suggestions for further work

Within 14 days of receiving the written text on the master thesis, the candidate shall submit a research plan for his project to the department.

When the thesis is evaluated, emphasis is 'put on processing of the results, and that they are presented in tabular and/or graphic form in a clear manner, and that they are analyzed carefully.

The thesis should be formulated as a research report with summary both in English and Norwegian, conclusion, literature references, table of contents etc. During the preparation of the text, the candidate should make an effort to produce a well-structured and easily readable report. In order to ease the evaluation of the thesis, it is important that the cross-references are correct. In the making of the report, strong emphasis should be placed on both a thorough discussion of the results and an orderly presentation.
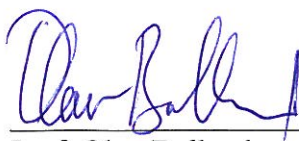
The candidate is requested to initiate and keep close contact with his/her academic supervisor(s) throughout the working period. The candidate must follow the rules and regulations of NTNU as well as passive directions given by the Department of Energy and Process Engineering.

Risk assessment of the candidate's work shall be carried out according to the department's procedures. The risk assessment must be documented and included as part of the final report. Events related to the candidate's work adversely affecting the health, safety or security, must be documented and included as part of the final report.

Pursuant to "Regulations concerning the supplementary provisions to the technology study program/Master of Science" at NTNU §20, the Department reserves the permission to utilize all the results and data for teaching and research purposes as well as in future publications.

The final report is to be submitted digitally in DAIM. An executive summary of the thesis including title, student's name, supervisor's name, year, department name, and NTNU's logo and name, shall be submitted to the department as a separate pdf file. The final report, with summery and all other material and documents have to be given to the supervisor in digital format on a CD.

Department of Energy and Process Engineering, 16. January 2012

Prof. Olav Bolland
Department Head

Prof. Trygve M. Eikevik
Academic Supervisor

Research Advisors:
Armin Hafner, SINTEF Energy Research, e-mail: armin.hafner@sintef.no

Abstract

This paper summarizes my master thesis during the spring semester 2012 at the Institute of Energy and Process Engineering, NTNU, Norway. The project was given to me as a collaboration with an ongoing project at SINTEF Energy Research. The focus represent electricity production offshore by applying a Rankine cycle with surplus heat as the energy source. Investigations concern foremost a comparison between steam and organic cycles and the effect the waste heat recovery unit (WHRU) has on the cycle as a whole.

I

Sammendrag

Tittelen på denne oppgaven - "Offshore Rankine Cycles" - er svært generell og dekker et stort spekter av tekniske felt, f.eks. termodynamiske sykluser (Rankine, ORC, Brayton, Kalina, etc.), mekanisk utstyr (gass-/dampturbin, varmevekslere og ekstra utstyr) og sikkerhetsaspekter (brennbar og/eller giftig væske, høye temperaturer og trykk) for å nevne de viktigste. Avhandlingen forsøker å gi en kortfattet oversikt over alle kritiske punkter og alternativer, og over implementering av en varmegjenvinningsprosess på offshore-anlegg, selv om fokus har vært på to mer spesifiserte tilfeller, nemlig:

- Sammenligning av en dampsyklus vs. en organisk syklus (ORC) ved høye varmegjenvinningstemperaturer.

- Studie av varmevekslerparametere med hensyn til den helhetlige prosessen.

Disse to punktene er studert sammen med en analyse av et modulært ekspanderoppsett kontra en enkelt-ekspander for å se om bedre effekt kan oppnåes for et modulært oppsett med hensyn til frekvente variasjoner i gassturbinbelastningen.

For å sammenligne en dampsyklus med en organisk syklus så måtte det gjøres en analyse av hvilke arbeidsmedium som kunne brukes. Toluen ble valgt på grunn av at det er en "vanlig" væske med kjente egenskaper og den ble ansett for å være et godt alternativ for varmegjenvinning ved høye temperaturer, både ved sub-kritisk og superkritisk operasjon. Siden vann i dette tilfellet er begrenset til sub-kritiske trykk så ble en CO_2-syklus brukt i sammenligning til den superkritiske toluensyklusen. Hovedfokuset for sammenligningen var eksergitapet i varmeoverføringen og total effekt levert av syklusen.

Studien av varmevekslerparametere ble utført med en såkallt "printed circuit"-varmeveksler (PCHE) som eksempel. Studien av varmevekslerparameterene på den helhetlige prosessen har nære forbindelser til størrelsen på varmeveksleren, siden dette er en viktig parameter med hensyn til offshore-drift på grunn av kostbart "fotavtrykk". Prosessen sin avhengighet av varmeveksleren er hovedsakelig gjennom varmeoverføringen, eller varmebelastningen påført prosessen. Varmebelastningen er gitt av varmevekslerens evne til å redusere temperaturen på avgassene. Denne evnen er avhengig av de to væskene som er involvert og geometrien til varmeveksleren. Mens valget av arbeidsmedium og "pinch points" fastsetter hvor mye varmeenergi som overføres, vil den resterende analysen hvile på varmeovergangskoeffisienten (UA) som skal balansere varmebelastningen. Når fluidegenskapene er fastsatt så avhenger UA-verdien på varmevekslergeometrien, og videre variasjon av disse parameterene gir oss størrelsen på varmeveksleren. Når et arbeidsmedium er valgt på den kalde siden av varmeveksleren så kan varmevekslervolumet optimaliseres ved en gitt varmebelastning.

En VBA-makro er laget der ekspanderparametere (effekt, og virkningsgrad vs volumstrøm) kan implementeres til å beregne effekten av to ekspandere i et modulært oppsett i forhold til en enkel ekspander brukt som referanse.

Summary

The title of the thesis - "Offshore Rankine Cycles" - is very general and cover a large range of engineering fields, e.g. thermodynamic cycles (Rankine, ORC, Brayton, Kalina, etc.), mechanical equipment (gas/steam turbine, heat exchangers and additional equipment) and safety concerns (flammable and/or toxic fluids, high temperature and pressures), to name the most important. The thesis try to give a brief overview of all critical points and alternatives, concerning employment of a waste heat recovery machine on offshore facilities, although focus has been on three more specified cases, namely:

- Comparison of a steam cycle vs. an organic Rankine cycle for high temperature operating conditions.

- Study of heat exchanger parameters on total cycle performance.

- Investigation of a modular expander setup versus a single expander.

To compare a steam cycle to an organic cycle, a choice of working fluid for the organic cycle had to be made. After some investigation, toluene was chosen as it is a "common" fluid with known properties and was found to be a viable option for high temperature heat sources, both for subcritical and supercritical operation. Due to water being constricted to subcritical operation a CO_2 cycle was implemented as a comparison to the supercritical toluene cycle. The main focus of the comparison was exergy losses during heat transfer and power output.

The heat exchanger parameter study was conducted with a printed circuit heat exchanger as an example. The study of overall cycle performance has close connections to the heat exchanger size, since it is an important parameter concerning offshore employment due to costly "footprint". The cycle's dependency on the heat exchanger is mainly by the heat transfer rate, or heat load, which the heat exchanger applies to the cycle. The heat transfer rate is given by the heat exchanger's ability to reduce the temperature of the exhaust gases. This ability depends on the two fluids involved and the geometry of the heat exchanger. While the choice in working fluid and pinch points sets the amount of heat transferred, the remaining analysis rest on the overall heat transfer coefficient (UA) to balance the heat load. When fluid properties are determined, the UA - value is again dependent on heat exchanger geometry and further variation of these parameters will in turn reveal the size of the heat exchanger. When imposing a working fluid to the cold side of the heat exchanger an optimization in heat exchanger volume could be found at specified heat load.

A VBA macro has been made where expander parameters (rated power and efficiency vs. volumetric flow rate values) could be used as inputs to calculate the power output of two expanders in a modular setup relative to a single expander as reference.

Limitations

- Calculations conducted on the working fluid side of the WHRU are done with the use of constant properties due to the complicated physics involving evaporation of a fluid (both sub- and supercritical) in a heat exchanger.

- Analysis concerning the condenser was neglected due to the assumed impact on the cycle, both in power and size, was small relative to the importance of the WHRU. This, in addition to the aforementioned use of constant properties (low precision) when evaluating the heat transfer on the working fluid side of the heat exchanger, resulted in less focus on the condenser.

- Investigations on a cycle with OTSG as evaporator was not performed.

- Cycle comparison is limited to a single pressure, i.e. it does not concern the effect e.g. reheating has on the cycle.

- Reliable information regarding expander efficiencies and gas turbine load variation was difficult to obtain. Expander manufacturers do not easily give away classified material and information from the literature are rather sparse. Due to the limited information gathered, the focus of the expander module calculations were of creating a functional program, were reliable inputs could be implemented when collected.

Contents

List of Figures

List of Tables

Nomenclature

Thermodynamic

Symbol	Description	Unit
E	energy	J
u	internal energy	J/kg
Q	heat energy	J
$\dot{Q}, q$	heat transfer rate	W
W	work	J
$\dot{W}$	power	W
$\dot{E}_Q$	exergy transferred by heat transfer	W
$\dot{E}_W$	exergy transfer by work	W
e_x	flow exergy	J/kg
p	pressure	Pa
T	temperature	$K, \,^\circ C$
t	time	s
m	mass	kg
$\dot{m}$	mass flow	kg/s
h	enthalpy	J/kg
s	entropy	$J/kg - K$
V	velocity	m/s
z	elevation	m
v	specific volume	m^3/kg
$\dot{V}$	volumetric flow rate	m^3/s
$\dot{S}_{gen}$	entropy generation	W/K
c_p	specific heat capacity	$J/kg - K$
k_f	thermal conductivity	$W/m - K$
ρ	density	kg/m^3
(hA)	heat transfer conductance	W/K
UA	overall heat transfer coefficient	W/K
T_0	ambient temperature	$^\circ C$
p_0	atmospheric pressure	Pa
T_c	cooling water temperature	$^\circ C$
$\Delta T_H, \Delta T_L$	approach temperature	$^\circ C$
P_H	cycle high pressure	Pa
P_L	condensing pressure	Pa
T_{ex}	exhaust temperature	$^\circ C$
T_{pp}	pinch point	$^\circ C$
g	gravitational constant	m/s^2

Dimentionless

Symbol	Description	Unit
St	Stanton number	-
Pr	Prandtl number	-
Nu	Nusselt number	-
Re	Reynolds number	-
f	friction factor	-
ϵ	heat exchanger effectiveness	-
η_{th}, η_1	1st law efficiency	-
η_c	Carnot efficiency	-
η_2	Exergetic efficiency, 2nd law	-
η_{is}	Isentropic efficiency	-
η_p	Pump efficiency	-
η_e	Expander efficiency	-
$\eta_{Brayton}$	Brayton efficiency	-
NTU	number of transfer units	-
C_r	heat capacity ratio	-

Geometry

Symbol	Description	Unit
#	number of channels	-
N_H	number of channels in the vertical direction	-
N_W	number of channels in the horizontal direction	-
D_h	channel diameter hot side	m
D_c	channel diameter cold side	m
A	heat transfer area	m^2
H	overall height	m
W	overall width	m
L	overall length	m
V	volume	m^3
w_H	wall thickness, vertical	m
w_W	wall thickness, horizontal	m

Chemical compounds

Symbol	Description	Unit
CO_2	Carbon dioxide	
NO_x	Nitrous oxide	
H_2O	Water	
NH_3	Ammonia	

Expander map variables

EM_{ratio}	expansion matching ratio	-
VFM_{ratio}	volumetric flow matching ratio	-
N_s	specific speed	-
N	rotational speed	rpm
D	diameter	ft
H_{ad}	adiabatic enthalpy drop	$ft * lb/lb$
D_s	specific diameter	-
Q	flow rate	ft/s

Expander VBA Macro

$VRExOPT$	optimum flow rate of expander x relative to the reference expander	-
P_{Ex}	rated power of expander x	W
P_R	rated power of reference expander	W
VFR	volumetric flow rate	m^3/s
k	sizing factor	-
N_R	reference expander efficiency	-
N_{Ex}	modular expander x efficiency	-
W'_R	reference work output	m^3/s
W'_{Ex}	modular expander work output	m^3/s

1 Background

There is a worldwide concern about the increasing CO_2 levels in our atmosphere and there is a consensus among scientists that CO_2 in particular are the primary cause of global warming. The environmental impacts is difficult to predict and, consequently, there is an ongoing discussion on the topic. In Norway, the petroleum sector alone accounts for 30% of the overall emissions where 78, 9% of these emissions are electricity production from gas turbines [2] [3]. In addition to emissions from gas turbines there is substantial emissions from ships (oil-/gas tankers, production, exploration and drilling, etc) as well.

A few countries, including Norway, has taken steps to try reducing the CO_2 emissions from burning of fossil fuels by introducing a tax on carbon emissions. This will produce incentives towards better efficiencies and/or the use of other, cleaner energy sources. Offshore structures/-ships have a large energy consumption and if a connection to the land-based electricity grid is to expensive, or difficult, the only real solution is to utilize a gas- or diesel engine for electricity needs. This implies that to reduce emissions you have to make either the energy consuming processes more efficient or the power production more efficient. This text concerns the latter.

All combustion power plants have substantial heat losses that occur mainly at the exhaust and intercooler. In addition there will be heat losses from diesel engine cooling or cylinder cooling. All these losses creates an opportunity to produce work and if they are utilized the overall efficiency will go up. The overall effect will be a reduction in fuel consumption given the same power output. One popular method to utilize waste heat is to employ a Rankine cycle which can absorb these heat losses in the evaporator and pass it to the working fluid. The main issue is to get the Rankine cycle to be economically feasible. This can mainly be done by increasing the efficiency and, in the offshore context, reduce the physical "footprint".

With the Snorre platform (which got 1 of currently 3 employed offshore combined cycles on the Norwegian shelf) as an example the addition of a Rankine cycle gives a reduction in fuel consumption of 39 $millSm^3/yr$ and a CO_2 reduction by 92 000 ton/yr [4]. If the fact that the reduction in CO_2 emissions is not a goal in itself it can be shown that with a current CO_2 - tax of 48 øre per Sm^3 fuel burned, in addition to the CO_2 quota (approximately 350NOK/ton) this will amount to 50.92 million NOK in tax savings. The gas price applies on top of that again.

1.1 EFFORT

EFFORT is a project carried out by Petrobras, Shell, Statoil and Total with SINTEF Energy Research and the Norwegian University of Science and Technology (NTNU) as research partners. The overall objective being research in more efficient energy solutions with respect to offshore processes. Offshore installations and -machinery require substantial energy supply, thus the potential in energy savings by increased efficiency would be equally substantial. Since a large amount of offshore installations are driven by combustion of fossil fuels as energy source there is environmental concerns to be accounted for as well. By focusing on excess heat recovery, case studies at Kristin and Draugen platforms revealed the following sources:

1. Gas turbine exhaust heat

2. Gas compressor aftercooling/intercooling

3. Well stream energy

4. Diesel engine exhaust heat

5. Gas expansion

The list above is ranked by decreasing energy recovery potential, with gas turbine exhaust heat as the source with greatest potential.

1.2 Energy sources

The case study carried out by EFFORT revealed several sources where useful work can be extracted. As this text concern the method by which a Rankine cycle is implemented to perform the energy recovery, the list will be shortened somewhat, e.g. energy from gas expansion is done by replacing the throttle valve by a gas expander and the Rankine cycle is not applicable in this scenario. The energy from a well stream is of a considerable amount but the temperature level is low and would not be suitable for energy recovery (ref EFFORT). The three remaining sources; Gas turbine exhaust heat, gas compressor aftercooling/intercooling and diesel engine exhaust heat is given further attention. A summary is shown in Table 1

Heat source	Location	Temperature (°C)	Pressure (Mpa)	Mass flow (kg/s)
Gas turbine	Exhaust	486		90
Gas compressor	Intercooler	126	6	150
	Aftercooler	126	18	150
ICE Gas (3MW)	Exhaust	470	-	4,35
	Jacket cooling	80-90	-	-
ICE Diesel (8,9MW)	Exhaust	346	-	17,5
	Jacket cooling	80-96	-	-

Table 1: Temperature and pressure levels for various offshore heat sources (EFFORT)

1.2.1 Gas turbine exhaust heat

There are in total 167 gas turbines deployed on the Norwegian shelf, with a total of 3000 MW installed power ([5], 2007). Most of these are in the 20MW - 30MW range. The exhaust gases rejected from the gas turbine contains in the range of 35% to 40% of the fuels energy which again holds a high potential for heat recovery[6]. In offshore facilities most gas turbines are of the aerodervative type, which are gas turbines originally developed for aircraft propulsion but has undergone minor modifications to be utilized as power turbines. These turbines has different attributes compared to industrial or land based turbines. The most important being

- Lighter. Aeroderivative turbines are made of lighter materials.

- More efficient. Higher firing temperatures and compression ratio

- More expensive.

- Less flexible when it comes to fuel types, usually gas driven.

- Slightly more fragile

The positive attributes such as size/weight and high efficiency outweighs the negative, i.e. equipment cost and flexibility. With heat recovery in mind the aeroderivative gas turbine's exhaust temperature is slightly lower than for conventional gas turbines, ranging from 415°C to 540°C. This will negatively effect the efficiency of an added Rankine cycle. Table 2 shows data from a typical aeroderivative gas turbine used on offshore facilities.

General Electric LM2500+	
Power output	30.2 MW
Exhaust flow	85.9 kg/s
Exhaust temperature	518C

Table 2: LM2500+ data (ge.com)

1.2.2 Gas compressor intercooling/aftercooling

Export gas needs to be cooled down prior to transport through the pipelines. The case used by EFFORT as an initial approach is concerning 2 compressors where the process line follow this setup: compressor 1, intercooling, TEG (to dehydrate the gas stream), compressor 2 and aftercooling. The thermodynamic properties of the stream are summarized in Table 3

	Intercooler		Aftercooler	
	Inlet	Outlet	Inlet	Outlet
Temperature (C)	126	Below 35	126	Below 100
Pressure (MPa)	6	6	18	18
Flow rate (kg/s)	150			

Table 3: Temperature and pressure of gas stream processing prior to transport (EFFORT)

1.2.3 Internal combustion engine exhaust heat

This heat source is given less attention in the EFFORT project due to additional problems with respect to fluctuating exhaust heat levels and, in addition, the relatively small units (3-4 MW). Although the unit size is small there is substantial heat recovery potential considering the number of diesel engines utilized, both on vessels and platforms. Several studies has been conducted for smaller engines in the 250kW - 300kW range [7], [8] and [9]. Vaja and Gambrotta [10] did a study on a 3MW natural gas ICE with three cases: a simple subcritical cycle with exhaust gases as the only thermal source, a simple subcritical cycle with use of both exhaust gases and engine cooling water, and finally a regenerated cycle. It was found that the preheat cycle (utilizes the engine cooling water as preheater)

and regenerative cycle gave the same increase in efficiency ($\approx 12, 5\%$). Benzene was used as the working fluid. It has to be noted that the regenerative cycle requires gas-liquid heat exchange whilst the preheat cycle has a liquid-liquid heat exchanger. The engine studied had exhaust temperature of $\approx 470°C$ and cooling water temperature of $80 - 90°C$ with exhaust massflow of 4.35 kg/s. Furthermore Bombarda et al.[11] conducted a study on two diesel engines (Wartsila 20V32), each with power output of 8900 kWe, where results from an ORC and a Kalina cycle was compared. Exhaust temperature of this engine was at 346°C with a massflow of 17,5 kg/s. The engine cooling water temperature was set between 80 and 96°C. The potential for heat recovery is found to be twice as large from the exhaust heat.

2 Theory

2.1 1st Law of Thermodynamics

The 1st law of thermodynamics can be expressed by one sentence: **Energy is conserved**, or for a closed system:

$$\Delta E_{system} = Q - W \tag{2.1}$$

Equation (2.1) states that *any change in a systems total energy is equal to the difference between the energy transfer by heat into the system and the energy transfer by work done by the system.*

2.1.1 Open system

For an open system (also mentioned as a *control volume*) you have to add the difference between energy transferred by mass into and out of the system, i.e.

$$\frac{d\,E_{cv}}{dt} = \sum_{j=0} \dot{Q}_j - \dot{W} + \sum_i \dot{m}_i(u + \frac{V^2}{2} + gz)_i - \sum_e \dot{m}_e(u + \frac{V^2}{2} + gz)_e \tag{2.2}$$

given in time rate form. The subscripts mean; inlet, i, exit, e, and heat transfer boundary, j.
The work can be divided into two parts:

$$\dot{W} = \dot{W}_{cv} + [\dot{m}_e(p_e v_e) - \dot{m}_i(p_i v_i)]$$

where the term enclosed in the square brackets is flow work at the exit and inlet of the system respectively, and $\dot{W}_{cv}$ is all other work done by the control volume on the surroundings. Substituting this into (2.2) gives us an expression in terms of *enthalpy* ($h = u + pv$)

$$\frac{d\,E_{cv}}{dt} = \sum_{j=0} \dot{Q}_j - \dot{W}_{cv} + \sum_i \dot{m}_i(h + \frac{V^2}{2} + gz)_i - \sum_e \dot{m}_e(h + \frac{V^2}{2} + gz)_e \tag{2.3}$$

2.1.2 1st law efficiency

The 1st law efficiency, also known as *thermal efficiency*, is defined as the ratio between useful work output to the heat added to the system

$$\eta_1 = \frac{\dot{W}_{out}}{\dot{Q}_{in}} \tag{2.4}$$

2.2 2nd Law of Thermodynamics

We start with two historical statements concerning the 2nd Law:
Clausius Statement

> *It is impossible for any system to operate in such a way that the <u>sole result</u> would be an energy transfer by heat from a cooler to a hotter body.*

This statement does not exclude the fact that you can transfer energy by heat from a cold to a hot body (as is done by a refrigeration system) but for a system containing <u>only</u> a hot and a cold body there would not be any heat transfer from the cooler to the hotter body.

Kelvin-Planck Statement

> *It is impossible for any system to operate in a thermodynamic cycle and deliver a net amount of energy by work to its surroundings while receiving energy by heat transfer from a single thermal reservoir.*

In other words, a thermodynamic cycle has to be in contact with two thermal reservoirs with different temperatures and have to reject heat to give a net output of work. This statement can be summed up mathematically by

$$W_{cycle} \leq 0$$

for a single reservoir.
With reference to the 1st law this implies that

$$Q_{cycle} \leq 0 \qquad \text{or} \qquad \oint \delta Q \leq 0$$

and with the inclusion of the *thermodynamical temperature*, T, this becomes

$$0 \geq \oint \left(\frac{\delta Q}{T} \right)_b \tag{2.5}$$

where b denotes the portion of the system boundary where the temperature is T and heat transfer δQ. The inequality is balanced when the cycle is reversible, or in other words: *when the cycle is reversed there will only be a change in sign, not magnitude* (see equation 2.7 but with both "paths" being reversible).
Changes in this quantity from one state to another is called the **entropy change** and is defined by Rudolf Clausius (1822-1888) as:

$$S_2 - S_1 = \int_1^2 \left(\frac{\delta Q}{T_b} \right)_{int \ rev} \tag{2.6}$$

where the subscript *int rev* mean that the system is reversible, although the surroundings may not be.

2.2.1 Entropy generation

The entropy generation shows the strength of the inequality in eq. (2.5). A cycle can be mathematically written with the reversed cycle taking a reversible path

$$\int_1^2 \frac{\delta Q}{T} + \int_2^1 \frac{\delta Q_{rev}}{T} \leq 0 \qquad (2.7)$$

By using eq. 2.6 in the above equation you get the definition of entropy generation:

$$S_{gen} = (S_2 - S_1) - \int_1^2 \frac{\delta Q}{T} \geq 0 \qquad \Rightarrow \qquad \frac{d\,S}{d\,t} = \int_1^2 \frac{\delta \dot{Q}}{T} + \dot{S}_{gen} \qquad (2.8)$$

where $S_{gen} \geq 0$.

The equation above is the 2nd law of thermodynamics for a closed system (usually written in the form on the right) and is very important when it comes to cycle efficiencies since it show how much of the heat transfer to the cycle that **cannot** be converted to work.

2.2.2 Control volume

For a control volume we get

$$\dot{S}_{gen} = \frac{d\,S_{cv}}{dt} - \sum_{j=0} \left(\frac{\dot{Q}}{T}\right)_j + \sum_e (\dot{m}s)_e - \sum_i (\dot{m}s)_i \qquad (2.9)$$

where the subscript j denotes the number of heat transfer boundaries. As with the entropy generation defined for a closed system, eq. (2.8), equation (2.9) is always positive as well.

2.2.3 Irreversibilities

The difference between a reversible and an irreversible process has to be explained since it is of great importance regarding thermodynamic cycles. The definition given in [12] is:

> A process is said to be *reversible* if it is possible for its effects to be eradicated in the sense that there is some way by which *both* the system and its surroundings can be *exactly restored* to their respective initial states. A process is *irreversible* if there is no way to undo it. That is, there is no means by which the system and its surroundings can be exactly restored to their respective initial states.

Examples of irreversibilities are: heat transfer by a finite temperature difference, unrestrained expansion, spontaneous chemical reaction, mixing of matter, friction, etc., which cannot be "undone" without additional work input. A system can be brought back to its initial state and still be irreversible (as is done with a Rankine cycle) but that implies that the surroundings can **not** be brought back to its initial state. This leads us to the subdivision **internal and external irreversibility** which means irreversibilities in the system and the surroundings respectively. By defining the temperature gradient of the heat transfer **outside** the system boundary, it can be thought of as an external irreversibility. Internal irreversibilities, wrt. the Rankine cycle, is irreversibilities occurring in the system without any energy communication to the surroundings, e.g. non-isentropic compression/expansion and duct friction. In an internal reversible process all intensive properties are assumed uniform (in equilibrium) at each phase.

2.3 Exergy

Exergy - a potential for utilization. The notion of exergy is of imperative use when working with heat engines as it relates the amount of work that is possible to extract from a temperature difference driven cycle to the amount of work transferred with heat.

The derivation of the equations used in the exergy analysis starts with a reference to the 1st and 2nd law of thermodynamics for a control volume, (2.3) and (2.9), with the purpose of maximizing the work output, $\dot{W}_{cv}$. The next step is to eliminate the heat transfer interaction with the environment, $\dot{Q}_0$, from the two equations. The resulting equation will be

$$
\begin{aligned}
\dot{W}_{cv} =\ & -\frac{d}{dt}(E - T_0 S_{cv}) + \sum_{j=1}\left(1 - \frac{T_0}{T_j}\right)\dot{Q}_j + \sum_i \dot{m}(h + \frac{V^2}{2} + gz - T_0 s) \\
& - \sum_e \dot{m}(h + \frac{V^2}{2} + gz - T_0 s) - T_0 \dot{S}_{gen}
\end{aligned}
\tag{2.10}
$$

The pressure interaction between the system and the environment is not included in these derivations because of the use of rigid equipment (the displacement work of the system wrt the environment is negligible). If needed, the total exergy will become: $\dot{E}_W = \dot{W}_{cv} - P_0 dV/dt$. $\dot{E}_W = \dot{W}_{cv}$ is assumed throughout the text.

The first four terms on the right side can be though of as reversible work and the equation can be reduced to

$$
\dot{W}_{cv} = \dot{W}_{rev} - \dot{W}_{lost}
\tag{2.11}
$$

which denotes the reversible, or maximum available work ouput, W_{rev}, the actual work produced from the process, $\dot{W}_{cv}$, and finally the work lost due to irreversibilities, $\dot{W}_{lost}$, where

$$
\dot{W}_{lost} = T_0 \dot{S}_{gen}
\tag{2.12}
$$

As shown above, for the same machine design, ($\dot{W}_{rev} = const$) to maximize the power output is equivalent to minimizing the power lost, $\dot{W}_{lost}$. These equation are very important since they show the maximum power output and the potential in improving the thermal design.

The second term on the right side is exergy transfer via heat transfer and is defined as

$$
\dot{E}_Q = \sum_{j=1}\left(1 - \frac{T_0}{T_j}\right)\dot{Q}_j
\tag{2.13}
$$

2.3.1 2nd law efficiency for heat cycles

The 2nd law efficiency, or utilization factor, is defined as the real available work divided by the maximum available work

$$
\eta_2 = \frac{\dot{E}_W}{\dot{E}_{W,rev}} = 1 - \frac{T_0 \dot{S}_{gen}}{\dot{E}_{W,rev}}
\tag{2.14}
$$

7

A relationship between 1st and 2nd law efficiencies can be showed to be

$$\eta_1 = \eta_2 \left(1 - \frac{T_L}{T_H} \right) \tag{2.15}$$

noting that for the completion of one cycle (and steady state) $E_{W,rev}$ is equal to equation (2.13).

2.3.2 Flow exergy

When evaluating power cycles with different fluids there is also important to perform an analysis to compare the different values of exergy losses in the fluids. The flow exergy is defined as

$$e_x = h' - h'_0 - T_0(s - s_0) \tag{2.16}$$

where $h' = h + V/2 + gz$. Equation (2.16) can be replaced by h' terms in eq. (2.11) and finally be used to evaluate exergy losses in each component of the Rankine cycle.

2.4 Rankine Cycle

In short, a Rankine cycle is a system that converts heat energy to mechanical work. It is named after the Scottish scientist William John Macquorn Rankine (1820 - 1872) for his contribution on steam engine science and the science of thermodynamics as a whole. In Figure 1 there is an example of how the Rankine cycle is incorporated into a power plant. The Rankine cycle is shown with the letter **A**. The cycle receives energy by heat from sub-system B and energy is transfered out by work (sub-system D) and waste heat (sub-system C).

The amount of useful work extracted is the difference in the heat energy supplied by sub-system B minus the heat removed in sub-system C. The efficiency increase attained by applying a steam driven Rankine cycle in combination with a gas turbine would typically be from 37% without heat recovery, and up to 50% with the Rankine cycle applied. The reduction in CO_2 and NO_x emissions would be approximately in the range of 25%.

2.4.1 Principle

To explain the principle behind the Rankine cycle it is easiest to use a *T-s diagram* which shows the temperature versus entropy through the cycle. A simple T-s diagram is shown in Figure 2 with according machinery setup.

The line j-k-l shown in Figure 2b is the saturation line for water/steam with k as the critical point. With the figure as reference the cycle is described step-by-step starting with the pump. Bare in mind that each process is idealized, i.e. no pressure loss in heat exchangers and isentropic compression/expansion in pump/expander (therefore known as an *ideal cycle*). A real cycle will deviate from these idealizations.

Feed pump: The pump increase the pressure of the saturated fluid isentropically from point 1 to 2.
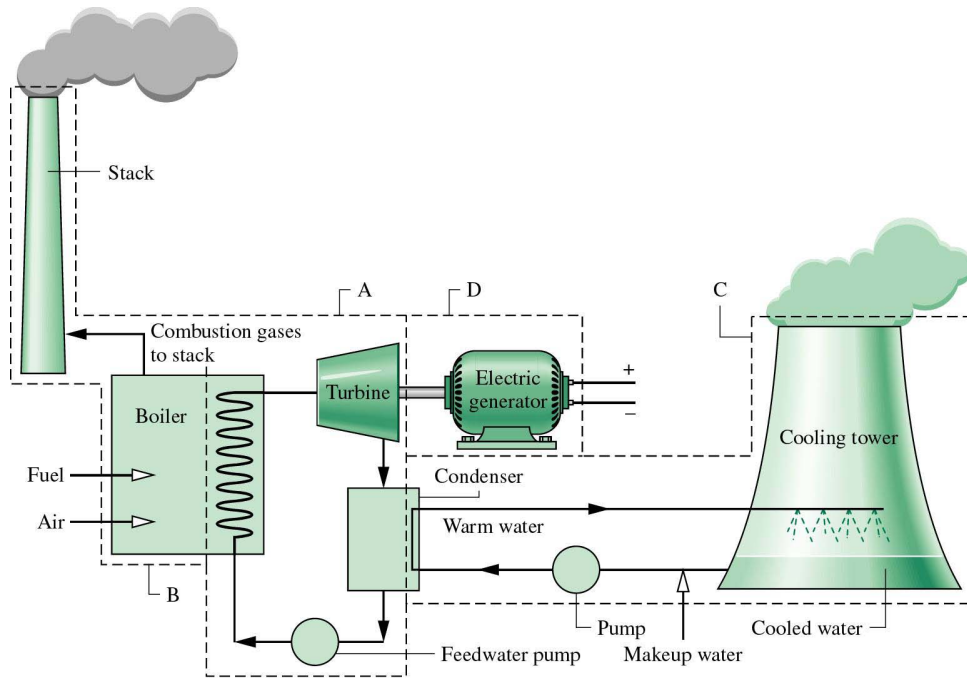
Figure 1: Example on how a Rankine cycle is incorporated in a power plant (Incropera)

Boiler: At point 2 the fluid enters the boiler and is heated isobaric until it reaches the point 3 where the fluid is superheated.

Turbine: From point 3 the fluid is expanded isentropically through a turbine/expander to point 4.

Condenser: At point 4 the fluid is condensed at constant pressure until it reaches the saturation point at 1, and then the cycle repeats itself.

2.4.2 1st and 2nd law applied on component level

Equations (2.3) and (2.9) in combination with (2.12) will be used to describe the energy transfer in each component.

Pump

$$\dot{W}_p = \dot{m}(h_2 - h_1)$$
$$\dot{W}_{p,\,lost} = T_0 \dot{m}(s_2 - s_1)$$

Boiler

$$\dot{Q}_b = \dot{m}(h_3 - h_2)$$
$$\dot{W}_{b,\,lost} = T_0 \left[\dot{m}(s_3 - s_2) - \frac{\dot{Q}_b}{T_{ex}} \right]$$
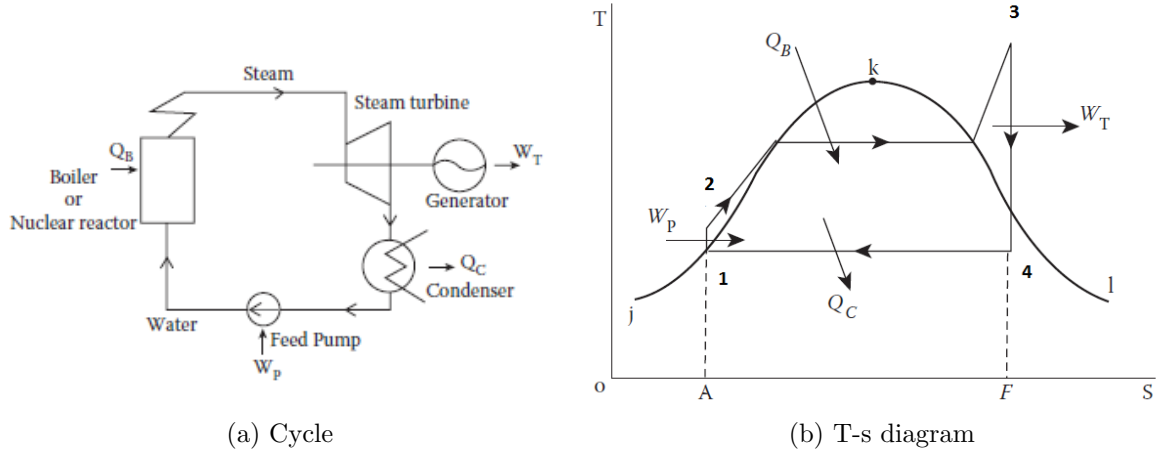
Figure 2: Simple Rankine cycle (Nuclear Engineering Handbook)

Expander/Turbine

$$\dot{W}_t = \dot{m}(h_3 - h_4)$$

$$\dot{W}_{t,\,lost} = T_0 \dot{m}(s_4 - s_3)$$

Condenser

$$\dot{Q}_c = \dot{m}(h_4 - h_1)$$

$$\dot{W}_{c,\,lost} = T_0 \left[\dot{m}(s_1 - s_4) + \frac{\dot{Q}_c}{T_0} \right]$$

2.4.3 Thermal efficiency

The **thermal efficiency** (also known as the 1st law efficiency, see section 2.1.2) of the cycle is calculated below using the enthalpies of the different stages

$$\eta_{th} = \frac{\dot{W}_{out}}{\dot{Q}_{in}} = \frac{\dot{W}_t - \dot{W}_p}{\dot{Q}_b} = \frac{(h_3 - h_4) - (h_2 - h_1)}{h_3 - h_2} = 1 - \frac{h_4 - h_1}{h_3 - h_2} \left(= 1 - \frac{\dot{Q}_c}{\dot{Q}_b} \right) \quad (2.17)$$

By using the expression $\Delta h = T\Delta s + v\Delta p$ and noting that the heat transfers occur at constant pressure ($\Delta p = 0$) and $\Delta s_{4 \to 1} = \Delta s_{2 \to 3}$ we get for an ideal cycle

$$\eta_{th} = 1 - \frac{\bar{T}_{4 \to 1}}{\bar{T}_{2 \to 3}} \quad (2.18)$$

where $\bar{T}$ is the average temperature between the states where heat addition and -rejection occurs. This temperature can be calculated by e.g. the LMTD-method with Kelvin as a unit.

Eq.(2.18) gives us an understanding on how the average temperature ratio affects the thermal efficiency for isentropic compression/-expansion. With Figure 2b as a reference and eq. (2.18) in mind it can be readily seen that the thermal efficiency can be increased

by decreasing the temperature ratio, i.e. increasing the evaporator temperature and decreasing the condenser temperature.

2.4.4 Carnot cycle

It is useful to compare a cycle efficiency with the maximum efficiency allowed, i.e. the efficiency of a reversible cycle (shown in Figure 3).
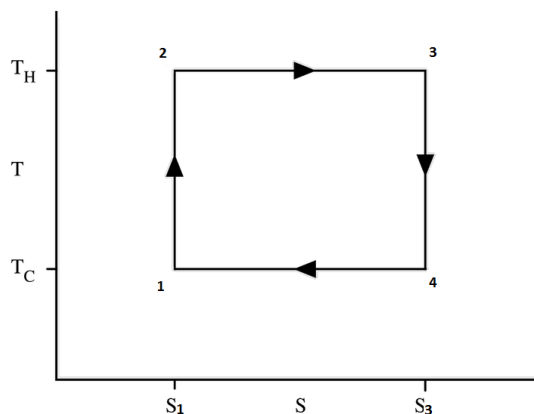
Figure 3: Carnot cycle

This cycle is called the Carnot [1] cycle and consists of the following stages:

Expander Isentropic expansion.(No irreversibilities in the expander, $3 \rightarrow 4$)
Condenser Isothermal heat rejection.(Heat removal occurring entirely in the 2-phase region, $4 \rightarrow 1$)
Pump Isentropic compression.(No irreveribilities in the pump/compressor, $1 \rightarrow 2$)
Boiler Isothermal heat addition.(Heat addition occurring entirely in the 2-phase region, $2 \rightarrow 3$)

The Carnot efficiency will be dependent only on the upper and lower temperatures, which will be constant, and the maximum (reversible) 1st law efficiency can be written:

$$\eta_c = 1 - \frac{T_L}{T_H} \tag{2.19}$$

This is also known as *Carnot efficiency*, which is reached when $\eta_2 = 1$, see eq. (2.15)

2.4.5 Trilateral cycle

The trilateral cycle is essentially a more realistic definition of the Carnot cycle in the sense that the assumption of an infinite heat source, i.e. heat transfer occurring at a constant heat source temperature, is not a practical assumption for waste heat appliances.

---

[1]Nicolas Léonard Sadi Carnot (1796-1832) - French engineer and scientist who, in his book *Reflections on the motive power of fire*, gave the first successful theoretical account of heat engines.

The solution is the trilateral cycle where the heat source is considered to be an infinite number of constant temperature heat sources, each in communication with the respective infinitesimal Carnot cycle. By integration of these Carnot cycles you will get the trilateral cycle as shown in Figure 4.
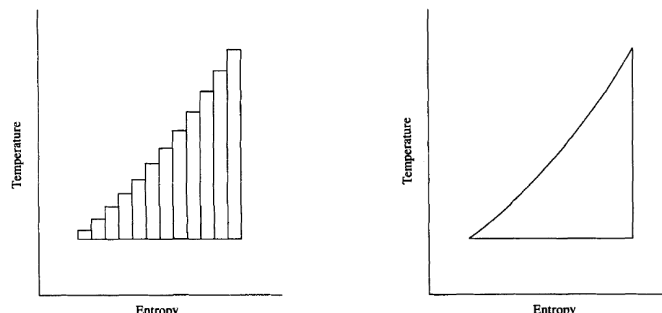
Figure 4: Trilateral cycle by integration of infinitesimal Carnot cycles. (Smith [1])

The efficiency can be shown to be

$$\eta_{trilateral} = 1 - \frac{T_L ln(T_H/T_L)}{T_H - T_L} \tag{2.20}$$

Studies has been done by Smith [1] comparing the trilateral cycle versus organic Rankine cycles and steam cycles with heat source temperatures ranging from 100°C to 200°C. The cycle is shown in Figure 5. At lower temperatures the trilateral cycle showed an improvement of about 80% with respect to the simple steam cycle. It also showed that the trilateral cycle is almost independent of the working fluid due to the almost ideal temperature match between heat source and working fluid. Difficulties lay on the expansion occurring entirely in the 2-phase region, and further technical advances in expander machinery is needed to make the trilateral cycle a viable solution for extended heat recovery loads.

2.4.6 Additions/Improvements

The Rankine cycle can be modified in several ways to accomplish different criteria when it comes to higher turbine inlet temperature, higher efficiencies, higher power output, the quality of the fluid at the turbine exit, etc. The main methods are described in the following paragraphs.
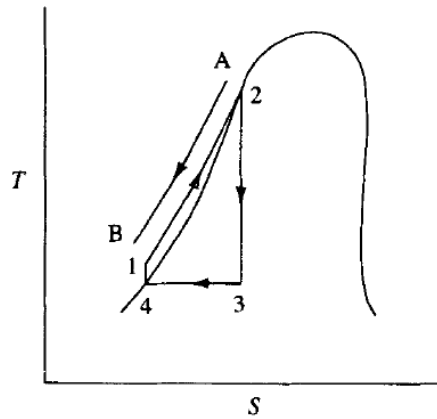
Figure 5: Trilateral cycle in a T-s diagram (Smith [1])
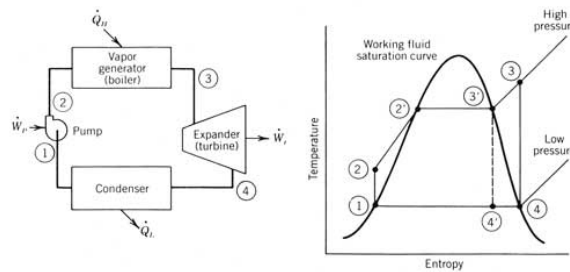
Figure 6: Rankine cycle with superheating (powerfromthesun.net)

If the temperature of the fluid exiting the boiler is too low the following expansion in the turbine can result in a low quality two-phase fluid which will cause erosion by liquid droplets in the last stages of the expander. This will damage the expander and produce lower overall efficiency. The solution is to further superheat the fluid and thereby increasing the fluid quality at the expander exit. If the heat source contain a sufficient temperature level then this is done by decreasing the approach temperature. If the heat source got a lower temperature than needed for superheating the working fluid another heat source with higher temperature has to be applied. For a HRSG (sec. 3.2.1) this can be accomplished by supplementary firing. The superheated cycle is shown in Figure 6 where superheating occurs by moving state 3' on the saturated vapor line to state 3 further into the gas region of the T-s diagram.

Note that this is only needed when the working fluid is classified as a *wet fluid*, i.e. the saturation line has a negative slope, which is the case for water but not for other fluids.

Reheat Another way to ensure high quality is by reheating the fluid. This is done by a multiple-stage expander, or multiple expanders, where the fluid is expanded in the first stage until it reaches the saturation line where it will be heated again at an intermediate pressure, before entering subsequent expander stages. With given heat

13

source temperature together with upper and lower pressures the optimum intermediate pressure could be found that maximizes the cycle efficiency, shown e.g. by Ust et. al. [13]. The cycle is shown in Figure 7. By doing this, superheated gas could be ensured at all expander stages. The reheating of the fluid can be done in the same boiler as the preliminary heating as there is no need for higher temperatures. The negative side is the added machinery investment.
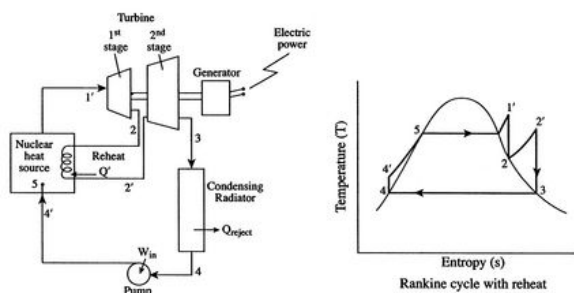
Figure 7: Reheat (mit.edu)

Regeneration Instead of reheating the fluid that is exiting the first stage expander you can use a fraction of it to preheat the fluid at some point between the pump and the evaporator, shown in Figure 8. The mixing of the extracted steam and the condensed fluid is done in a *contact heater* which has its own pump to bring the condensed fluid pressure up to the steam pressure. The effect will be increased thermal efficiency because of the elevated average temperature. The same goes for the 2nd law efficiency due to the higher evaporator inlet temperature reducing the temperature difference, consequently reducing the irreversibilities in the evaporator. Because of the extraction of mass flow from the first stage expander the power output will go down in total, although the efficiency increase is slightly better than reheat. This build is used when the added increase in 1st- and 2nd law efficiencies surpass the need for higher power output, i.e. when heat source are sparse and fuel costs are high.
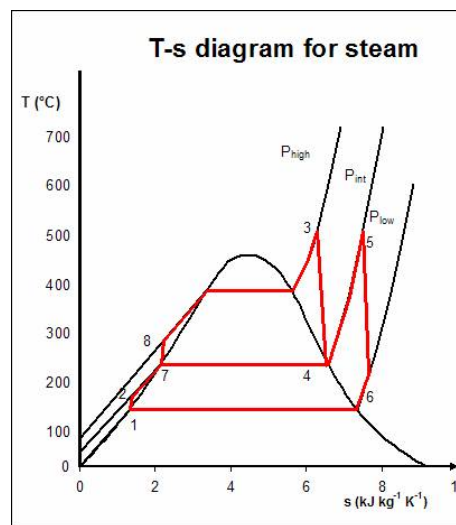
Figure 8: Regeneration (commons.wikimedia.org)

2.4.7 Supercritical Rankine cycle

The supercritical Rankine cycle is a cycle where heat addition occur at pressures above the critical point. It takes advantage of the gliding temperature increase of the working fluid in the boiler. By removing the constant temperature (2-phase) evaporation there is a reduction in entropy generation in the boiler and the cycle will reach higher 2nd law efficiencies, due to heat transfer with decreased temperature difference. To reach

supercritical levels in a steam cycle the pressure has to be above the critical pressure for water ($p_{crit} \approx 220 bar$) and consequently, the heat source temperature has to be well above the critical temperature ($T_{crit} \approx 374°C$) to ensure expansion in the gaseous phase. This will practically leave out all heat sources shown in Table 1 and focus will thereby be on supercritical organic cycles with much less critical pressure/temperature, e.g. CO_2 with $p_{crit} \approx 74 bar, T_{crit} \approx 31°C$. Additional care has to be taken when doing calculations close to the critical point as the fluid properties are not well defined, in addition to a jump in the specific heat capacity of the working fluid during the heat transfer in the boiler, as shown in Figure 9.
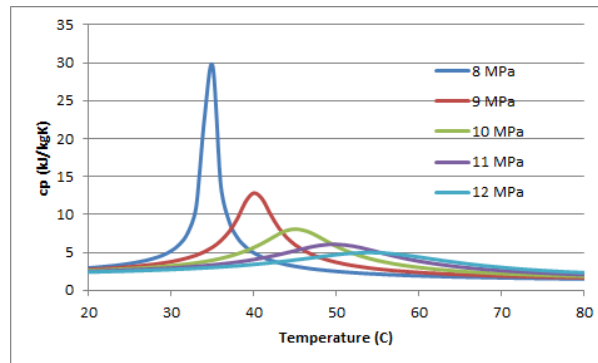
Figure 9: Variation in heat capacity vs temperature for CO_2 at supercritical pressures (calculated using REFPROP)

2.4.8   Kalina cycle

A Kalina cycle is a Rankine cycle which uses a mixture of two different fluids as the working fluid, more precisely, a water/ammonia mixture. The Kalina cycle offer several advantages with respect to a conventional steam cycle. The primary advantage is the mixture's ability to have a variable boiling and condensation temperature due to the different boiling temperatures of the respective fluids. This effect would make the boiling of the mixture follow the heat source temperature more closely in the boiler, as discussed in section 2.4.7. Other advantages that should be mentioned is: much lower freezing point reduces the risk of freezing during condensation, regulation can be done easily by regulation the amount of ammonia in the water and it allows higher condensation pressure, thus higher density at the expander exit, and consequently smaller expander size for the same power output [14].

2.5   ORC working fluid

Usually the working fluid in a Rankine cycle is water since it is cheap, abundant, non-toxic, environmentally friendly and it is thermodynamically suitable. Besides the apparent positive sides of water there is a few negative sides when the temperature of the heat source is low. For instance, at temperatures below 370°C water does not allow efficient recovery of waste heat [15].

Temperatures for surplus heat sources could be well below 370°C, thus water has to be replaced by another fluid with a lower boiling point. These fluids are often organic and the cycle is thereby termed Organic Rankine cycle, although non-organic fluids, e.g ammonia and CO_2, could be used as well. For the best efficiency, the fluids are chosen by their saturation curve and latent heat at low pressures. That is, isentropic (i.e. vertical saturation curve) [16] and high latent heat [17] for the best performance. These criteria promotes the use of R-123 for lower temperatures and p-Xylene for higher temperatures [18]. The saturation curve is mostly dependent on molecular weight of the fluid. High molecular weight implies a "dry fluid" (the saturation line has a positive slope) and a high molecular weight could be beneficial in terms of turbine design as well. CO_2 has also been tested [19] as a working fluid with heat exchange in the supercritical pressure region. This is done because the working fluid will "follow" the temperature of the heat source better and thereby reduce the exergy loss in the boiler. In addition to reduction in exergy losses, higher pressures result in higher fluid density, thus higher heat transfer coefficient, and the physical size of the boiler can be reduced.

Several studies has been performed with a multitude of working fluids. The fluid in this study is chosen to be toluene [15], [20]. The relative high critical values of toluene are more suitable for high temperature heat recovery [21], [17]. Toluene has a low GWP of 2.7 (ipcc.ch), low toxicity, low price and very good availability. The negative side is toluene being highly flammable (flash point of 4°C and auto-ignition point of 508°C) and should not be directly heated by the exhaust gases as it could auto-ignite at a temperature below the exhaust temperature when mixed with sufficient amounts of oxygen. Supplementary firing could reduce this risk and the fact that safety procedures for highly flammable fluids should already be well implemented on offshore facilities reduces the impact of this hazard to a certain degree. CO_2 is chosen as well, as a comparison to the toluene supercritical cycle [22].

2.6 Machinery

Four components are needed for a functional Rankine cycle, i.e. pump, boiler, expander and condenser. The pump and expander will get a description here as the two remaining heat exchangers are discussed more thoroughly in the latter part of the text.

2.6.1 Pump

The pump is the least critical equipment in the cycle. It operates entirely in the liquid (incompressible) region and since it requires a small amount of power relative to the output of the cycle, a large variation in pump efficiency would effect the cycle power output in a negligible degree. The efficiency of the pump is given as

$$\eta_p = \frac{h_{2,\,is} - h_1}{h_2 - h_1} \tag{2.21}$$

where $h_{2,\,is}$ is the enthalpy at state 2 for isentropic compression from state 1.

2.6.2 Expander devices

The expander efficiency, on the other hand, has a very large effect on total cycle output due to a much higher enthalpy drop. For the expander the isentropic efficiency is defined as:

$$\eta_e = \frac{h_3 - h_4}{h_3 - h_{4,\,is}} \tag{2.22}$$

where $h_{4,\,is}$ is the isentropic expansion from state 3. The isentropic efficiency is dependent on several factors, but mainly heat exchange losses to the ambient and friction losses in the expander.

Two other important factors are the **expansion matching ratio** and the **volumetric flow matching ratio** defined below:

$$\texttt{EM}_{ratio} = \frac{(v_1/v_2)_{fluid}}{(V_{in}/V_{out})_{exp}} \tag{2.23}$$

$$\texttt{VFM}_{ratio} = \frac{v_1 \dot{m}}{V_{in} N} = \frac{\dot{V}_{fluid}}{\dot{V}_{exp}} \tag{2.24}$$

$\texttt{EM}_{ratio}$ shows how close an expansion is to the isentropic expansion and $\texttt{VFM}_{ratio}$ shows the ratio between the volumetric flow of the fluid compared to the swept, or built-in, volumetric flow of the expander. If $\texttt{VFM}_{ratio}$ is above unity there has to be leakage through the expander. Both ratios should be close to unity.

2.6.3 Turboexpander

A turboexpander is used when there is high mass flow and power output from the cycle. They are generally subdivided into two classes: axial and radial inflow. Typical examples of constructions are shown in Figure 10. The inlet flow direction and area could be varied

(a) Radial inflow rotor (b) Axial rotor

Figure 10: Turboexpander (Barber-Nichols)

by internal guide vanes (IGV) on both models. The radial inflow turbine in Figure 10a is usually enclosed in a spiral-shaped casing which directs the flow in a tangential direction towards the turbine blades, where the pressure drop are divided between both nozzle and the wheel. It tolerates high shaft speed and are generally suitable for organic Rankine

cycles. The axial turboexpander can further be divided into impulse and reaction type, Figure 10b shows the reaction type. The difference lay in the curvature of the turbine blades. The reaction types are formed more like an airfoil and the pressure drop are divided between blade and nozzle (as with the radial inflow turbine) whereas the impulse blades are formed more like buckets and the pressure drop occur in the nozzle, thus the rotor are driven by mostly kinetic energy. The impulse type are generally more suitable at low flow rates (barber-nichols.com).

2.6.4 Number of expander stages

Marciniak et al. [15] suggested to make the selection of number of expander stages dependent on enthalpy drop, thus maintaining high expander efficiencies, or approximately the same efficiencies, for different cycles. A rough division was made encompassing the following enthalpy drop ranges in kJ/kg.

$$
\begin{array}{rcll}
0 & < & 250 & \text{1-stage} \\
250 & < & 450 & \text{3-stages} \\
450 & < & & \text{More than 3 stages}
\end{array}
$$

2.6.5 Other expander solutions

Rolling piston
The high pressure gases enters in the suction hole and leaves through the discharge valve. The pressure difference between suction and discharge are pushing the spring loaded roller in a clockwise motion inside the static cylinder. The induced motion of the roller is transmitted to the shaft which will rotate in a counterclockwise direction.

Evaluation Testing has been conducted by Åge Guddingsmo at Norges Landbrukshøgskole, Ås 2004[23]. During the tests there were a negative total work on the shaft. Because of the mechanical design there will be a small negative moment on the shaft at the first stage of expansion but this should not prevail through the cycle. The probable reasons for the negative work is listed as:
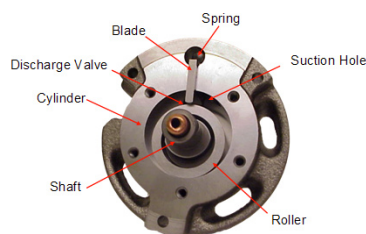
Figure 11: Rolling piston (Xpressar™)

- Large tolerance between cylinder and roller.

- Uncertainty in the effect the lubricant used to seal the gap between cylinder and roller.

- Small relative speed between cylinder and roller which effects the amount of lubricant introduced into the expander.

- Design flaw which increases the negative moment experienced in the first stage of expansion.

18

Screw

Figure 12 shows a screw compressor/expander. It consists of two interlocking helical screws, both are free to rotate. At the start of an expansion cycle the male screw fits into the female part on the high pressure side, as the screw rotates the volume between the screws gets larger and larger until the gas is released to the low pressure side. One of the screws will have a shaft for work extraction.

Evaluation

Smith et al. [24] conducted experimental tests on a screw expander with "N-profile" and R-113 as the working fluid and they obtained a peak isentropic efficiency of 76%. A negative property of the screw expander is its high rotational speed and therefor reduction gearboxes are required [25]
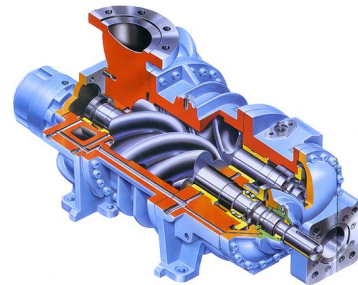
Figure 12: Screw compressor (Eltacon Engineering BV)

Scroll

The scroll compressor mainly consist of two spirals, or scrolls, positioned as seen in Figure 13. One scroll is stationary while the other is connected eccentrically to a shaft and is "free" to move inside the first scroll. The movement is induced by high pressure gas entering at the center of the scrolls and is being expanded as it moves towards the outer edge. The scroll expander has several preferable characteristics such as a simple design, low cost and low noise (low vibration). It typically has as 10% higher machine efficiency (η_m) than a similar piston compressor [26].
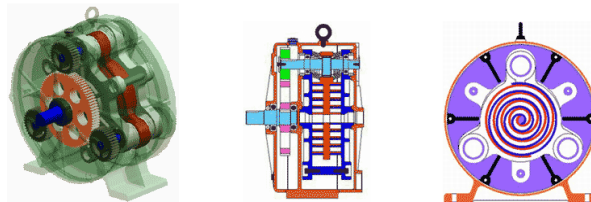
Figure 13: Scroll expander (scrollcomp.com)

Evaluation

Experimental tests has been performed by e.g. Ingley et al. [26] and Mathias et al. [27]. Ingley used a scroll compressor in reverse as an expander and NH_3/H_2O mix as the working medium. The bottomline test results indicated that scroll compressors function poorly as an expander but could be improved with further sealing between the scrolls. Mathias et al. found that selecting the scroll expander with EM_{ratio} and VFM_{ratio} closest to unity, the isentropic efficiency predicted would be at least 0.82. During experimental tests of 3 scroll expanders they got VFM_{ratio} down to 1.07 i.e. low leakage through the expander.

There are several other types of compressors that can be utilized as an expander, below follows four examples with a short description.

Vane Figure 14a (oilmaintenance.com) shows a compressor, so for an expander the flow

19
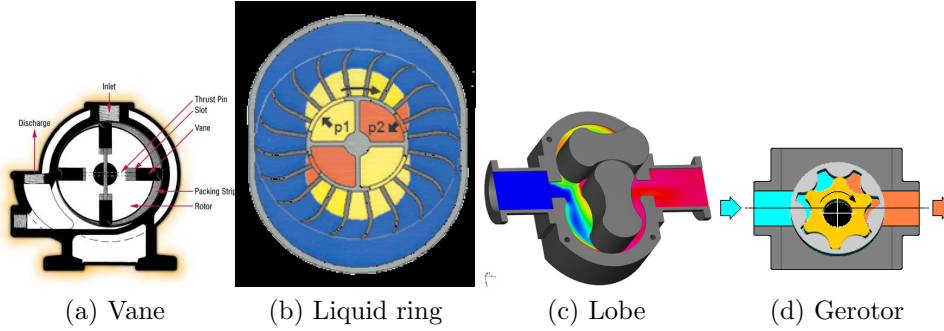
Figure 14: Collection of compressors

will be reversed. The high pressure gas enters at the "discharge" port were it expands towards the "inlet" port. These expanders has high leakage [25].

Liquid ring In figure 14b (garo.it) the gas will go from the static high pressure port (p_2) following the counterclockwise rotation of the vanes to the outlet port. The liquid in the machine is forced to the edges by the rotation of the vanes. This means that the expander needs to be applied with a start engine to ensure the centrifugal forces on the liquid before the expansion starts.

Lobe Figure 14c (pump-zone.com) shows a lobe expander with high pressure on the right side. The pressure difference forces the lobes to rotate as the fluid travels on the inner edges of the casing. One of the lobes has a shaft for extraction of mechanical energy.

Gerotor Figure 14d (sealantequipment.com) shows the high pressure on the left side as it forces the eccentric rotor to rotate inside the casing. Has been tested by [27] and showed some problems with leakage.

2.6.6 Expander selection

Kreider [28] proposed a set of dimensionless numbers to perform similarity analysis on expanders. The dimensionless numbers were the Reynolds number (Re), the Mach number (Ma), specific diameter (D_s) and specific speed (N_s). The latter two are defined below:

$$N_s \equiv NQ^{1/2}H_{ad}^{-3/4} \tag{2.25}$$

$$D_s \equiv DH_{ad}^{1/4}Q^{-1/2} \tag{2.26}$$

N is rotational speed in rpm, D diameter in ft, H_{ad} adiabatic enthalpy drop across the expander in $ftlb/lb$ and Q inlet flow rate in ft/s.
If the Reynolds number is high ($> 10^6$) and Mach number low (< 0.7) these two dynamic effects are of less concern, thus leaving N_s and D_s as the main parameters. By plotting N_s and D_s together with expander efficiencies, a map can be created to see what type of expanders could be most effective given specific speed and specific diameter. The map is shown in Figure 15. A more thoroughly description of the procedure is given by Balje [29]

20
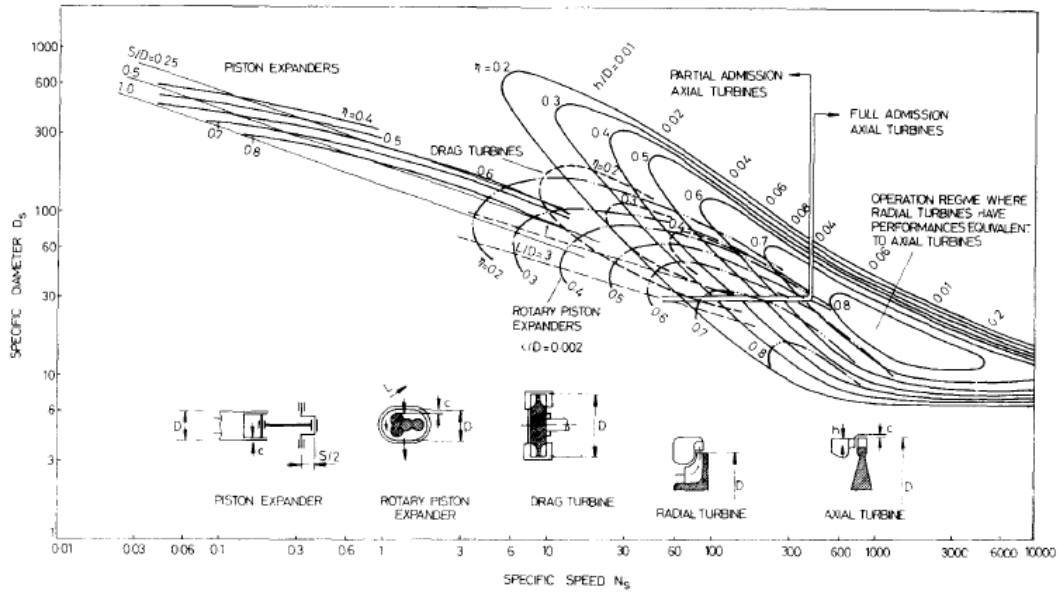
Figure 15: Performance map of different types of expanders (Kreider)

2.7 Gas turbine

2.7.1 Brayton cycle

The Brayton cycle has a close resemblance to the Rankine cycle, the difference being the working fluid in a Brayton engine is in the gaseous state throughout the entire cycle, as seen in Figure 16. Using an open Brayton cycle with air as the working fluid is the most common way to run a gas turbine, although there is a possibility to run it in a closed cycle as well (with a heat exchanger/cooler between state 1 and 4). An advantage with the closed cycle is the possibility of utilizing a higher pressure in the cycle. By doing this you would get a smaller gas turbine and the added regulation opportunity in pressure level variation [30]. With heat recovery in mind, the closed cycle intercooler could be smaller in size (increased fluid density in the closed Brayton cycle increases heat transfer, thus a reduction in heat transfer area) than a heat exchanger mounted on the exhaust of an open cycle gas turbine.

2.7.2 Brayton cycle efficiency

The Brayton efficiency for a polytropic process is derived from the Carnot efficiency as shown below

$$\eta_{Brayton} = 1 - \frac{T_{turbine,\,exit}}{T_{turbine\,inlet}} = 1 - \left(\frac{p_{turbine,\,exit}}{p_{turbine\,inlet}}\right)^{\frac{n-1}{n}} \tag{2.27}$$

where n is the polytropic temperature coefficient. The subscript *turbine inlet* denotes the thermodynamic properties after the combustion chamber. The efficiency is highly dependent on exit temperature and to a lesser extent, exit pressure.

21
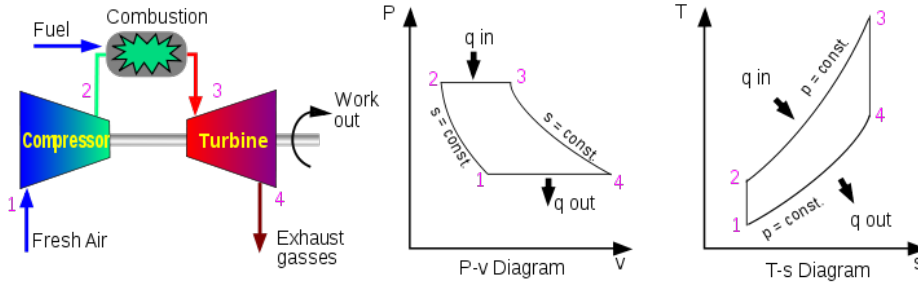
Figure 16: Open Brayton cycle (commons.wikimedia.org)

2.7.3   Variable load strategies for gas turbines

The efficiency and power output of the combined cycle is dependent on the load strategies used for variable load operation of the gas turbine. The most common methods of load regulation is fuel flow and air flow management. Each of these methods give different combined cycle output regarding both efficiency and power. The consequence of reduction in fuel flow is mainly a decrease in exhaust temperature with a negligible decrease in mass flow, whereas reduction in air flow increases exhaust temperature with a larger decrease in mass flow. A study has been conducted by Muñoz de Escalona et al. [31] in which the bottom line being the variation in air flow by internal guide vanes gives increased combined cycle efficiency compared to the variation in fuel flow management. These results where conducted at gas turbine loads below optimum only and with toluene as working fluid.

2.7.4   Water-augmented gas turbine

Gas turbine exhaust heat recovered can be used to enhance gas turbine efficiency directly instead of applying a Rankine cycle. As this is beyond the scope of this text, the different systems will be given a short presentation. The subject is discussed more thoroughly in [32]. Water heated by the gas turbine exhaust gases could be used to increase the gas turbine efficiency in several ways. Recuperated water injection (RWI, Rolls-Royce) injects the heated water prior to each compressor stage. The result is a close to isothermal, and thus more efficient, compression. This is also known as the Sprint-system (GE). Another way to enhance power in the gas turbine is a more complex system called *humidified air turbine* (HAT) which (along with several intercooling and aftercooling methods) humidifies the air in a column prior to the combustion chamber. The result would be a higher density of the working fluid and higher power output. This technique suffer from high complexity. Also known as *evaporative gas turbine (EvGT)*. A more simplified method is the Cheng cycle (GE has a similar system called steam injected gas turbines, STIG, LM2500 is available with this system) which uses a conventional HRSG and injects steam/water directly into the boiler. International Power Technologies (IPT) holds the patent and they report over 130 Cheng Cycle installations installed worldwide [33].

22

2.8 Heat transfer

Heat transfer between fluids is based foremost on the balancing of two equations. The first one is the 1st Law of Thermodynamics considering a heated fluid flowing through a control volume (e.g. a pipe) at steady state with no work done on the boundary and with negligible kinetic and potential energy changes. By applying these criteria on eq. (2.2) the result is

$$\dot{Q} = \dot{m}c_p(T_{out} - T_{in}) \tag{2.28}$$

The second equation is **Newtons law of cooling** which relates the heat transfer to the temperature potential between two fluids.

$$\dot{Q} = (UA)\Delta T \tag{2.29}$$

where $\dot{Q}$ and ΔT is the heat transfer and temperature difference, respectively, between the fluids. (UA) is the overall heat transfer coefficient and is dependent on several factors e.g. the convective heat transfer coefficient (h) on both sides of the heat exchanger, conduction resistance, overall surface efficiency and fouling.

2.8.1 Convective heat transfer

The convective heat transfer coefficient is found by using the Gnielinski corrolation

$$Nu_D = \frac{hD}{k_f} = \frac{(f/8)(Re_D - 1000)Pr}{1 + 12.7(f/8)^{1/2}(Pr^{2/3} - 1)} \tag{2.30}$$

which is valid for $0.5 < Pr < 2000$ and $3000 < Re_D < 5000000$ and could be applied for both uniform surface heat flux and uniform temperature heat transfer. Note that if the channel diameter become very small (< 1.09 mm) a correction of the Gnielinski corrolation given by Adams et al. [34] should be considered, another important point is the transition from laminar to turbulent flow in microchannels occur at Reynolds number of approximately 900, not 2300 as in conventional circular channels [35]. The Darcy friction factor for smooth surfaces needed to calculate eq. (2.30) could be found by the logarithmic overlap law derived by Prandtl (1935) but the more simple explicit formula provided by Filonenko (1954) is used here.

$$f_D = (1.82 * log_{10}(Re_D) - 1.64)^{-2} \tag{2.31}$$

Figure 17 show how the corrolation will give a slightly lower friction factor compared to the more precise logarithmic overlap law. The error is within 1% up to $Re_D = 1 * 10^6$.

The pressure drop in a channel is calculated with

$$\Delta p = f_D \frac{L}{D} \frac{\rho V^2}{2} \tag{2.32}$$

One important fact to bare in mind is the strong effect the tube length (WHRU length) has on the pressure drop while the convective heat transfer coefficient remain constant throughout the tube if the tube length/diameter ratio is larger than 10. This is a rule of thumb for turbulent flow with constant properties [36]
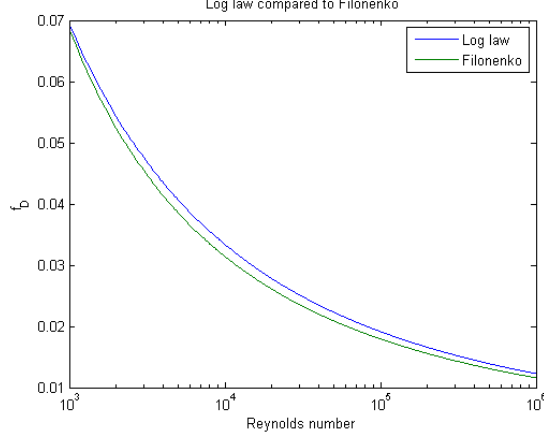
Figure 17: Comparison between the logarithmic overlap law and the Filonenko corrolation (calculation done in Matlab)

2.8.2 Optimal division of heat transfer conductance between WHRU and condenser

By maximizing the power output at fixed heat source input, the heat transfer conductance (hA) division between the two heat exchangers can be optimized as shown below. By setting a constraint on total heat transfer conductance, i.e. $(hA)_{tot} = (hA)_L + (hA)_H$, and the ratio between the "hot" exchanger and the total to: $(hA)_H/(hA)_{tot} = x$ it can be showed that

$$\eta = 1 - \left(\frac{T_L}{T_H}\right) \bigg/ \left[1 - \frac{\dot{Q}_H}{T_H \bar{h}A}\left(\frac{1}{x} + \frac{1}{1-x}\right)\right] \tag{2.33}$$

Optimizing $\eta(x)$ results in maximum efficiency at $x_{opt} = 1/2$ and the efficiency will become

$$\eta_{max}(x_{opt}) = 1 - \left(\frac{T_L}{T_H}\right) \bigg/ \left(1 - \frac{\dot{Q}_H}{T_H(hA)}\right) \tag{2.34}$$

The derivation reveal two interesting points. First, the heat transfer conductance should be split equally between the heat exchangers to obtain maximum power output and secondly, the maximum efficiency (η_{max}) with fixed heat input between T_H and T_L is a function of heat transfer conductance only[37].

2.8.3 Internal irreversibilities, heat transfer vs friction in heat exchanger

By combining the 1st and 2nd Law of Thermodynamics with $dh = Tds + vdP$ evaluated at a duct passage of length dx it can be shown that the entropy generation becomes

$$\dot{S}'_{gen} = \frac{(q')^2 D_h}{4T^2 \dot{m} c_p St} + \frac{2\dot{m}^3 f}{\rho^2 T D_h A^2} \tag{2.35}$$

per unit length. By using correlations for the Nusselt number (Nu) and the friction factor f for turbulent flow in circular smooth pipes equation (2.35) becomes dependent on only

24

the Reynolds number and consequently the pipe diameter ($Re = 4\dot{m}/\pi D\mu$ for circular pipes). Solving $d\dot{S}_{gen}/d(Re) = 0$ gives us

$$Re_{opt} = 2.023 Pr^{-0.071} B_0^{0.358} \qquad (2.36)$$

where $B_0 = \dot{m}q'\frac{\rho}{\mu^{5/2}(kT)^{1/2}}$ By employing this equation in the start of the analysis an estimate of the tube diameter can be obtained. Corrections can be done when more data (physical/thermodynamic restrictions) are collected.

3 Cycle comparison and heat exchanger parameter study

Higher fuel prices and elevated environmental concerns promotes the need for waste heat recovery as a mean to increase efficiency of power producing devices, or more general, to produce power where any heat source is readily available. Offshore installations are prone to these methods, first of all since connection to the land based power grid could be difficult and/or cost inefficient. Secondly, heat sources suitable for recovery are readily available as presented in section 1.2. The evaluation will focus on high temperature heat sources, which leaves gas turbine and ICE exhaust heat as a base for discussion. Gas turbine exhaust heat has the greatest potential and will be used as the working example, more specifically the General Electric's LM2500+ G4 (Figure 18) exhaust heat as a load on the Rankine cycle's WHRU. The LM2500+ G4 is chosen because it has wide usage and can be utilized both on marine vessels and offshore structures. The technology is proven as well (G4 stands for 4th generation).
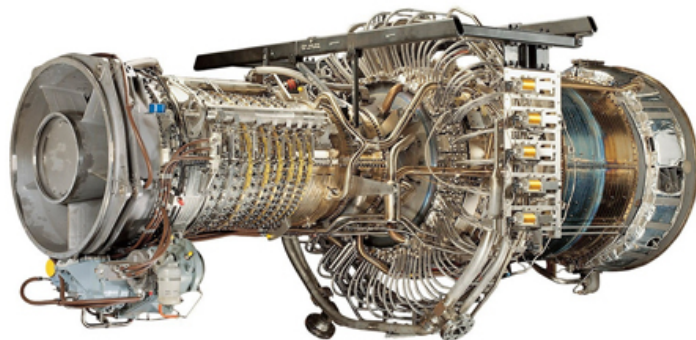
Figure 18: General Electric LM2500+ G4 (ge.com)

An ORC (organic Rankine cycle) could be used with a large range of different organic fluids and several studies has been done to try locating the best ones. In general, the fluids with the best efficiency is chosen by their saturation curve and their latent heat at low pressure. That is, isentropic (i.e. vertical saturation curve) [16], low liquid specific heat and high latent heat together with high density [17] for the best performance. These criteria promotes the use of R-123 for lower temperatures and p-Xylene for higher

General Electric LM2500+ G4	
Power output	35,3 MW
Exhaust flow	93 kg/s
Exhaust temperature	549°C

Table 4: Exhauxt data from LM2500+ G4 (60Hz, 15C, sea level, 60% rel. humidity)

temperatures [18]. CO_2 has also been tested [19] as a working fluid with heat exchange occurring in the supercritical region. As the scope of this evaluation is a comparison between steam cycle and ORC in general, less attention is given to the selection of working fluid. R-123 is scheduled to be completely phased-out by 2030 so toluene is chosen for both subcritical and supercritical cycle. A supercritical CO_2 cycle is chosen as a comparison to the supercritical toluene cycle. The selection is primarily based on availability (toluene has high availability) and environmental/personnel impacts such as ODP, GWP, toxicity and flammability. Toluene and CO_2 does not cover all these criteria, e.g. toluene is highly flammable, but considering highly flammable fluids are already present at offshore facilities the safety measures should already be implemented. These fluids are non-corrosive as well, which reduces the threat of leakage. Although CO_2 does not fit the definition of an "organic" fluid it will be presented here as such.

3.1 Comparison criteria and important parameters for evaluation

Important parameters to be evaluated in this comparison is listed below together with a short description:

Power output High relevance. High power output reduces the need for additional power producing equipment.

System size/Weight High relevance, especially in an offshore context which have costly "footprint".

Efficiency, 1st and 2nd law Decreases fuel costs and emissions per kW output.

Complexity and reliability More complex system often mean less reliability and equipment failure could become critical in the offshore environment.

Environmental and personnel safety Has to be well above certain criteria. Added risks means added costs.

By doing a comparison between cycles where all can be modified in a multitude of different conformations there has to be some "ground rules":

1. Same heat source load with no variation. (LM2500+ G4 exhaust heat, Table 4)

2. Expander is of either radial inflow or axial single-stage turboexpander (no reheating or multi-pressure HRSG/WHRU).

3. Same environmental reference properties and condensing water temperature ($T_0 = 15°C, p_0 = 1bar, T_c = 10°C$)

26

3.2 Physical system

As mentioned in section 2.4.1 the Rankine cycle consist of four main components in addition to the working fluid, these are: waste heat recovery unit (WHRU, working fluid evaporator), expander, condenser and pump. Further components might be introduced to the cycle if necessary. The main component which has the largest effect on all the mentioned parameters is the WHRU and will be presented here.

3.2.1 Heat recovery steam generator - HRSG

A HRSG is a heat exchanger widely used in chemical processing, to cool process gases down to desired temperatures, and in CHP/CC (combined heat and power/combined cycle) plants to utilize excess heat from exhaust gases. As the name implies, water is used as the cooling fluid. The structure is simple with hot gases going straight through, with inlet on one side and outlet on the opposite side, and the cooling liquid is routed through pipes inside the gas stream, usually with extended surfaces if the gas stream is clean. This set-up is called *water tube boiler*, in contradiction to *fire tube boilers* where the hot gases runs inside the pipes. The water tube boiler is discussed here since it can handle a large gas flow and has the opportunity to extract multiple steam pressures. Although the basic HRSG is a simple structure there could be made several modifications depending on its usage. The main modifications being the need for multi-pressure steam extraction and/or high superheating. If the hot gases is not sufficiently hot enough to heat the steam up to required superheating, the HRSG can be equipped with a boiler section to provide this. The added heat input in the boiler section has its origin from combustion of fuels. Since the fuel used in the HRSG "skips" the gas turbine part of the system, extended use of it should be avoided in a combined cycle. In other words: why having a gas turbine if you will be using the fuel only to run the steam engine? The incentive to use supplementary firing is to make the steam engine less dependent of the variations in heat load from the waste gases. If a forced-draft fan is added to provide the necessary pressure at the HRSG inlet, the fired HRSG could run the steam cycle even if the gas turbine is shutdown.

Multi-pressure HRSG One modification often used is the opportunity to produce steam with different pressures in the HRSG. Usually the pressure is divided into 3 levels: High pressure (HP) up to 170 bar, Intermediate pressure (IP) at 25 to 35 bar and low pressure (LP) at 3 to 6 bar [6]. The first two pressure levels are used for power production, i.e. superheat and reheat, and the latter is used for process heating, preheating the condenser fluid or deaeration (see section 3.2.2). Each pressure level is further divided into economizer, evaporator and superheat tube banks as shown in Figure 19. Counter-current flow is used throughout the HRSG except in the superheat tube bank where parallel flow is applied. As the allowable heat flux decreases with higher steam quality, parallel flow avoids the risk of departure from nucleate boiling (DNB).
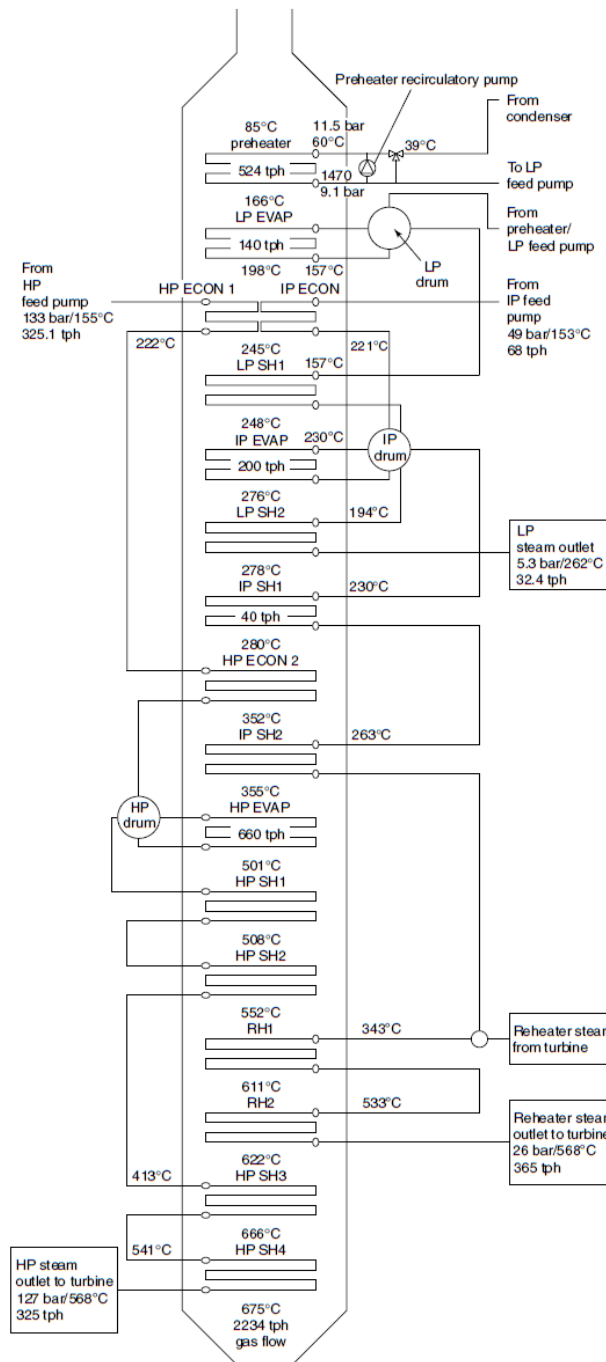
Figure 19: Different pressure levels in HRSG (Rayaprolu)

The HRSG can be sub-divided into 3 categories: vertical, horizontal and once-through (OTSG), where the different configurations are shown in Figure 20.

| (a) Horizontal | (b) Vertical | (c) Once-Through |
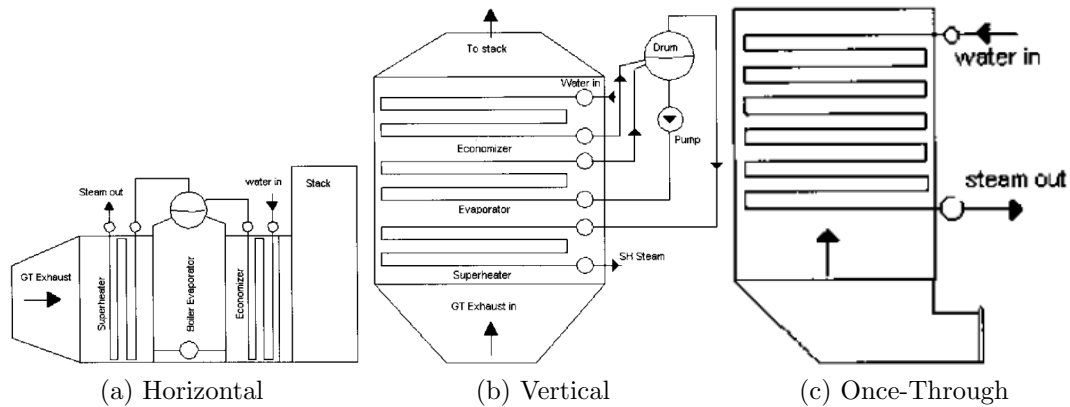
Figure 20: Types of HRSG (Ganapathy)

Horizontal

- Vertical tubes driven by natural circulation. Removes the need for circulation pumps and consequently reduces the risk of failure (pump failure, power outage...). Care has to be taken to prevent departure from nucleate boiling (DNB) where the heat transfer from the hot gases exceeds the maximum heat transfer to the steam/water. The result will be overheating of the tubes and possible tube failure.

- Simple installation and low installation time.

- Lower heat transfer coefficients resulting in larger heat transfer area needed.

- Due to the horizontal position it will occupy more floor space.

- Less flexible for cycling duty

Vertical

- Horizontal tubes require circulation pumps for pressures above 130 bar.

- Less footprint but taller and more exposed to wind loads.

- Easy access to tube banks.

- Handles cycling duty well.

Once-Through

- Requires no drum, risers, downcomers, blowdown system, etc.

- No distinct economizer, evaporator or superhaeting section, i.e. a single bank.

- Vertical design, approximately half the size of a vertical HRSG although only a slight decrease in footprint.

- Made of Inconel, not steel.

- Lower installation time.

- More expensive largely due to the use of Inconel.

29

Boiler blowdown is needed to remove dissolved solids (carbonates and sulphates of calcium and magnesium which cannot be filtered out) that could accumulate in the boiler during operation, introduced primarily through make-up water. The water impurities do not evaporate with the steam and will reside in the boiler water. If not removed these dissolved solids could deposit on the heat transfer surfaces, thus reducing heat transfer which in turn could lead to overheating and loss of mechanical strength. To reduce the amount of total dissolved solids (TDS) there is some water extraction (a few percent of total mass flow dependent of concentration of TDS and/or make-up water conditions) from the steam drum to lower the concentration. Since the water is extracted from the steam drum a substantial amount of heat follows with it. This heat loss has potential to be recovered [38].

3.2.2 Deaerator

A deaerator is used to reduce the risk of corrosion in iron or steel boilers. Corrosion is mainly dependent on the feedwater temperature, pH level and oxygen content in the water. As with most chemical reactions the reaction rate increases with temperature. In addition, temperature also increases the diffusion rate of oxygen from the water. Together with low pH levels(see Figure 21), the temperature will determine the aggressiveness of the corrosion. The oxygen content is a factor that effects the magnitude of the corrosion, lower oxygen content means less corrosion. To reduce the oxygen content in the feedwater a deaerator is used. The principle is to spray water (reducing the travel distance of oxygen due to small droplets) at saturation temperature (lowers the solubility) while steam is passed through to carry out the oxygen. The oxygen mixed steam is then condensed while the oxygen is vented to the atmosphere. The deaerator will also remove any CO_2 in the water and thereby increasing the pH-value.
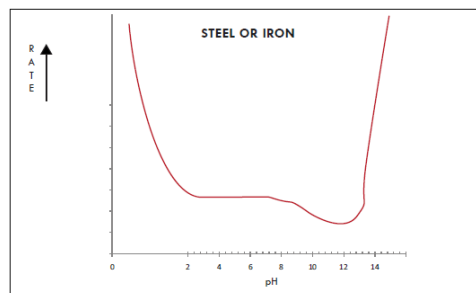
Figure 21: The effect of pH on corrosion rates (Noble Company)

3.2.3 Pinch point and approach temperature

The temperature profile through a HRSG can be found even without consulting manufacturers for specifications, i.e. without the use of physical and thermodynamical HRSG parameters. This can be done by choosing appropriate values for the *pinch point* and *approach point*. The pinch point is defined to be the temperature difference between the saturation temperature of the cold liquid and the temperature of the hot gases leaving

the evaporator at that point in the heat exchanger, and the approach point is the difference between the saturation temperature and the temperature of the water entering the evaporator. As seen in Figure 22 the approach point is located at the HRSG side where the superheated working fluid exits and the hot gases enters. This can be written as:

$$\text{Pinch point} = T_{ex,x} - T_{sat,water} \tag{3.1}$$

$$\text{Approach point}_1 = (T_{sat} - T_{in})_{working\ fluid} \tag{3.2}$$

$$\text{Approach point}_2 = T_{ex,\ inlet} - T_{working\ fluid,\ exit} \tag{3.3}$$

The approach temperature (1) ensure there is no steaming occurring in the economizer as well. Both values are usually 10°C plus/minus a few degrees. Lower pinch point and approach point result in better performance but increasingly larger heat transfer area.
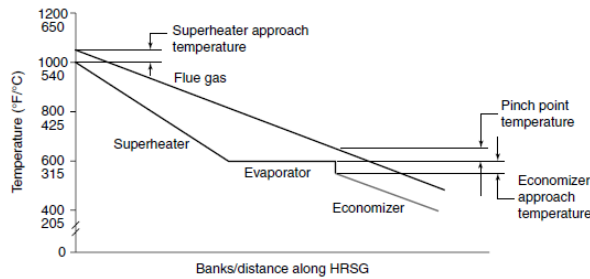
Figure 22: Temperature profiles in hot and cold streams showing the location of pinch point and approach temperatures. (Boilers for power and process - Rayaprolu)

3.2.4 Summary HRSG

Among the 3 different constructions above, the OTSG looks most promising for a steam cycle especially in terms of compactness and low maintenance. As for now the constraint of a single-pressure leaves the OTSG as the best option. The main difference in size is the absence of the steam drum in OTSG vs HRSG. Water enters at one end of the tube bundle and as the fluid exits fully evaporated at the other end there is no need for circulation and water/steam separation in a steam drum. The lack of steam drum decreases startup time and reduces weight substantially, on the other hand, the water contamination has to be at a minimum prior to injection to the boiler since the OTSG lack the blowdown system where contaminants can be rejected. The water treatment in a OTSG is done by all-volatile treatment (AVT) or oxygenated treatment (OT). AVT introduces chemicals to the stream that increases the pH-value thus provides better corrosion protection for steel. OT increases the electrochemical potential which reduces the iron oxide in the feedwater. Both methods could be combined with successful results [39].

3.2.5 Heat exchangers

Due to the wide range of usage there exist also an equally wide range of heat exchangers available. A few of the different categories are listed below with a following description. This is not an exhaustive coverage but will focus on the possibilities concerning the

object of this text where the first "filter" will be size, capacity, temperature and pressure requirements. Due to these standards, the most common heat exchanger, shell and tube, will not be presented here owing to its large size. High pressure and temperature leaves out gasketed heat exchangers as well. In addition to the already mentioned standards there is other important criteria as well, which the heat exchanger need to meet. These are: reliability, durability, low maintenance and above all, operation safety.

3.2.6   Plate heat exchangers (PHE)

Plate heat exchangers are made of plates (see Figure 23) stacked on top of each other and sealed by either gaskets, brazing or welding according to pressure requirements. The gasketed type has one important feature in the opportunity to fully dismantle the heat exchanger for cleaning or easily adding/reducing the number of plates. The plates could have different corrugation patterns to enhance turbulence and heat transfer. Usually plate heat exchangers are less resistant to high pressures (especially in the case of plate and frame heat exchangers) than tubular types although added strength can be procured by brazing or welding the plates together at contact points made by the corrugation pattern. Typical pressure and temperature limitations are: 40 bar and 350°C (limitations given for Alfarex welded HE by Alfa Laval).

For higher temperature and pressures a **plate and shell** heat exchanger (PSHE) is available. Due to the stronger and more rigid circular shell the heat exchanger can endure higher mechanical forces. As an example the Vahterus model shown in Figure 23b has temperature and pressure limitations of up to 200 bar and 899° C.

(a) Plate   and   frame   (Alfa (b) Plate and shell (Vahterus)
Laval)
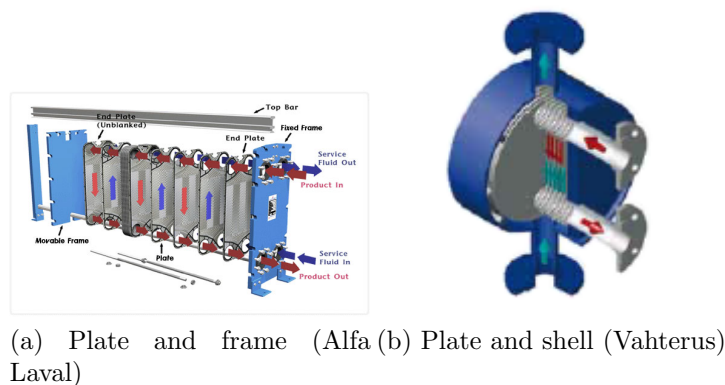
Figure 23:   Two types of plate heat exchangers

3.2.7   Plate-fin heat exchanger (PFHE)

By adding fins to the plates the total heat exchange surface could be increased by 5 to 12 times the primary surface, although the heat transfer coefficient could be either lower or higher, the sole result would be an increase in heat transfer surface area density (m^2/m^3). The strongest types are made with diffusion bonding. The manufacturing involves the adding of bond inhibitors between two plates where the flow path should be. The plates

are then extruded into the final shape resulting in a very large area density and strong structure with limitations of 200 bar and 400°C (Rolls Laval).

3.2.8 Printed-circuit heat exchanger (PCHE)

These models has the highest temperature and pressure limits of all types of heat exchangers and can operate in excess of 600 bar and 900°C (Heatric). The reason is the manufacturing method which has some similarities with the manufacturing of circuit boards (thus the name printed circuit HE). The process starts with chemical etching of the flow paths onto sheets of metal. The metal sheets are then stacked and fusion bonded together. The fusion bonding of the plates makes the joining points between the plates as strong as the parental metal. Channel diameter can be made very small (down to 0.1 mm) resulting in very high heat exchange surface to volume ratio.

3.3 Thermodynamic cycle analysis

The thermodynamic analysis has two main goals, first of all to determine 1st and 2nd law efficiencies together with an exergy analysis and total work output. Secondly, and equally important, the dimensioning of the machinery will be determined with focus on heat exchanger size.
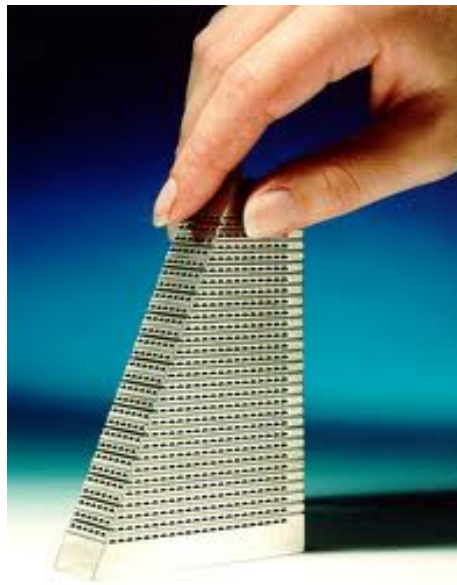
Figure 24: A section of a printed circuit heat exchanger (Heatric)

3.3.1 Preliminary study

Water, toluene and CO_2 was selected as discussed in section 2.5. The preliminary study is conducted on an ideal cycle with no pressure drops in the heat exchangers and isentropic compression/expansion in the pump/expander. The study is simply to investigate the effect of P_H on cycle efficiency and determine suitable pressure ranges for further calculations. Some constraints has been imposed on the cycle, these are:

- Ideal cycle.

- Pump inlet temperature kept at 20°C.

- Expander inlet temperature at 539°C.

- Pressure range from 1 MPa to the imposed maximum pressure limit of 15 MPa

Due to the high fluid pressure of CO_2 at condensing temperature (5.73 MPa) the efficiency is evaluated above the critical point at 7.38 MPa, i.e. from 8 to 15 MPa. This range

33

will not encompass the subcritical pressures for CO_2 and the cycle will be supercritical throughout the pressure range. The efficiency is simply evaluated with

$$\eta_1 = 1 - \frac{T_{L,avg}}{T_{H,avg}} \tag{3.4}$$

where

$$T_{x,avg} = \frac{1}{\Delta s} \int T \, ds \tag{3.5}$$

The results are shown in Figure 25
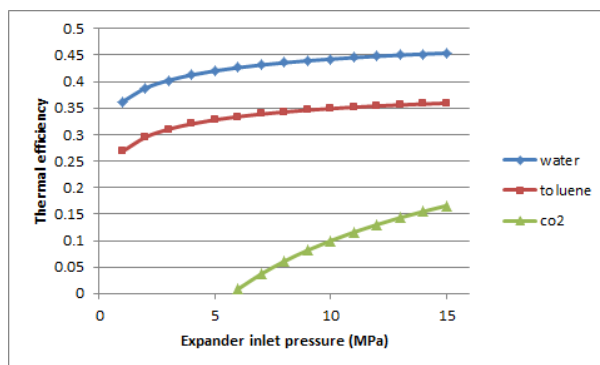
Figure 25: Efficiency vs heat recovery pressure for water, toluene and CO_2
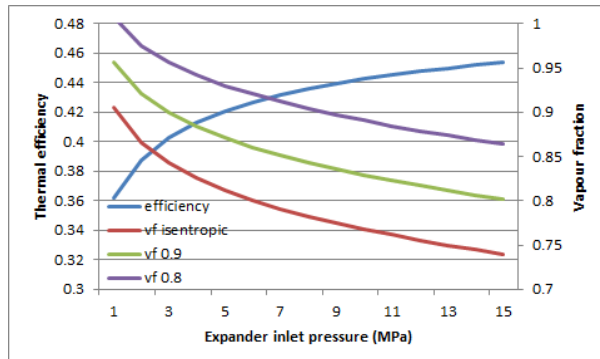
Figure 26: Chart showing the vapor fraction at 3 different expander efficiencies over a range of pressures

Higher pressures result in higher $T_{H,avg}$ as expected but the relative increase will level off as the pressure increases. For toluene the whole range is valid and can be used in further calculations. For water on the other hand, there is a risk of steam condensation in the expander at higher pressures. To reduce wear on the expander the vapor fraction should at least be above 0.8 for isentropic expansion. The cycles are constricted to one pressure level, thus reheat is not applied to the water cycle to increase the vapor fraction. Figure 26 shows that a vapor fraction of 0.8 occur at a pressure of approximately 6 MPa for isentropic expansion. With an expander efficiency of 0.8 the vapor fraction at

6 MPa increases to 0.92. As a consequence further calculations with the steam cycle involves pressures below 6 MPa. It is assumed that the vapor fraction will increase with calculations departing from an ideal cycle. The study resulted in the selection of the following high pressure levels of the cycle shown in Table 5. The pressures are chosen to be as high as possible due to assumed increase in heat transfer by increasing the fluid density (a consequence of high pressure).

Set pressure at Expander inlet (T_3)		
Working fluid	Description	Pressure
Water	Subcritical	6 MPa
CO2	Supercritical	15 MPa
Toluene	Subcritical	3,5 MPa
	Supercritical	15 MPa

Table 5: Selected pressure for each cycle

3.3.2 Defining the states for the Rankine cycle

All of the four different states of the Rankine cycle could be defined by the listed inputs in Table 6 except state 4 (condenser inlet) which depends on the pressure drop (i.e. the cycle mass flow) through the condenser, which is not known.

Cycle input values		
Cooling water temperature, T_c	10	°C
Approach point condenser, ΔT_L	10	°C
Gas turbine exhaust temperature, T_{ex}	549	° C
Approach point WHRU, ΔT_H	10	°C
Pump isentropic efficiency, η_p	0.8	-
Expander isentropic efficiency, η_e	0.8	-
Expander inlet pressure P_3	Table 5	MPa

Table 6: Set values for calculation of cycle states

State 1 - Pump inlet

$$T_1 = T_c + \Delta T_L$$

$$P_1 = f(T_{1,sat\ liquid})$$

State 2 - WHRU inlet

$$h_2 = h_1 + \frac{h_{2,is} - h_1}{\eta_p}$$

where

$$h_{2,is} = f(p_3, s_1)$$
$$T_2 = f(p_3, h_2)$$

State 3 - Expander inlet

$$T_3 = T_{ex} - \Delta T_H$$

$$p_3 \quad \text{Table 5}$$

State 4 - Condenser inlet

$$p_4 = p_1 + \Delta p_L$$

where Δp_L is the pressure drop in the condenser.

$$h_4 = h_3 - \eta_e(h_3 - h_{4,is})$$

where

$$h_{4,\,is} = f(p_4, s_3)$$

Assumption which need to be checked: Properties at state 2 are evaluated at P_2 as the pressure drop in the WHRU is assumed to be negligible relative to the high pressure, i.e.

$$\frac{\Delta p_H}{P_3} = \text{negligible}$$

That assumption is not valid for the low pressure where P_1 and ΔP_L could be closer in magnitude, especially for the low condensation pressure of water, thus Δp_L has to be calculated before state 4 is fixed. The pressure drop on the working fluid side of the WHRU with a length of 3.5m and channel diameter of 0.8mm (see the rest of the assumptions in section 3.4.2) turns out to be $\approx$ 2.5 kPa which is negligible relative to the high pressure of the working fluids (3.5 to 15 MPa).

3.3.3 Determine heat input and working fluid mass flow

The heat transfer to each of the four different cycles can be found by setting the pinch point for the subcritical cycles. For the supercritical cycles the temperature difference at the subcooled side of the heat exchanger has to be set, which is not a *pinch point* in the conventional sense, but will be regarded as such. After these points are specified a simple heat balance will determine the amount of heat transferred to the each cycle. The calculation are conducted as shown below and the two heat transfer rates are divided as seen in Figure 27. The first step is to choose a pinch point temperature, ΔT_{pp}, normally around 10°C, and then find the amount of heat transferred from the exhaust gases down to this temperature, i.e.

$$\dot{Q}_1 = \dot{m}_{ex}[h(T_{ex,\,in},\ p_{ex,\,in}) - h(T_{sat\,liq,\,working\,fluid} + \Delta T_{pp},\ p_{ex,\,x})]$$

$p_{ez,\,x}$ is the pressure at that particular point in the exhaust stream. The heat transfer $\dot{Q}_1$ is then used to find the mass flow of the working fluid

$$\dot{m}_{working\,fluid} = \dot{Q}_1/(h(T_3) - h(T_{sat\,liquid}))$$

where both enthalpies are evaluated at the working fluid high pressure. When the mass flow is obtained the heat transfer needed to bring the subcooled liquid up to saturation temperature is found by

$$\dot{Q}_2 = \dot{m}_{working\,fluid}(h(T_{sat\,liquid}) - h(T_2))$$

36

The total heat transfer $\dot{Q} = \dot{Q}_1 + \dot{Q}_2$ determine the exhaust temperature at the exit of the WHRU

$$h(T_{ex,\,out},\ p_{stack}) = h(T_{ex,\,in},\ p_{ex,\,in}) - \dot{Q}/\dot{m}_{ex}$$

where $T_{ex,\,out} = f(h, p)$ which is known. $p_{stack} \approx$ atmospheric pressure. The results are plotted on a T-Q diagram (Figure 28) which shows the temperature distribution along the length of the heat exchanger as well as the total heat transferred to the fluid.
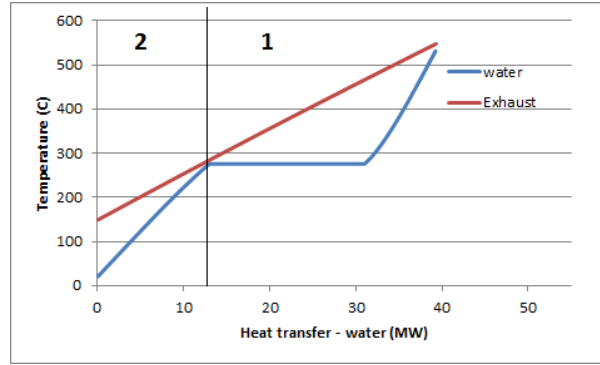
Figure 27: Division of the two heat transfer rates from the heat source

(a) Water · (b) Toluene - subcritical

(c) CO2 · (d) Toluene - supercritical
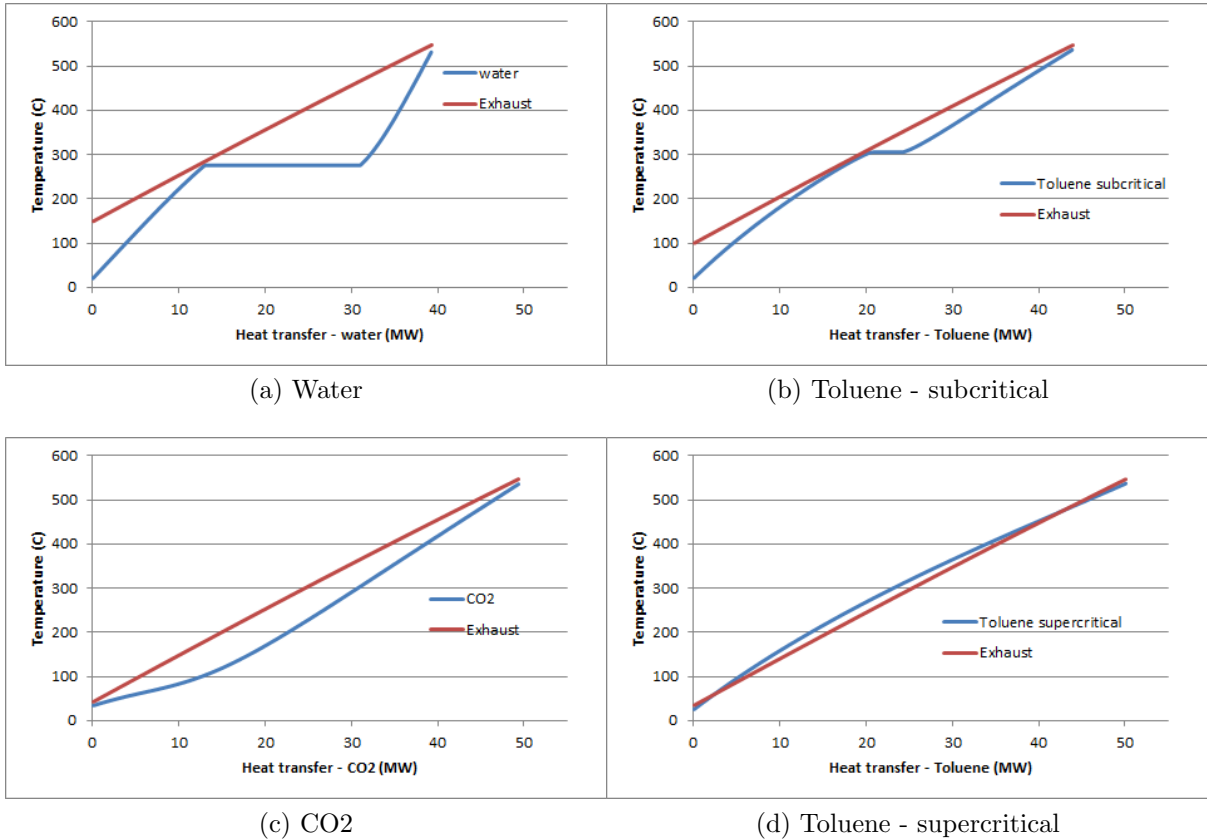
Figure 28: Graphs showing the temperature distribution along the WHRU and total heat transfer to the cycle for four different cycles. Approach temperature and pinch point at 10°C.

It is evident that the supercritical toluene cycle is not physically possible and there has to be some adjustment to the "pinch point". The reason for the "overlap" in Figure 28d is the variation in specific heat capacity for toluene. Figure 29 explain this by showing the specific heat capacity (c_p) versus temperature for air, toluene and CO_2.
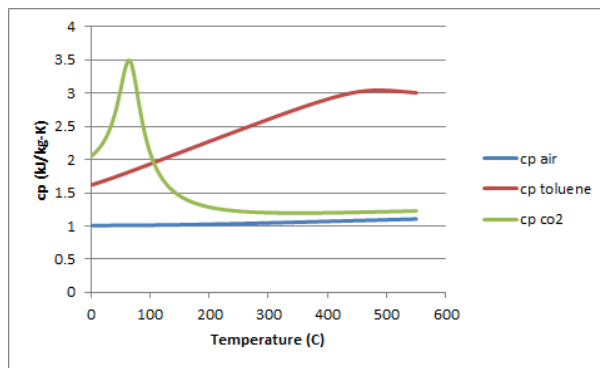
Figure 29: Specific heat capacity versus temperature for air, toluene and CO_2

Although CO_2 has a jump in cp at lower temperatures, due to its properties being

38

close to the critical point, it becomes a constant at higher temperatures similar to the specific heat capacity of air. Toluene, on the other hand, has a steadily increasing cp. This is not favorable as the working fluid cp curve should inherently have the same shape (or as close as possible) as the heat source over the given temperature ranges for the best temperature matching.

For a temperature difference above 10°C throughout the entire WHRU a pinch point of 90°C (instead of $10°C$ used in the other cycles) is required for supercritical toluene. The most important parameters from the analysis is summarized in Table 7 and the corrected supercritical toluene cycle shown in Figure 30.
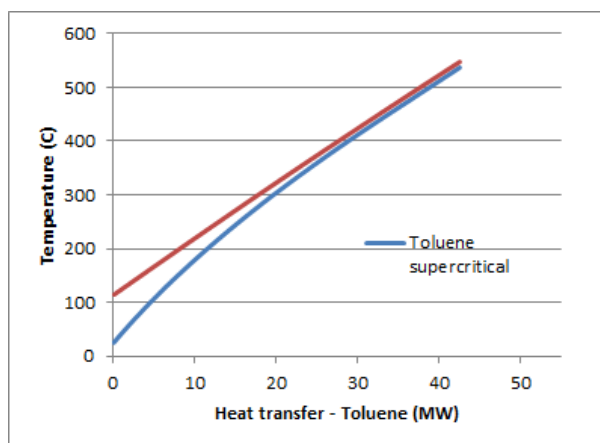
Figure 30: Supercritical toluene cycle with corrected pinch point at $90°C$

	Water	Toluene subcritical	Toluene supercritical	CO2
Heat transfer (kW)	39225	42898	42569	49237
Mass flowrate (kg/s)	11.46	30.81	33.16	65.21
Pinch point (°C)	10	15	90	10
Exhaust temperature (°C)	150	110	115	44
Exergy transfer via heat transfer (kW)	20823	21939	21814	23096
Exergy lost, WHRU (kW)	5617	2629	2217	4844
Exergy lost wrt transferred	27.0%	12.0%	10.2%	21.0%

Table 7: Cycle values given by exhaust properties and set approach and pinch point

As seen from both Figure 28 and Table 7, CO_2 will match the "temperature-glide" of the heat source best and as a result CO_2 is able to absorb more heat given the same criteria. Water, on the other hand, does not have this ability to transfer heat (at least from a single-phase heat source) and is restricted by the saturation temperature which will "choke" the heat transfer. Subcritical toluene inhere the same negative effect, although the effect will be smaller due to the lesser heat of vaporization of 116.7 kJ/kg compared to 1570.6 kJ/kg for water at their respective pressure levels. The cycle most comparable to CO_2 is the supercritical toluene cycle. It suffer from the aforementioned imbalance in c_p, wrt air being the heat source. The pinch point had to be raised for both toluene

cycles due to the mentioned c_p imbalance, although equal (or better) effect could be accounted for by increasing the approach temperature. For the sake of cycle comparison, the approach temperature was left at the same magnitude as the other cycles.

Another interesting point is the amount of exergy destruction in the WHRU for each cycle. Water has the worst "temperature match" in the heat exchanger, thus the highest amount of exergy destruction. On the other end of the scale we find toluene with a temperature distribution matching the heat source better along the heat exchanger. Due to the low heat of vaporization of the subcritical cycle it can bring the exhaust temperature down to 110°C, thus absorbing more heat than the supercritical cycle, although worse temperature matching makes it less efficient in term of exergy transfer. From Table 7 it can be shown that the exergy transferred to the cycle *after* heat transfer is 19310 kW for the subcritical cycle while the super-critical cycle transfer 19597 kW of exergy.

Although CO_2 transfer the highest amount of heat to the cycle it suffers from the "c_p-peak" shown in Figure 29 resulting in the "bend" in Figure 28c which effects the temperature matching throughout the heat exchanger. This result in a high amount of exergy destroyed during heat transfer leaving the total amount of exergy to the cycle (after heat transfer) to 18252 kW. This effect could be reduced by allowing less heat to be transferred to the CO_2 cycle, thus increasing the exhaust temperature exiting the WHRU resulting in a better temperature match between the fluids, although with less heat transferred. As an added bonus; by decreasing the heat transfer smaller sized WHRU could be applied. Finally, the net exergy transfer to the cycle with water as the working fluid is 15206 kW.

3.3.4 Energy and exergy analysis

The exergy discussion started in the previous section due to the high dependency of the temperature mismatch in the WHRU on overall exergy destruction. The exergy lost due to the heat transfer across the finite temperature difference in the WHRU is calculated by the equation below

$$\dot{W}_{lost} = \sum_{i=1}^{n} \left(1 - \frac{T_{L,i}}{T_{ex,i}} \right) \dot{Q}_i \tag{3.6}$$

where T_L is the temperature of the working fluid and n is the number of partitions of the WHRU length and should be high enough to get approximately constant temperatures at each evaluation point i.

The total exergy transferred to the cycle by heat is calculated by

$$\dot{E}_Q = \sum_{i=1}^{n} \left(1 - \frac{T_c}{T_{ex,i}} \right) \dot{Q}_i \tag{3.7}$$

where T_c is the cooling water temperature which is assumed to be constant during the heat rejection in the condenser, i.e. a temperature reservoir. The net exergy after heat transfer would then be

$$\dot{E}_{Q,net} = \dot{E}_Q - \dot{W}_{lost} = \sum_{i=1}^{n} \left(\frac{T_{L,i} - T_c}{T_{ex,i}} \right) \dot{Q}_i \tag{3.8}$$

As seen from eq. (3.8), if $T_{L,i} \to T_{ex,i}$ then $\dot{E}_{Q,net} \to \dot{E}_Q$.

By using the 2nd law equations presented in section 2.4.2 for the pump and the expander together with the net power output defined as

$$\dot{W}_{cycle} = \dot{m}(h_3 - h_4) \tag{3.9}$$

the exergy lost in the condenser is readily available as

$$\dot{W}_{c,lost} = \dot{E}_{Q,net} - \dot{W}_{p,lost} - \dot{W}_{e,lost} - \dot{W}_{cycle} \tag{3.10}$$

The exergy losses for each cycle is shown in Figure 31
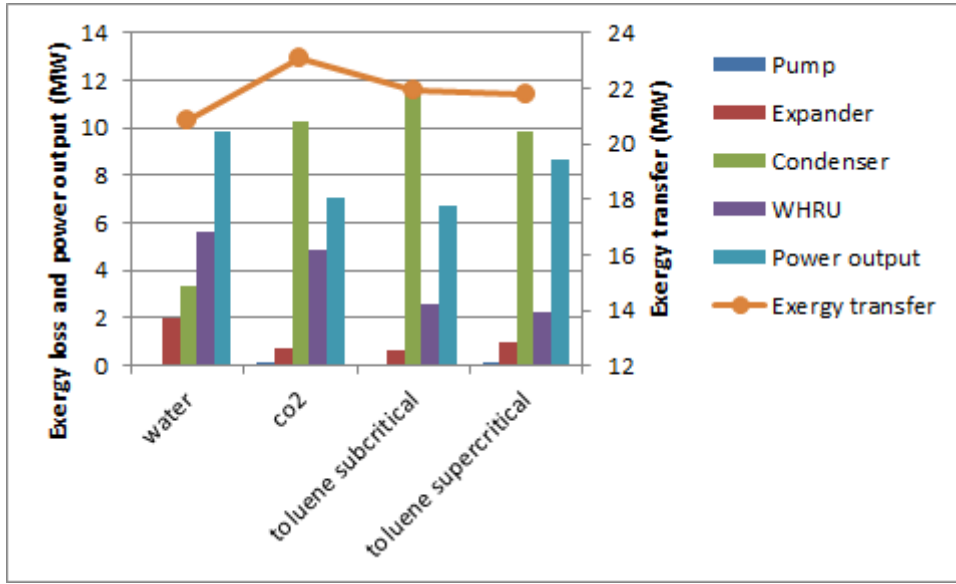
Figure 31: Exergy losses in each component for all cycles plotted together with work output and exergy transferred to each cycle

Figure 31 depicts very variable component losses, regarding each cycle. Water has the "normal" division in losses where the components are ranked in the following way with the component experiencing least losses first: pump, expander, condenser and WHRU. All cycles follow this trend with exception of the condenser losses in the organic cycles. The reason for this is the high temperatures at the condenser inlet and high heat transfer load on the condenser. With reference to equation (3.6) it is apparent that large heat loads and temperature differences result in high exergy losses. Figure 32 shows the heat load and inlet temperature at the condenser for each cycle.

The reason for the high temperatures at the condenser inlet is mostly because of the low enthalpy difference between the low and high pressures of the organic cycles. The respective enthalpy drop through the expander for each cycle is shown in Table 8. Water has a substantially higher enthalpy drop than the other cycles, thus more work per mass flow rate can be extracted through the turbine. The negative side to the high enthalpy drop is the expander's inability to handle this range in one stage, usually the isentropic efficiency goes down for high enthalpy drops. To maintain the efficiency for
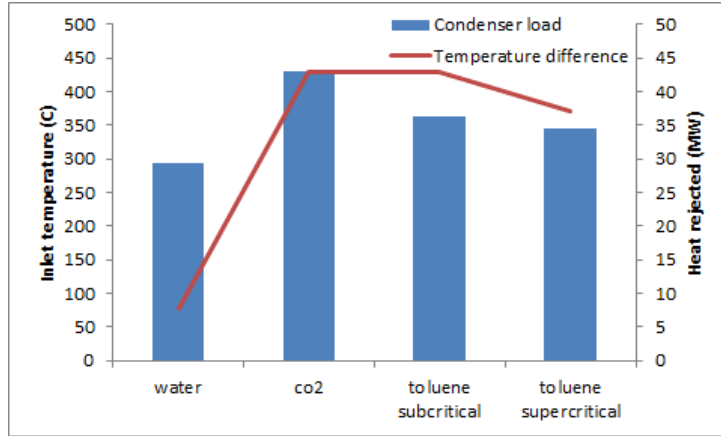
Figure 32: Condenser load and inlet temperature for each cycle

	Water	CO_2	Toluene subcritical	Toluene supercritical
Enthalpy drop (kJ/kg)	859.2	108.9	219.6	261.5

Table 8: Enthalpy drop for each cycle

the expander more stages has to be added. As discussed in 2.6.4 the high enthalpy drop require more than three stages to maintain the efficiency, while for the organic cycle one stage is sufficient. More expander stages will result in larger and more costly equipment.

One way to reduce inefficiency of the organic cycles (high temperature heat load is wasted during condensation) is to utilize the excess heat for process heating or other form of heating needs. This will affect the power output of the Rankine cycle in a negative way because up to now the heat sink is regarded to be a temperature reservoir, in contrast to an assumed glide in the condenser cooling fluid temperature for a combined heat and power cycle, although the thermal efficiency will go up substantially for the latter cycle.

3.4   WHRU hot side - Gas turbine exhaust

The thermodynamical study of the heat exchanger parameters starts with an analysis of the hot side of the WHRU which is assumed to be the deciding factor in evaluating the WHRU size (the cold side is assumed to have a higher heat transfer coefficient). The heat exchanger is chosen to be of the printed circuit type (see section 3.2.8) shown in Figure 33 due to high temperature requirements above 500°C and pressure difference between the two fluids of up to 15 MPa.

Geometry relations, WHRU   The WHRU is a rectangular shaped box with overall height, H, width, W, and length L as shown in Figure 33. The relation between channel numbers are
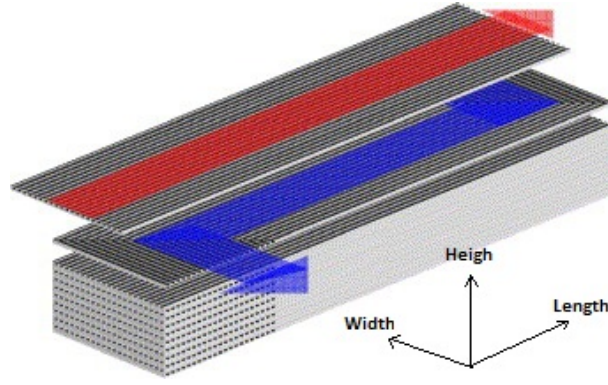
$$\# = N_H N_W$$

Figure 33: The flow path of a printed circuit heat exchanger (heatric.com)

where # are the total number of channels in one stream and N_H/N_W are the number of channels in the vertical and horizontal direction respectively. By setting $N_W = 2N_H$ (the overall number of channels are equal in both directions) the channel numbers in each direction can be represented by the total number of channels for one stream, i.e.

$$N_W = \sqrt{2\#}$$

and

$$N_H = \frac{\sqrt{2\#}}{2}$$

The height and width are further reduced to the height with the wall separating the channels subtracted H':

$$H' = N_H(D_h + D_c)$$

where D_h and D_c are the hot side and cold side channel diameter. The width with the wall thickness subtracted is

$$W' = (N_W D)_x$$

where x denotes either the cold or the hot side parameters.
The heat transfer area is thus

$$A = W' * L * (2N_H - 1) \tag{3.11}$$

where all parameters are independent of the choice of hot or cold side stream. The heat transfer area can thus be seen as a plate heat exchanger (no wall thickness between channels) with $(2N_H - 1)$ being the number of "plates".

Heat transfer   The heat transfer to the cycle from the exhaust gas is calculated by

$$q_i = \dot{m} \left(\frac{c_p(T_i) + c_p(T_{i+1})}{2} \right) (T_i - T_{i+1})$$

43

where T_i and T_{i+1} are evaluated at (p_i, s_i) and (p_{i+1}, s_{i+1}) respectively. To calculate the heat transfer from the exhaust gases to the cycle, Newton's law of cooling is used. It is defined as

$$q = UA\Delta T \tag{3.12}$$

where ΔT is the temperature difference between the two fluids and the overall heat transfer coefficient (UA) for unfinned surfaces, no fouling and negligible conduction resistance is defined below

$$\frac{1}{UA} = \frac{1}{(hA)_h} + \frac{1}{(hA)_c} \tag{3.13}$$

where h are the convective heat transfer coefficient and the subscripts denotes the hot and the cold side.

ϵ-NTU method   From the definition of heat exchanger effectiveness we get ϵ to be dependent on the WHRU approach point and working fluid outlet pressure, p_3 ($\Delta T_H = T_{exhaust, in} - T_3(\Delta T_H, p_3)$).

$$\epsilon = \frac{q}{q_{max}} = \frac{T_3 - T_2}{T_{exhaust, in} - T_2} = 1 - \frac{\Delta T_H}{T_{exhaust, in} - T_2}$$

where $q_{max} = C_{min}(T_{exhaust, in} - T_2)$. $C_{min} = \dot{m}c_p$ for the fluid experiencing the highest temperature difference, in this case it is the working fluid by the criteria that the approach point temperature difference is smaller than that of the pinch point. To find the overall heat transfer coefficient the $\epsilon - NTU$ method is used where

$$NTU = \frac{UA}{(\dot{m}c_p)_{min}} = \frac{\epsilon}{1 - \epsilon} \qquad\qquad C_r = 1$$

and

$$NTU = \frac{1}{C_r - 1}ln\left(\frac{\epsilon - 1}{\epsilon C_r - 1}\right) \qquad\qquad C_r < 1$$

where C_r is defined to be

$$C_r = \frac{(\dot{m}c_p)_{min}}{(\dot{m}c_p)_{max}} = \frac{T_{exhaust, in} - T_{exhaust, out}}{T_3 - T_2}$$
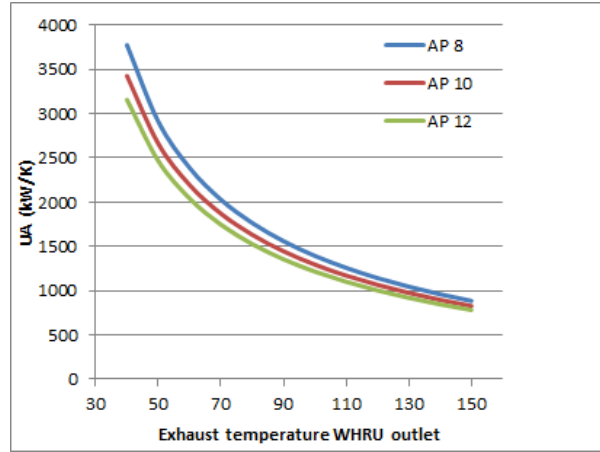
Figure 34: Variation in the UA value with a change in temperature differences on both sides of the WHRU

Figure 34 shows a plot of the UA - values needed from the heat exchanger while varying the temperature differences on both side of the WHRU. The calculations has been done by assuming the temperature on the inlet of the cold side of the WHRU being constant at $T_2 = 20°C$. Since a change in ΔT_H affects the cycle output as well as size of the WHRU it will be chosen to be $10°C$. At that approach point the thermal effectiveness is calculated to be $98,1\%$, which is a high number but assumed to be reachable (Heatric reports thermal effectiveness in excess of 98%). By fixing the temperature difference, the exhaust temperature at the WHRU outlet remain as the main parameter in deciding the heat exchanger overall size. The 1st Law of Thermodynamics demands the exhaust temperature to be as low as possible to obtain the highest heat input to the cycle and thus reducing the exergy loss by the temperature difference during the heat transfer as well. The decision on how low the pinch and approach points should be has to balance the (exponential) increase in the overall heat transfer coefficient (i.e. cost).

Heat transfer coefficient analysis   With reference to Figure 33 the total heat transfer area is calculated with eq. (3.11). If the goal is to reduce the heat transfer area but keep the overall heat transfer coefficient constant it implies that the "U-value" has to be increased.

With reference to eq. (3.13) and noticing the areas on the hot and cold side to be of equal size as the overall area it reduces to

$$U = \frac{h_h h_c}{h_h + h_c} \tag{3.14}$$

which clearly shows that to increase the U value both h_c and h_h need to be as large as possible. Another criteria seen from eq. (3.13) is that both convection heat transfer coefficients has to be larger than the overall heat transfer coefficient, i.e.

$$h_h, h_c > U$$

45

As the convective heat transfer coefficient on the exhaust side has to be higher than the U value but assumed to be lower than the cold side convection coefficient (higher densities on the cold side due to higher pressures enhances the heat transfer), it is regarded the main variable in deciding the overall size of the WHRU. Another important fact is the strong effect h_h has on the needed magnitude of the cold side coefficient h_c as seen in Figure 35
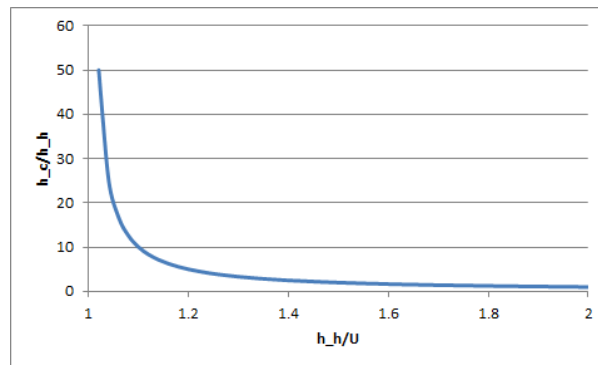
Figure 35:   Relative magnitude of heat transfer coefficients

If the smaller heat transfer coefficient (hot side) goes below about 1.15 times the overall heat transfer coefficient the needed relative magnitude of the heat transfer coefficient on the other side increases rapidly towards infinity when $h_h \rightarrow U$. If $h_h/U = 1.2$, h_c has to be 5 times larger than h_h, for $h_h/U = 1.4$, h_c/h_h equals 2.5. Thus, the goal is to enhance the assumed lowest heat transfer coefficient as much as possible.

3.4.1   Reduction of variables

To reduce the convective heat transfer coefficient on the hot side, h_h, several methods can be utilized. The most apparent are listed below with positive and negative properties.

1. Increasing exhaust pressure

   - Positive: Increases the allowable pressure drop in the WHRU thus smaller tube diameter and longer tube lengths can be used.
   - Negative: Reduction in gas turbine output.

2. Increasing the number of tubes

   - Positive: Increases the total heat transfer surface. Decreases the pressure drop by decreasing the massflow through each tube.
   - Negative: Proportionally increase in WHRU size. Decreases heat transfer due to lower Reynolds number.

3. Decrease the tube diameter

   - Positive: Increases h while decreasing the overall WHRU size.

- Negative: Increases pressure drop.

4. Increase WHRU length

   - Positive: Increases the total heat transfer surface.

   - Negative: Proportionally increase in WHRU size and pressure drop. h will remain approximately constant throughout the tube length.

Point 4 - Increasing the WHRU length - does not affect the convective heat transfer coefficient in any noticeable degree (ref [36]) and calculations can be made per unit length with proportional increase in both heat transfer area and pressure drop. Since the gas turbine is very sensitive to back pressure increase, a limitation is set to a pressure drop of 0.2 MPa in the WHRU and the effective back pressure at the gas turbine exit will be 0.3 MPa assuming the ambient pressure to be 0.1 MPa. This restriction removes point 1 from the list above. By implementing the pressure limit, parameter 2 and 3 (tube diameter and number of tubes) can be grouped together since for each tube diameter there corresponds a certain amount of tubes to reduce the pressure loss down to sufficient levels. Thus, two remaining independent variables (length and the group, number of channels/channel diameter) are left and results can be produced with respect to heat transfer area versus heat recovery. Figure 36 is plotted with a fixed pressure drop of 0.2 MPa and $h_h/U = 1.4$. It produces the size (length, L and width, W') of the WHRU given the exhaust temperature at the WHRU exit (exhaust properties from Table 4). The procedure starts in Figure 36b by selecting the exhaust temperature, by moving vertically from that point the $(hA)_h$ needed on the hot side is found, and thereafter, by moving horizontally to Figure 36a and selecting the length, the tube diameter is found. The two remaining graphs, Figure 36c and 36d shows the heat surface area and number of channels for the selected exhaust temperature and WHRU length.

(a) 2

(b) 1

(c) 3

(d) 4
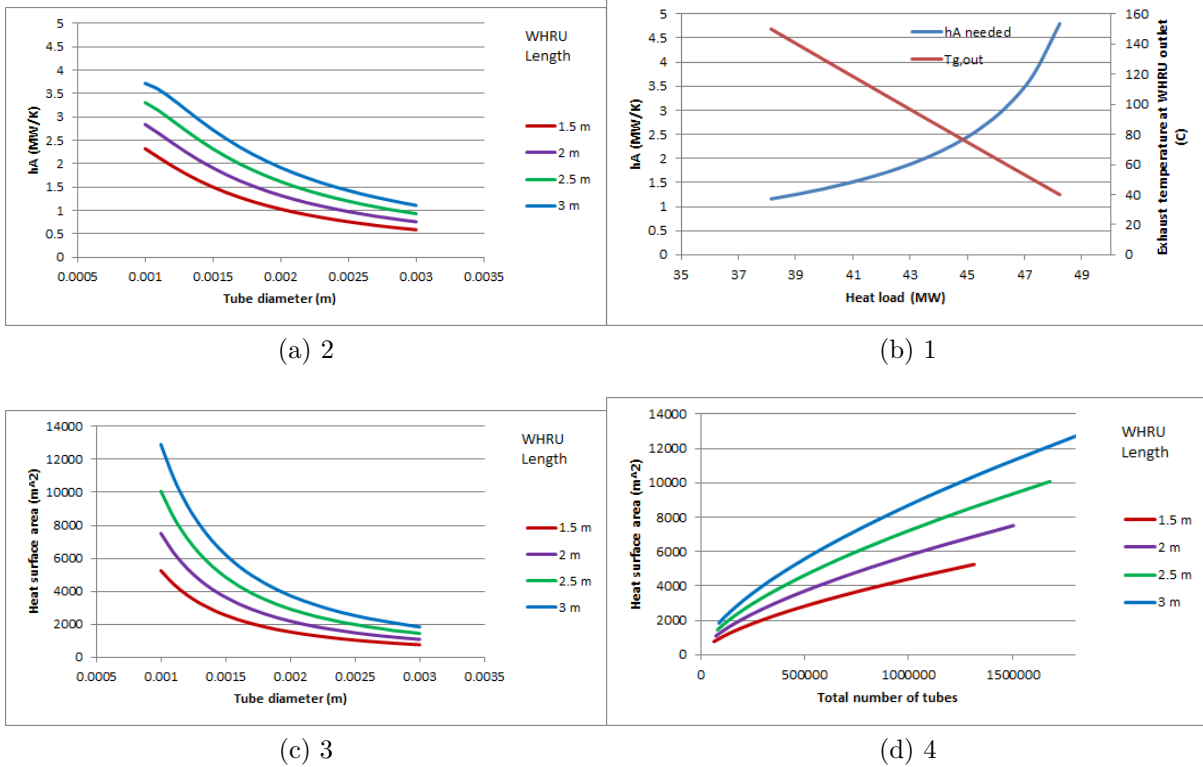
Figure 36: WHRU parameters given the selected heat load (exhaust temperature) - WHRU hot side. The procedure to retrieve the parameters involves selecting the exhaust temperature and WHRU length and then drawing vertical or parallel lines between the graphs starting at 36b

3.4.2 Overall WHRU size (WHRU cold side)

Although Figure 36 gives a hint of the overall size it is not sufficient. To estimate the overall dimensions of the WHRU a description of the cold side of the heat exchanger is needed as well, mainly to find the cold side channel diameter, D_c. Before the evaluation begins, it is necessary to mention the low precision in the following calculations due to the use of constant fluid properties, in reality these properties will change drastically when evaporating a liquid and further superheating it into the gas region. To get a "reasonable" estimate of the properties an Excel function is created, which is described in the appendix. A more precise method can be applied by looking into the *three-zone flow boiling*-model described by Thome et al. [40]

Another limitation is the fact that the fluid properties (viscosity and thermal conductivity) are not defined in REFPROP for toluene, thus the following results are reduced to water only.

The cold side channel diameter, D_c By implementing the results from the exhaust side of the WHRU and results from Table 7 the required $(hA)_c$ value on the cold side can be found. To produce the (hA) values for both sides the ratio $(hA)_h/UA$ need to be selected. As a starting point this value is chosen to be 1.4 which is then used in equation

48

(3.14) (solved here for $(hA)_c$)

$$(hA)_c = \frac{h_h/U}{h_h/U - 1} UA = 3.5 UA = 1160 kW/K$$

The UA - value in the equation above is the needed value to bring the exhaust gas temperature down to 150°C which is the case for water. With both heat transfer conductances set, all parameters on the hot side is readily available (given the pressure restriction), except the channel (WHRU) length. Given the assumption that the convective heat transfer coefficient (h) being constant throughout the length of the heat exchanger it implies that the heat transfer area remains constant as well ($(hA)_c$ is set by $(hA)_h$ and T_{ex}). **Note:** An investigation considering the change in convective heat transfer coefficient reveals a decrease of approximately 6% when the channel length is increased from 2m to 3.5m. With the heat transfer area set by the hot side the cold side convective heat transfer coefficient is determined by

$$h_c = \frac{(hA)_c}{A}$$

and the Nusselt number on the cold side is found (independent of WHRU length as well). With the Nusselt number and the heat transfer area set by the hot side, the cold side channel diameter is determined. For a $(hA)_h/UA$ value of 1.4 the cold side channel diameter is found to be 0.8mm.

WHRU Volume   The volume of the WHRU equals

$$V = HWL$$

where L is the length and H is the height in meter and calculated by

$$H = N_H \left[D_h + D_c + w_H \right]$$

where w_H is the wall thickness in the vertical direction.
The width, W, is calculated by

$$W = \sqrt{2\#} \left[D_h + w_W \right] = N_{W,h} \left[D_h + w_W \right]$$

or; number of channels in a horizontal row times the size of a channel diameter/wall thickness pair.
An overview of the terms constituting the volume equation reveals that the only independent variables for a given $(hA)_h/UA$ value is the hot side channel diameter, D_h, and channel length, L, remembering that the total number of channels on the hot side is dependent only on the same two variables. 3D plots can then be made for a given $(hA)_h/UA$ value. The plot for $(hA)_h/UA = 1.4$ is shown in Figure 37 where $w_H = w_W = 1mm$
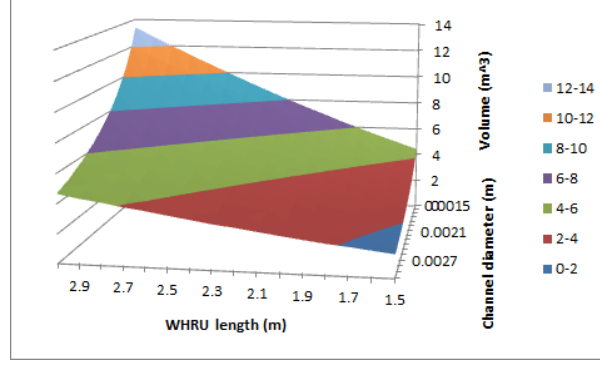
Figure 37: WHRU volume by variation in hot side channel diameter and channel length for $(hA)_h/\mathrm{UA} = 1.4$

There is a clear linear dependency on the volume by the variation in length. Further inspection show that the total volume decreases with a decrease in length and increase in hot side channel diameter. An important fact is the restriction in the hot side channel diameter (at a specific length) given by the set heat transfer area, e.g. for a length of 2m the channel diameter cannot be larger than 1.8mm and for a length of 3m the channel diameter is restricted to 2.6mm. Thus, the variation in length and channel diameter is potentially prone to optimization at the set heat transfer area. With reference to eq. (3.11) the heat transfer area can be written as

$$A(L,\ D_H) = L D_H \sqrt{2\#_h}(\sqrt{2\#_h} - 1) \approx L D_H 2\#_h \tag{3.15}$$

remembering $\#_h$ being a function of length and hot side channel diameter. Equation (3.15) needs iteration to be solved and the procedure is shown in the appendix. The result is shown in Figure 38.
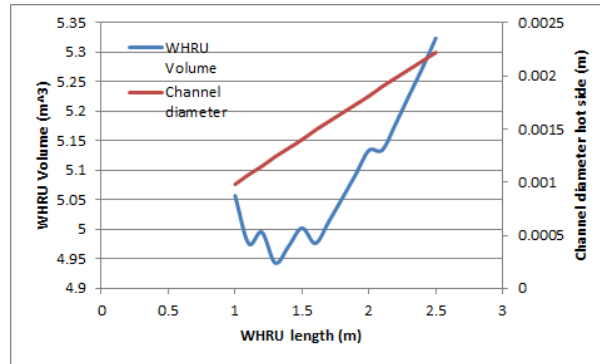
Figure 38: WHRU volume by variation in hot side channel diameter and channel length for $(hA)_h/\mathrm{UA} = 1.4$

The numeric results should be taken lightly as the calculations are done with constant properties, although the procedure leading up to the result will be the same for different cycle parameters (fluid type, mass flow, heat load, etc.). Figure 38 is dependent on two parameters (in addition to w_H and w_W) and that is the pressure drop restriction

50

in the heat exchanger and the $(hA)_h$/UA- value. The pressure drop is assumed it could be optimized with respect to combined power output (Brayton + Rankine cycle) and the required $(hA)_h$/UA-value could be found with better knowledge of the working fluid properties. Thus, with these 2 values optimized (Δp and Volume) the total combined cycle will be optimized regarding both power and WHRU size.

4 Evaluation of single versus modular based expander setup

Electrical power consumption offshore could vary at a great extent and the gas turbine load need to vary accordingly. This variation will in turn influence the heat source load on the Rankine cycle. If the gas turbine is regulated by IGV, thus leaving the exhaust temperature constant (as discussed in section 2.7.3) the Rankine cycle will compensate by varying the mass flow of the working fluid accordingly, thus maintaining the specific properties throughout the cycle constant. As the efficiency of an expander varies with flowrate it will become inefficient as the flowrate moves away from the optimal flowrate (see Figure 39). It could therefore be productive to utilize two expanders (instead of one), with smaller power output, but could operate with a flowrate closer to each respective optimal flowrate. Calculations has been conducted with single expander of 8 MW as a reference. For a modular set-up to be an option it has to perform better than the reference.

4.1 Calculation setup

Expander data are hard to obtain due to corporate secrecy and most data from the literature are of a "typical" order which do not specify all important parameters. Consequently, these calculations are unfortunately based on the efficiency curve for a "typical" 6 MW expander provided by an operator, Figure 39.
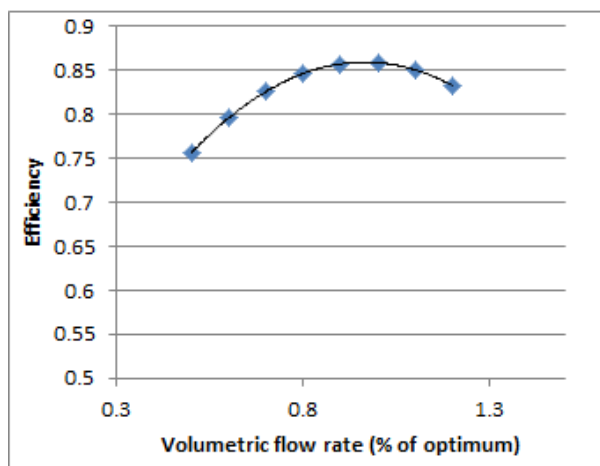
Figure 39: Efficiency vs Volumetric flow rate (VFR) for a typical 6 MW expander

With the 6 MW expander as a reference similar graphs has been made by a linear

increase/decrease in efficiency for the range of 1 to 8 MW (Figure 40). The linear scaling coefficient used are from a graph by Marcuccilli, [41].
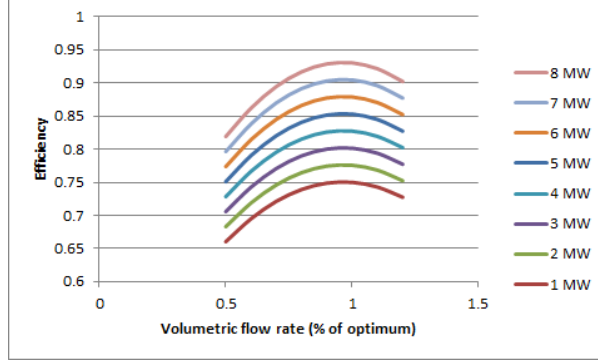
Figure 40: Efficiency vs Volumetric flow rate (VFR) for an expander range from 1 to 8 MW measured at a percent of optimum for each expander

Note: The calculations are based on these calculated efficiencies as a rough estimate until more reliable values are gathered. The proceeding calculations are not dependent on exact values but to get reliable output the efficiency values has to be substituted.

4.2 Program

Calculations are conducted in Microsoft Excel with the use of Visual Basic for Applications. Input values (expander efficiency vs VFR for a specified power output) are directly entered in the Excel Worksheet and calculates two parameters used in the VBA program. The first one is the optimum volumetric flow rate (VREOPT)

$$VRExOPT = \frac{P_E}{P_R}$$

where P_E and P_R are the power at optimum VFR for a modular expander and the reference expander respectively. $VRE1OPT$ show the optimum VFR for Expander 1 relative to the optimum VFR for the reference which is normalized to be 1, i.e. $0 < VRE1OPT \leq 1$. The second parameter is the sizing factor k which is defined as

$$k_x = \frac{N_x}{N_{Rx}} \tag{4.1}$$

which is the ratio of the efficiency of one of the modular expanders to the efficiency of the reference expander at a certain normalized VFR, (x). As the efficiency chart used here (Figure 40) is created with a linear scaling the k-value will be constant throughout the whole VFR range. When all these values from the test range of expanders are included in the calculation sheet a VBA macro calculates the result which can be graphed as seen in Figure 41.

Due to the unreliable input data conclusions are difficult to make. If the created efficiency graphs are assumed to be correct, Figure 41 show increased power output only for a modular set-up with a 8 MW expander plus any expander from the set range.
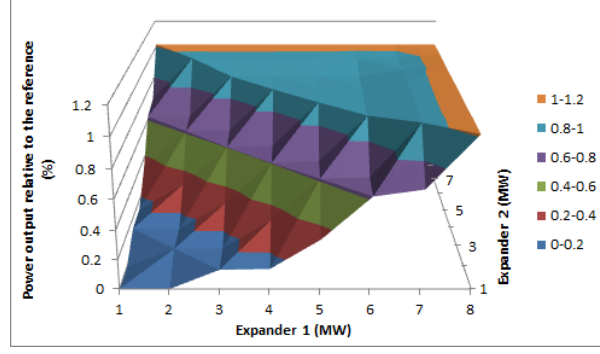
Figure 41: Calculated power from a modular setup (2 expanders) with respect to a reference case (8 MW expander)

The reason for the relative power output being constant (the "plateau") for the no. 1 expander throughout a certain range of no. 2 expanders is that the first expander are running at optimum efficiency and the 2nd one is shut-down, i.e. there is no further reward in subtracting mass flow from the 1st expander (and divert it from the optimum point) to operate the 2nd expander. If the VFR for the 2nd expander is above or below the operating range of $0.5 < VFR < 1.2$, it is shut-down.

4.3 Analytical model

The reference case is described by

$$W'_R = VFR_R * N_R$$

where W'_R is the "specific" reference work output, i.e. divided by density and enthalpy drop which is assumed to be the same for the reference case and all modular configurations regarding the states on both inlet and outlet to be constant. VFR_R and N_R are the reference volumetric flow rate and efficiency respectively. The same goes for Expander 1

$$W'_{E1} = VFR_{E1} * N_{E1}$$

and Expander 2

$$W'_{E2} = VFR_{E2} * N_{E2}$$

By summing these two we get the modular work output, W'_M

$$
\begin{aligned}
W'_M &= W'_{E1} + W'_{E2} = VFR_{E1}N_{E1} + VFR_{E2}N_{E2} \\
&= xVFR_R * k_1N_R + (1-x)VFR_R * k_2N_R = W'_R[xk_1 + (1-x)k_2] \quad (4.2)
\end{aligned}
$$

The second equation is balanced by the use of eq. (4.1) and $x = VFR_{E1}/VFR_R$ which leaves $(1-x) = VFR_{E2}/VFR_R$. The last expression on the right side of eq. (4.2) shows that if a modular set-up to be a viable option it has to reach the following criteria.

$$xk_1 + (1-x)k_2 > 1$$

4.4 VBA Macro

The VBA macro consist of 3 "Sub" procedures called *REFERENCE*, *MODULAR* and *CalcAll.*

REFERENCE

This procedure calculates the expander load variation (which is not known at this point, thus randomly generated) throughout a year in cycles of 8 hours. The load is either 50%, 80%, 100% or 120% VFR. Given the load variation the reference expander output is calculated for each load cycle throughout the year.

MODULAR

The *MODULAR* procedure is the main part of the calculations. For a set expander configuration (e.g. expander1 = 5MW, expander2 = 4MW) it goes through the overall load variation from 50% to 120% in steps of 5% to find the best load combination of the two expanders for optimum power output at each step. The best output at 50%, 80%, 100% and 120% is then tabulated together with the corresponding load variation and reference output.

The best load combination is found by first going through the allowable load range (50% to 120%) of the 1st expander with the highest rated power and calculate the relative VFR (e.g. an expander of 6 MW running at 100% consumes 75% of the total flow rate) which again is used to find the remaining VFR to the 2nd expander at each point in the range. If the VFR for the 2nd expander is below 50% or above 120% it is shut-off, if it is between 50% to 120% it is added to the first expander power output. The procedure then finds the best value for the specific overall load and stores it. All the result from the variation in load and VFR in the different expanders are stored in the "calculations" sheet. An example is shown in Figure 42.

VR	VE1	VE2	Power
1	0.5	1.250	
1	0.55	1.175	0.795
1	0.6	1.100	0.809
1	0.65	1.025	0.819
1	0.7	0.950	0.827
1	0.75	0.875	0.832
1	0.8	0.800	0.834
1	0.85	0.725	0.834
1	0.9	0.650	0.833
1	0.95	0.575	0.830
1	1	0.500	0.826
1	1.05	0.425	
1	1.1	0.350	
1	1.15	0.275	
1	1.2	0.200	
		BEST	0.834

Figure 42: Example from the "calculations" sheet with a 6 and a 4 MW expander at 100% load

As the 1st expander (in this example, 6 MW) VFR varies, the according power output is shown in the right column. The brown color means that the specified VFR for the 1st expander is not within ±5% of the relative load and cannot be used at that point. The

red color means that the 2nd expander is out of range and shut-down.

CalcAll The procedure simply goes through all the different configurations (64 in total) by automatically setting the different expander ratings and calling *MODULAR*. The final results are stored in the "results" sheet.

5 Conclusion

Cycle comparison

Results concerning energy transfers are summarized in Table 7 and Figure 31. By the restrictions implemented on each cycle to investigate them on "equal ground" (single pressure expansion, fixed approach temperature and condensation temperature (state 1), same heat source/heat sink), the different cycles can be evaluated.

Heat absorption in the WHRU is dependent on how low the WHRU and working fluid in combination can bring the exhaust temperature at the outlet of the heat exchanger. CO_2 has clearly the best ability to absorb heat, while water has the lowest. This is due to the "choking" of heat transfer at the pinch point of water. CO_2 does not inherit this heat transfer restriction and could therefore absorb more heat. Both toluene cycles got this pinch point, although to a lesser degree. They transfer approximately the same amount of heat to the cycle.

The pinch point contributes negatively to the exergy transfer in the heat exchanger as well, since it affects the temperature matching of the fluids during heat transfer. Although CO_2 does not have a pinch point in the conventional sense the exergy destuction in the WHRU for CO_2 is twice as high as for the toluene cycles. The cause being the c_p-peak (shown in Figure 29) which inhibits the temperature matching. A solution could be to increase the condensation temperature, up to say 150°C, this way the cycle does not encompass the jump in c_p and CO_2 will have a very good temperature match with the exhaust gases, of the expense of total heat absorption. This cycle would be completely in the gaseous phase (with close resemblance to the Brayton cycle), thus compressor work would increase substantial and power output is assumed to be lower than the "condensing-cycle".

Although the steam cycle has the least heat absorbed and the highest rate of exergy loss in the WHRU, it produces the highest amount of overall power output. This is due to the high enthalpy drop during expansion which yield two features; decreased load on the condenser and a lower temperature at the outlet of the expander (close to the condensation temperature). Both of these affects the exergy loss in the condenser, see eq. (3.6). If seen in context of maximum power output, this promotes the use of a steam cycle. Additional positive properties is the low mass flowrate for water (11.46 kg/s vs 65.21 kg/s for CO_2), low pressure (6 MPa vs 15 MPa for CO_2) and the assumption of water probably requiring a smaller WHRU. The latter assumption is made by the fact that water has a lower heat load on the WHRU (39 MW vs 49 MW). Which one of the fluids has the highest heat transfer coefficient is yet to be determined (a model with variable properties is needed) although the trend is higher thermal conductivity for water and lower viscosity for CO_2 while the densities are harder to separate. Both higher thermal conductivity and low viscosity (higher Reynolds number) promotes heat transfer, so a more thoroughly analysis has to be made. The high enthalpy drop during expansion in the steam cycle requires several expansion stages in the expander to maintain the efficiency. This means added equipment size and cost.

If a CHP cycle is employed the high heat loads and temperatures at the condenser inlet of the organic cycles could be utilized for e.g. regeneration, process heating or utilize the gas turbine augmentations mentioned in section 2.7.4, thus increasing the thermal

efficiency. This can be applied to the steam cycle as well, although to a lesser extent, since the exhaust gases leaving the WHRU has a temperature of $\approx 150°$C.

The toluene cycles show promising results, especially the supercritical cycle. Compared to CO_2 the supercritical toluene cycle deliver more power at lower heat load on the WHRU, meaning with an assumed smaller heat exchanger. The reason for this is the good temperature matching with the heat source which consequently increases the exergy transfer to the cycle, together with a relatively large enthalpy drop during expansion which decreases the heat load on the condenser. Due to high temperature at the expander outlet the supercritical toluene cycle is prone to modifications that could result in a higher power output than the steam cycle. If a CHP cycle could be applied both toluene cycles would be fitting due to the highest exergy delivered to the working fluid after heat transfer amongst the 4 cycles.

WHRU parameters

Tangible conclusions will not be presented as calculations has been conducted with constant properties on the working fluid side of the heat exchanger, although a calculation procedure has been created for the steam cycle previously investigated. The WHRU load used as example is set by the same gas turbine exhaust heat used in the cycle comparison. A pressure drop criteria is set on the WHRU which puts restrictions on channel length, channel diameter and number of channels, e.g. the number of channels becomes a function of channel diameter and length.

The states on all inlets/outlets on the heat exchanger is known and a needed UA-value for the WHRU can be found. By setting the $(hA)_h/UA$-fraction both heat transfer conductances is available. Since the heat transfer area is dependent on both channel diameter and length, but the conductive heat transfer coefficient is dependent only on channel diameter (a weak dependency on length) it forces the heat exchanger area to be constant for a given required heat transfer conductance on the hot side. At this specific heat transfer area an optimum channel diameter (due to the pressure drop restriction) can be found at a given channel length, i.e. the total volume becomes dependent on channel length only. These two values together with the cold side channel diameter (found to be 0.8mm with constant properties, independent of channel length) and wall thicknesses, constitutes the WHRU volume. By plotting the volume versus channel length, Figure 38 is created. It shows an optimum volume at approximately $5m^3$ with a length of 1.3m.

The values for pressure drop and $(hA)_h/UA$-fraction is "arbitrary"-chosen but it is assumed that an optimized pressure drop could be found regarding maximum combined power output and the $(hA)_h/UA$-fraction would be set by a better model of the cold side parameters, thus finding better values for the cold side heat transfer conductance and channel diameter.

Expander module analysis

Conclusions can not be made considering the low reliability in input values. An analytical model and an Excel based program is created which can produce reliable results as long as reliable values are used as inputs. Figure 41 shows how the results are plotted. Expander values used here are "manufactured" based on information from a 6 MW

expander together with a linear "sizing-factor" [41]

Suggestions for further work

This project cover a wide span of engineering subjects and due to the generalization, each subject are not covered as thoroughly as it could have been. By doing investigations concerning the overall system, several important subjects that need analysis gets revealed. Some of them are in close context with the limitations mentioned at the beginning of this thesis.

Working fluid for high temperature heat recovery. A more thoroughly investigation on applicable working fluids wrt safety measures, pressure levels, cost/availability, temperature matching in the WHRU, effect on expander efficiency, etc. Focus probably on natural working fluids (water, ammonia, CO_2, hydrocarbons) to screen out a few possible fluids and their range of application. It reduces the workload when doing investigations on the overall cycle drastically if the choice of a relevant working fluid can be reduced to one or two possibilities.

Effect of gas turbine regulation/variation on optimum pressure drop in the WHRU. Increasing the pressure drop on the hot side of the WHRU enhances heat transfer although the effective back pressure on the gas turbine increases as well, thus reducing the gas turbine efficiency. A comparison regarding combined power output of these two effects could be investigated to see if an optimal point could be found.

OTSG versus compact heat exchangers. This thesis chose compact heat exchangers while an OTSG (or general HRSG) could be applied as well. An introduction has been presented but calculations has not been conducted. An OTSG has lower pressure drop on the exhaust side but assumed lower heat transfer abilities, thus increased equipment size. The aforementioned point should be implemented because it is assumed that a compact heat exchanger affects the gas turbine power output more than an OTSG.

Heat exchanger analysis with variable properties on the working fluid side. A method to define the fluid properties at small increments along the heat transfer length is necessary to produce reliable results. Certain fluid properties for several relevant fluids were not defined in REFPROP, thus restricting the range of possible fluids to investigate. A model to retrieve these properties would be useful.

Regeneration or modular cycles As the working fluid temperature after expansion for high temperature organic cycles is still relatively high (≈ 350°C) regenerative cycle could be applied, or further power output could possibly be obtained by adding another Rankine cycle which utilizes the exergy content in the working fluid of the primary Rankine cycle, between the expander outlet and condensation point. Added machinery and complexity counts negatively in this case.

References

[1] I.K. Smith. Development of the trilateral flash cycle system: Part 1: Fundamental considerations. *Proceedings of the Institution of Mechanical Engineers, Part A: Journal of Power and Energy*, 1993.

[2] Statistisk sentralbyrå. Kraftig oppgang i klimagassutslippene. `http://www.ssb.no/emner/01/04/10/klimagassn/`, May 2011.

[3] Jon Ødegård Hansen, Signe Berg Verlo, and Evy Zenker. Fakta - norsk petroleumsverksemd 2011. `http://www.npd.no/Publikasjoner/Faktahefter/Fakta-2011/`, 2011.

[4] P. Kloster. Energy optimalization on offshore installations with emphasis on offshore combined cycle plants. *1999 Offshore Europe conference*, 1999.

[5] NVE/OD. Kraft fra land til norsk sokkel. `http://www.npd.no/Global/Norsk/3%20-%20Publikasjoner/Rapporter/PDF/Kraft%20fra%20land%20rapport.pdf`, 2007.

[6] Kumar Rayaprolu. *Boilers for power and process*. CRC Press 2009, 2009. Chap 14.

[7] V. Dolz, R. Novella, A. Garcia, and J. Sanchez. Heavy duty diesel engine equipped with a bottoming rankine cycle as a waste heat recovery system. part 1: Study and analysis of the waste heat energy. *Applied Thermal Engineering*, 36, 2011.

[8] J.R. Serrano, V. Dolz, R. Novella, and A. Garca. Hd diesel engine equipped with a bottoming rankine cycle as a waste heat recovery system. part 2: Evaluation of alternative solutions. *Applied Thermal Engineering*, 36, 2011.

[9] MingShan Wei, JinLi Fang, ChaoChen Ma, and Syed Noman Danish. Waste heat recovery from heavy-duty diesel engine exhaust gases by medium temperature orc system. *Science China - technological Sciences*, 54, 2011.

[10] Iacopo Vaja and Agostino Gambarotta. Internal combustion engine (ice) bottoming with organic rankine cycles (orcs). *Energy*, 35, 2009.

[11] Paola Bombarda, Costante M. Invernizzi, and Claudio Pietra. Heat recovery from diesel engines: A thermodynamic comparison between kalina and orc cycles. *Applied Thermal Engineering*, 30, 2009.

[12] Frank Kreith. *CRC Handbook of Thermal Engineering*. CRC Press 2000, 2000. Chap 1.

[13] Y. Ust, G. Gonca, and H. K. Kayadelen. Determination of optimum reheat pressures for single and double reheat irreversible rankine cycle. *Journal of the Energy Institute*, 84, 2011.

[14] A. Ganapathy. *Industrial Boilers and Heat Recovery Steam Generators: Design, Applications, and Calculations*. Marcel Dekker, Inc, 2003.

[15] T.J. Marciniak, J.L. Krazinski, J.C. Bratis, H.M. Bushby, and E.H. Buycot. Comparison of rankine-cycle power systems: effects of seven working fluids. 1981.

[16] T.C. Hung, T.Y. Shai, and S.K. Wang. A review of organic rankine cycles (orcs) for the recovery of low-grade waste heat. 1996.

[17] Huijuan Chen, D. Yogi Goswami, and Elias K. Stefanakos. A review of thermodynamic cycles and working fluids for the conversion of low-grade heat. *Renewable and sustainable energy reviews*, 14, 2010.

[18] T.C. Hung. Waste heat recovery of organic rankine cycle using dry fluids. *Energy conversion and management*, 42, 2001.

[19] Harald Taxt Walnum, Yves Ladam, Petter Nekså, and Trond Andresen. Off-design operation of orc and co2 power production cycles for lower temperature surplus heat recovery. *9th International conference on sustainable energy technologies; Shanghai, China*, 2010.

[20] G. Schmidt, P. Schmid, H. Zewen, and S. Moustafa. Development of a point focusing collector farm system. *Solar Energy*, 31, 1993.

[21] Bertrand F. Tchanche, Gr. Lambrinos, A. Frangoudakis, and G. Papadakis. Low-grade heat conversion into power using organic rankine cycles a review of various applications. *Renewable and Sustainable Energy Reviews*, 15, 2011.

[22] Tony Ho, Samuel S. Mao, and Ralph Greif. Comparison of the organic flash cycle (ofc) to other advanced vapor cycles for intermediate and high temperature waste heat reclamation and solar thermal energy. *Energy*, 40, 2012.

[23] Åge Guddingsmo. Test of organic rankine cycle with rolling piston ekspander, 2004.

[24] Ian K. Smith, Nicolay Stosic, and Ahmed Kovalevic. Power recovery from low cost two-phase expanders. `http://www.staff.city.ac.uk/~ra601/exp.pdf`.

[25] O. Badr, P.W. O'Callaghan, M. Hussein, and S.D. Probert. Multi-vane expanders as prime movers for low-grade energy organic rankine cycle engines. *Applied energy*, 16, 1984.

[26] Herbert A. Ingley, D. Yogi Goswami, and Robert Reed. Optimalization of a scroll expander applied to an ammonia/water combined cycle system for hydrogen production. *Energy*, 36(1645), 2004.

[27] James A. Mathias, Jr Jon R. Johnston, Jiming Cao, Douglas K. Priedeman, and Richard N. Christensen. Experimental testing of gerotor and scroll expanders used in, an energetic and exergetic modeling of, an organic rankine cycle. *Journal of Energy Resources Technology*, 131, 2009.

[28] Jan F. Kreider. *Medium and high pressure solar processes*. Academic Press, inc, 24 Oval Road, London NW1 7DX, 1st edition, 1979.

[29] O.E. Balje. A study on design criteria and matching of turbomachines: part a - similarity relations and design criteria of turbines. *ASME*, 1962.

[30] H.I.H. Saravanamuttoo, P. Straznicky, H. Cohen, and G. Rogers. *Gas Turbine Theory*. Pearson Education Limited, Edinburgh Gate, Harlow, Essex, England, 6th edition, 2009.

[31] J.M. Munoz de Escalona, D. Sanchez, R. Chacartegui, and T. Sanchez. Part-load analysis of gas turbine & orc combined cycles. *Applied Thermal Engineering*, 131, 2011.

[32] Ronald L. Klaus. *Encyclopedia of Energy Engineering and Technology - 3 Volume Set*. CRC Press 2007, 2007. Chapter 181 Water-Augmented Gas Turbine Power Cycles.

[33] International Power Technology. `http://intpower.com/`, April 2012.

[34] T.M. Adams, S.I. Abdel-Khalik, S.M. Jeter, and Z.H. Qureshi. An experimental investigation of single-phase forced convection in microchannels. *International Journal of Heat Mass Transfer*, 41, 1997.

[35] W. Peiyi and W.A. Little. Measurement of friction factors for the flow of gases in very fine channels used for microminiature joule-thomson refrigerators. *Cryogenics*, 23, 1982.

[36] F.P. Incropera, D.P. DeWitt, T.L. Bergman, and A.S. Lavine. *Fundamentals of Heat and Mass Transfer*. John Wiley & Sons, Inc., 111 River Street, Hoboken, NJ, 6th edition, 2007.

[37] A. Bejan. *Advanced engineering thermodynamics*. John Wiley & Sons, Inc., 2nd edition, 1997.

[38] Alireza Bahadori and Hari B. Vuthaluru. A method for estimation of recoverable heat from blowdown systems during steam generation. *Energy*, 35, 2010.

[39] Frank Gabrielli and Horst Schwevers. Design factors and water chemistry practices - supercritical power cycles. *Chemical Engineering*, 2008.

[40] J.R. Thome, V. Dupont, and A.M. Jacobi. Heat transfer model for evaporation in microchannels. part 1: presentation of the model. *International Journal of Heat and Mass Transfer*, 47, 2004.

[41] Frederic Marcuccilli and Samuel Zouaghi. Radial inflow turbines for kalina and organic rankine cycles. *Proceedings European Geothermal Congress 2007*, 2007.

Appendices

A Constant cold side Reynolds number

The Reynolds number becomes a constant (independent of channel diameter D_c) at a given WHRU length.

Requirement: geometry (heat exchange area, width (W'), height (N_c)) is set by the hot side of the heat exchanger and constant fluid properties. The Reynolds number for a circular channel is defined as

$$Re = \frac{4\dot{m}_c}{\pi D_c \mu}$$

The mass flowrate through one channel is

$$\dot{m}_c = \frac{\dot{m}}{\#_c} = \frac{\dot{m} D_c}{W' N_c}$$

where W'/D_c is the number of channels in one row ("plate").

By assembling these two equations the Reynolds number becomes a function of constants only (given the above assumptions).

$$Re = \frac{4\dot{m}}{\pi W' N_c \mu}$$

B Excel tables

B.1 Preliminary analysis

Fluid	water	toluene	co2	
PL	0.002339	0.002919	5.729053	MPa
s1	0.296483	-0.49326	1.187731	kJ/kg-K
s_L, sat gas	8.665984	0.925156	1.706226	kJ/kg-K
Pcrit	22.064	4.1263	7.3773	MPa
Tcrit	373.946	318.6	30.9782	°C

Table 1: Cycle parameters defined by environmental values

	Condensing water		GT exhaust	
Temperature	10		549	°C
ΔT	10		10	°C
T_1	20	T_3	539	°C

Table 2: Environmental values and set temperature differences

A

Pressure	1	2	3	4	5	6	7
Water efficiency	0.362013	0.387792	0.402496	0.412673	0.42037	0.4265	0.431547
Toluene efficiency	0.26834	0.295312	0.310281	0.320444	0.328017	0.33397	0.338817
CO2 efficiency	-0.35925	-0.20879	-0.12584	-0.06897	-0.02588	0.008695	0.037164
Water vapor fraction isentropic	0.905052	0.865776	0.84235	0.825403	0.812001	0.800834	0.791205
$\eta_{is} = 0.9$ vapor fraction	0.956388	0.920653	0.899178	0.883529	0.871066	0.86061	0.851533
$\eta_{is} = 0.8$ vapor fraction	1.007725	0.97553	0.956005	0.941655	0.930131	0.920386	0.911862
8	9	10	11	12	13	14	15
0.435802	0.439449	0.442618	0.445397	0.447854	0.450038	0.45199	0.45374
0.342861	0.346293	0.349247	0.351816	0.354069	0.356058	0.357825	0.359407
0.061157	0.081808	0.099873	0.115883	0.130225	0.143186	0.154988	0.165803
0.782698	0.775043	0.768057	0.76161	0.755603	0.749965	0.744638	0.739575
0.843461	0.836152	0.82944	0.823207	0.817367	0.811852	0.806612	0.801607
0.904225	0.897261	0.890822	0.884804	0.87913	0.873739	0.868587	0.863638

Table 3: Table showing the calculated efficiencies at different pressures. Below the efficiencies the vapor fraction at the same pressure range are calculated for water with 3 different expander efficiencies

Table 4 see end of Appendices

B.2 Cycle

Working fluid			water	CO_2	subcritical toluene	supercritical toluene
State 1 - Pump inlet						
Temperature	°C		20	20	20	20
Pressure	Mpa		0.002339318	5.729053	0.002918943	0.002918943
Entropy	kJ/kg-K		0.296483337	1.187731	-0.49326357	-0.49326357
Enthalpy	kJ/kg		83.91414483	255.8685	-166.706855	-166.706855
Work lost	kW		16.58352925	173.6344	29.87132677	135.8530769
State 2 - WHRU inlet						
Temperature	°C		20.44922538	34.13579	21.3437493	25.660823
Pressure	Mpa		6	15	3.5	15
Entropy	kJ/kg-K		0.301595938	1.197136	-0.48983914	-0.47879546
Enthalpy	kJ/kg		91.41482075	270.2906	-161.669609	-145.183085
State 3 - Expander inlet						
Temperature	°C		539	539	539	539
Pressure	Mpa		6	15	3.5	15
Entropy	kJ/kg-K		6.999063664	2.784966	2.115854171	1.895477581
Enthalpy	kJ/kg		3515.390105	1025.367	1230.740679	1138.44959
Work lost	kW		1958.673942	717.3456	683.699064	959.8549314
State 4 - Condenser inlet						
Temperature	°C		86.98686919	439.5498	438.8883363	381.1553124
Pressure	Mpa		0.052339318	5.779053	0.052918943	0.052918943
Entropy	kJ/kg-K		7.602910919	2.823819	2.194232966	1.997700395
Enthalpy			2656.223922	916.4428	1011.157613	876.922152
vapor fraction	-		1.000708733			
Temperature difference	°C		76.98686919	429.5498	428.8883363	371.1553124
Enthalpy drop	kJ/kg		859.1661825	108.9244	219.5830659	261.5274375
Work lost heat transfer	kW		3388.238261	10258.1	11830.95762	9828.545602
Cycle properties						
Massflow	kg/s		11.45602155	65.20832	30.80811811	33.16320854
Heat input	kW		39225.13463	49237.27	42897.54061	42569.37808
Condenser out	kW		29468.43624	43074.94	36287.78764	34610.08639
Pump work	kW		85.92790488	940.4409	155.1880551	713.7972573
Work output	kW		9842.626299	7102.777	6764.94103	8673.08895
Efficiency	-		0.250926514	0.144256	0.157699974	0.203740091
Exergy transfer and destruction in WHRU (Directly copied from "heat input and mass flow")						
Exergy lost in WHRU	kW		5617.157682	4844.283	2629.235333	2217.051409
Exergy transfer via heat transfer	kW		20823.27971	23096.14	21938.70437	21814.39397
% of exergy lost vs. exergy transferred	-		26.98 %	20.97 %	11.98 %	10.16 %

Table 5: Cycle state points and energy/exergy transfers

Component exergy losses (kW)

	water	CO_2	toluene subcritical	toluene supercritical
Pump	16.58	173.63	29.87	135.85
Expander	1958.67	717.35	683.70	959.85
Condenser	3388.24	10258.10	11830.96	9828.55
WHRU	5617.16	4844.28	2629.24	2217.05
Work output	9842.63	7102.78	6764.94	8673.09
Exergy transfer	20823.28	23096.14	21938.70	21814.39

Table 6: Component exergy losses, exergy transfer and work output

B.3 Heat input and mass flow

Table 7 see end of Appendices

	water	Unit
"Tsat"	275.585	°C
q to PP	26365.66	kW
$\dot{m}$	11.45602	kg/s
q rest	12859.48	kW
sum q	39225.13	kW
hout exhaust	425.2389	kJ/kg
Temperature exhaust exit	150.4235	°C

Table 8: Sample of values calculated from Table 7 (for water)

B.4 WHRU hot side

Table 9 see end of Appendices

B.5 Reduction of variables

D	#	m/tube	Re	Nu	h	Width	"height"	Am^2	hA
0.001	1107000	8.4E-05	3601.102	12.23163	530.8951	1.48	1487	3318.876	1761975
0.0011	849000	0.00011	4268.573	14.46035	570.5721	1.43	1302	2799.392	1597255
0.0012	666000	0.00014	4988.013	16.71067	604.4176	1.38	1153	2395.267	1447741
0.0013	534000	0.000174	5742.466	18.9434	632.4687	1.34	1032	2079.696	1315343
0.0014	435000	0.000214	6545.845	21.20997	657.5615	1.30	932	1825.555	1200414
0.0015	360000	0.000258	7382.259	23.47277	679.1997	1.27	848	1618.992	1099619
0.0016	301000	0.000309	8277.45	25.80538	700.0266	1.24	775	1443.149	1010243
0.0017	255000	0.000365	9195.894	28.11906	717.9202	1.21	713	1298.419	932161.1
0.0018	218000	0.000427	10159.07	30.4726	734.7868	1.18	659	1174.877	863284.1
0.0019	188000	0.000495	11160.19	32.85138	750.4545	1.16	612	1069.523	802628.5
0.002	164000	0.000567	12153.72	35.15334	762.8882	1.14	572	982.7752	749747.6
0.0021	143000	0.00065	13274.79	37.68951	778.9787	1.12	534	899.5697	700745.6
0.0022	126000	0.000738	14381.02	40.1361	791.839	1.10	501	829.95	657186.8
0.0023	112000	0.00083	15475.23	42.50761	802.1641	1.08	472	770.6995	618227.5
0.0024	100000	0.00093	16610.08	44.92162	812.3974	1.07	446	718.0461	583338.8
0.0025	89000	0.001045	17916.49	47.64899	827.2525	1.05	421	666.0754	551012.5
0.0026	80000	0.001163	19165.48	50.20998	838.1873	1.04	399	622.44	521721.3
0.0027	72000	0.001292	20506.28	52.91354	850.6039	1.02	378	580.9357	494146.2
0.0028	66000	0.001409	21571.54	55.03066	853.0432	1.01	362	552.3888	471211.5
0.0029	60000	0.00155	22910.46	57.65608	862.9219	1.00	345	519.875	448611.6
0.003	55000	0.001691	24160.12	60.0734	869.1312	0.99	331	494.0113	429360.6

Table 10: WHRU heat transfer parameters at given length

From "WHRU hot side"				Multiplication factor	
				1.4	
Tg, out	q	UA	(hA)_h,needed	(hA)_c, required	
40	48226.43	3428284	4799598	11998996	
50	47295.45	2663475	3728865	9322162	
60	46367.9	2195719	3074006	7685015	
70	45443.58	1872765	2621871	6554679	
80	44522.29	1633113	2286358	5715894	
90	43603.83	1446498	2025097	5062743	
100	42687.94	1296070	1814499	4536247	
110	41774.39	1171609	1640252	4100630	
120	40862.91	1066508	1493111	3732778	
130	39953.22	976287.8	1366803	3417007	
140	39045.05	897789.1	1256905	3142262	
150	38138.09	828712.8	1160198	2900495	

Table 11: Calculation of the required (hA) values for given exhaust temperature at WHRU outlet

Table 12 and 13 see end of Appendices

L	1	1.1	1.2	1.3	1.4	1.5	1.6	1.7
D	0.00098	0.00107	0.00115	0.00124	0.00132	0.0014	0.00149	0.00157
Volume	5.057013	4.976282	4.995304	4.942971	4.971668	5.002373	4.976393	5.013173
	1.8	1.9	2	2.1	2.2	2.3	2.4	2.5
	0.00165	0.00173	0.00181	0.0019	0.00198	0.00206	0.00214	0.00222
	5.052276	5.092533	5.133808	5.134419	5.178789	5.226587	5.273323	5.323803

Table 14: Optimum hot side channel diameter at given lengths together with calculated WHRU volume at these parameters

C Excel Macros

C.1 Tavg

Tavg - Used in "Preliminary analysis" and "WHRU cold side" to obtain average temperatures at constant pressure.

Function Tavg(fluid, p, s1, s2, N)

Dim Ds, T, sn, i, Ttot

Ds = (s2 - s1) / N
Ttot = 0

For i = 0 To N
sn = s1 + Ds * i
T = refprop8.temperature(fluid, "ps", "C", p, sn)
Ttot = Ttot + T
Next i

Tavg = Ttot / (N + 1)

End Function

C.2 Average functions

Functions used in "WHRU cold side" to get a reasonable estimate of the working fluid properties during heat transfer in the WHRU.

C.2.1 Viscosity, water

Function Viscavgwater(fluid, p, s1, s2, N)

Dim Ds1, Ds2, Visc1, Visc2, sn1, sn2, i, Visctot1, Visctot2, sliq, svap, vliq, vvap, v2pavg

sliq = refprop8.Entropy(fluid, "pliq", "c", p)
svap = refprop8.Entropy(fluid, "pvap", "c", p)
vliq = refprop8.viscosity(fluid, "pliq", "c", p)
vvap = refprop8.viscosity(fluid, "pvap", "c", p)
v2pavg = (vliq + vvap) / 2

Ds1 = (sliq - s1) / N
Ds2 = (s2 - svap) / N
Visctot1 = 0
Visctot2 = 0
For i = 0 To N
sn1 = s1 + Ds1 * i
sn2 = svap + Ds2 * i
Visc1 = refprop8.viscosity(fluid, "ps", "C", p, sn1)
Visc2 = refprop8.viscosity(fluid, "ps", "c", p, sn2)
Visctot1 = Visctot1 + Visc1
Visctot2 = Visctot2 + Visc2
Next i

Viscavgwater = ((Visctot1 + Visctot2) / (N + 1) + v2pavg) / 3

End Function

C.2.2 Prandtl number, water

Function Prandtlwater(fluid, p, s1, s2, N)

Dim Ds1, Ds2, Pr1, Pr2, sn1, sn2, i, Prtot1, Prtot2, sliq, svap, prliq, prvap, pr2pavg

sliq = refprop8.Entropy(fluid, "pliq", "c", p)
svap = refprop8.Entropy(fluid, "pvap", "c", p)
prliq = refprop8.prandtl(fluid, "pliq", "c", p)
prvap = refprop8.prandtl(fluid, "pvap", "c", p)
pr2pavg = (prliq + prvap) / 2

Ds1 = (sliq - s1) / N
Ds2 = (s2 - svap) / N
Prtot1 = 0
Prtot2 = 0
For i = 0 To N
sn1 = s1 + Ds1 * i
sn2 = svap + Ds2 * i
Pr1 = refprop8.prandtl(fluid, "ps", "C", p, sn1)
Pr2 = refprop8.prandtl(fluid, "ps", "c", p, sn2)

G

Prtot1 = Prtot1 + Pr1
Prtot2 = Prtot2 + Pr2
Next i

Prandtlwater = ((Prtot1 + Prtot2) / (N + 1) + pr2pavg) / 3

End Function

C.2.3   Thermal conductivity, water

Function Kfwater(fluid, p, s1, s2, N)

Dim Ds1, Ds2, Kf1, Kf2, sn1, sn2, i, Kftot1, Kftot2, sliq, svap, kfliq, kfvap, kf2pavg

sliq = refprop8.Entropy(fluid, "pliq", "c", p)
svap = refprop8.Entropy(fluid, "pvap", "c", p)
kfliq = refprop8.thermalconductivity(fluid, "pliq", "c", p)
kfvap = refprop8.thermalconductivity(fluid, "pvap", "c", p)
kf2pavg = (kfliq + kfvap) / 2

Ds1 = (sliq - s1) / N
Ds2 = (s2 - svap) / N
Kftot1 = 0
Kftot2 = 0
For i = 0 To N
sn1 = s1 + Ds1 * i
sn2 = svap + Ds2 * i
Kf1 = refprop8.thermalconductivity(fluid, "ps", "C", p, sn1)
Kf2 = refprop8.thermalconductivity(fluid, "ps", "c", p, sn2)
Kftot1 = Kftot1 + Kf1
Kftot2 = Kftot2 + Kf2
Next i

Kfwater = ((Kftot1 + Kftot2) / (N + 1) + kf2pavg) / 3

End Function

C.2.4   Density, water

Function Densityavg(fluid, p, s1, s2, N)

Dim Ds, rho, sn, i, Rhotot

H

Ds = (s2 - s1) / N
Rhotot = 0
For i = 0 To N
sn = s1 + Ds * i
rho = refprop8.density(fluid, ”ps”, ”C”, p, sn)
Rhotot = Rhotot + rho
Next i

Densityavg = Rhotot / (N + 1)

End Function

C.3   qg

qg - used in ”WHRU - hot side” to calculate the heat input to the cycle from the exhaust gases.

Function qg(fluid, m, T1, P1, T2, P2)
Dim N, s1, s2, sn, si, sii, qi, Ti, Tii, pi, pii, i, q, C, pn, ci, cii, c1, c2, cn

q = 0
N = 5
Sets the precision. The results uses N=100 (an increase to N=200 returns negligible differences)
c1 = cp(fluid, ”TP”, ”C”, T1, P1)
c2 = cp(fluid, ”TP”, ”C”, T2, P2)
s1 = refprop8.Entropy(fluid, ”TP”, ”C”, T1, P1)
s2 = refprop8.Entropy(fluid, ”TP”, ”C”, T2, P2)

sn = (s1 - s2) / N
pn = (P1 - P2) / N
cn = (c1 - c2) / N
For i = 0 To N
si = s1 - sn * i
sii = s1 - sn * (i + 1)
pi = P1 - pn * i
pii = P1 - pn * (i + 1)
ci = c1 - cn * i
cii = c2 - cn * (i + 1)
Ti = temperature(fluid, ”PS”, ”C”, pi, si)
Tii = temperature(fluid, ”PS”, ”C”, pii, sii)
qi = m * ((ci + cii) / 2) * (Ti - Tii)
q = q + qi
Next i

I

qg = q

End Function

C.4   number

number - used in "Reduction of variables" to calculate the number of channels needed to get the pressure drop beneath a certain value. The maximum pressure drop in the report is 0.2 MPa.

Function number(dp, L, m, D, rho, mu)
Dim N, test, Re, pi, f

pi = WorksheetFunction.pi()
test = dp + 1
Do While test > dp
N = N + 1000   *N + x, where x sets the precision*

   Re = 4 * m / N / pi / D / mu

   f = filonenko(Re)
test = L * f * 8 * m^2 / N^2 / D^5 / pi^2 / rho
Loop
number = N

End Function

C.5   Friction factor and turbulent/laminar flow Nusselt number

filonenko
Function filonenko(Re)
'Returns the friction factor to use in gnielinski.

$filonenko = (1.82 * WorksheetFunction.Log10(Re) - 1.64)^{-2}$

End Function

gnielinski
Function gnielinski(Re, Pr)
'Returns the Nusselt number for turbulent CIRCULAR duct flow in smooth pipes
'D - tube diameter
'f - friction factor

'm - mass flow
'mu - dynamic viscosity
'cp - fluid heat capacity
'kf - fluid thermal conductivity
'Re - Reynolds number
'Pr - Prandtl number

Dim f, nom, denom

f = filonenko(Re)

nom = (f / 8) * (Re - 1000) * Pr
denom = 1 + 12.7 * Sqr(f / 8) * ($Pr^{2/3}$ - 1)

gnielinski = nom / denom

End Function

graetz
Function graetz(Re, Pr, L, D)
' Returns the Nusselt number for laminar duct flow in smooth pipes
Dim x

x = L / D / Pr / Re

graetz = 3.66 + 0.0668 / ($x^{1/3}$ * (0.04 + $x^{2/3}$))

End Function

C.6 bejan

Optimum channel diameter, by Bejan [37]
Function bejan(Pr, m, q, rho, Kf, mu, T)
'returns optimal tube diameter
' q is per meter tube length.
' T = (Th-Tc)/2
' All properties evaluated at T

Dim b, Reopt

b = (m * q * rho) / ($mu^{5/2}$ * $Kf * T^{1/2}$)

Reopt = 2.023 * $Pr^{-0.071}$ * $b^{0.358}$

bejan = (4 * m) / (WorksheetFunction.pi() * Reopt * mu)

End Function

C.7 dp

Returns the pressure drop in a circular channel for a smooth pipe.

Function dp(Re, m, L, D, rho, mu)

Dim f
f = filonenko(Re)

dp = (8 * f * m^2) * L / (rho * WorksheetFunction.pi()^2 * D^5)

End Function

C.8 Dopt and volume

Used in "Reduction of variables" to calculate the optimum hot side channel diameter and volume.

C.8.1 volume

Function volume(D, L, dp, m, rho, mu)

Dim wtw, wth, Dc, H, W

wtw = 0.001
wth = 0.001
Dc = 0.0008

H = ((2 * number(dp, L, m, D, rho, mu))$^{1/2}$ - 1) / 2 * (D + Dc + wth)
W = (2 * number(dp, L, m, D, rho, mu))$^{1/2}$ * (D + wtw)

volume = H * W * L

End Function

C.8.2 Dopt

Function Dopt(L, dp, m, rho, mu)
Dim A, test, Dh

A = 1854
test = A + 1
Dh = 0.0006

Do While test > A
test = 2 * L * Dh * number(dp, L, m, Dh, rho, mu)
Dh = Dh + 0.001
Loop

Dopt = Dh

End Function

D Expander module calculations

control

| | | "POWER" | |
LOADVAR	REFERENCE	R	MODULAR
1.2	0.902	1.083	1.083
0.5	0.819	0.410	0.410
1	0.930	0.930	0.974
1	0.930	0.930	0.974
0.5	0.819	0.410	0.410
0.5	0.819	0.410	0.410
1	0.930	0.930	0.974
1	0.930	0.930	0.974

Table 15: Sample from the first 8 load cycles. LOADVAR is the variation in load, REF-ERENCE is reference efficiency, R and MODULAR are the "power" from the reference case and the modular case respectively

inputs

REFERENCE		
Expander type	Radial reaction	
Power output (MW)	8	PR
EXPANDER 1		
Expander type	Radial reaction	
Power output	8	PE1
Relative V at opt point	1	VRE1OPT
EXPANDER 2		
Expander type	Radial reaction	
Power output	8	PE2
Relative V at opt	1	VRE2OPT

Table 16: Rated expander power are used as inputs

	Optimal efficiencies for the range of power output							
Vex	1	2	3	4	5	6	7	8
0.5	0.660356	0.683028	0.7057	0.728372	0.751044	0.773717	0.796389	0.819061
0.6	0.695003	0.718865	0.742727	0.766589	0.790451	0.814312	0.838174	0.862036
0.7	0.721292	0.746056	0.770821	0.795585	0.820349	0.845114	0.869878	0.894642
0.8	0.739221	0.764601	0.789981	0.815361	0.84074	0.86612	0.8915	0.91688
0.9	0.74879	0.774499	0.800207	0.825916	0.851624	0.877332	0.903041	0.928749
1	0.75	0.77575	0.8015	0.82725	0.853	0.87875	0.9045	0.93025
1.1	0.74285	0.768355	0.793859	0.819364	0.844868	0.870373	0.895877	0.921382
1.2	0.727341	0.752313	0.777285	0.802257	0.827229	0.852201	0.877173	0.902145
k value	0.806235	0.833916	0.861596	0.889277	0.916958	0.944639	0.972319	1

Table 17: Lookup table to get the correct efficiencies for chosen expanders

data

Not included here due to corporate secrecy.

results

	1	2	3	4	5	6	7	8
1	0	0	0.131673	0.13813	0.336156	0.620346	0.665842	1.016226
2	0	0.129515	0.130231	0.327883	0.613726	0.623361	0.986081	1.014913
3	0.131673	0.130231	0.315052	0.602805	0.617418	0.930036	0.987342	1.01474
4	0.13813	0.327883	0.602805	0.611227	0.924392	0.932937	0.986802	1.01474
5	0.336156	0.613726	0.617418	0.924392	0.928707	0.933638	0.985847	1.01474
6	0.620346	0.623361	0.930036	0.932937	0.933638	0.926937	0.981804	1.01474
7	0.665842	0.986081	0.987342	0.986802	0.985847	0.981804	0.983795	1.01474
8	1.016226	1.014913	1.01474	1.01474	1.01474	1.01474	1.01474	1.01474

Table 18: Result sheet showing the power relative to the reference case for each set of expander combinations. The rated power outputs are in the upper row and leftmost column.

D.1 Expander module macro

D.1.1 REFERENCE

Dim PR 'Cycle power at optimal load
Dim PE1 'E1 power at VRE1OPT or optimum VFR for that expander
Dim PE2 'E2 power at VRE2OPT or optimum VFR for that expander
Dim VR 'Cycle volumetric flow rate (VFR)
Dim VRE1OPT 'Optimal flow rate E1 relative to VR (VRE1OPT = PE1/PR)
Dim VRE2OPT 'Optimal flow rate E2 relative to VR (VRE2OPT = PE2/PR)
Dim VE1 'Flow rate E1 (50, 80, 100, 120Dim VE2 'Flow rate E2 (same)
Dim VRE1 'Absolute flow rate E1 (VRE1 = VRE1OPT * VE1)
Dim VRE2 'Absolute flow rate E2 (VRE2 = VRE2OPT * VE2)
Dim x 'Relative flow rate E1 (x = VRE1/VR)
Dim y 'Relative flow rate E2 (y = VRE2/VR)
Dim LOADVAR As range
Dim REFN As range
Dim REFP As range
Dim POWER As range
Dim r, c, start, cycles, a
Option Base 1 'Sets array position 1 to index 1, instead of 0

Sub REFERENCE()
Application.ScreenUpdating = False
start = Sheets("control").range("d11").Address
cycles = 1095 '8760/8 → hours/year divided by 8 hour cycles → 1095 cycles/year

r = range(start).Row
c = range(start).Column
Set LOADVAR = Cells(r, c)
Set REFN = Cells(r, c + 1)
Set REFP = Cells(r, c + 2)

O

```
For i = 1 To cycles
a = Int((4 * Rnd) + 1) 'sets 'a' to be a random number with range 1 to 4
If a = 1 Then
LOADVAR(i, 1) = 0.5
REFN(i, 1) = range("c4")
REFP(i, 1) = LOADVAR(i, 1) * REFN(i, 1)
ElseIf a = 2 Then
LOADVAR(i, 1) = 0.8
REFN(i, 1) = range("d4")
REFP(i, 1) = LOADVAR(i, 1) * REFN(i, 1)
ElseIf a = 3 Then
LOADVAR(i, 1) = 1
REFN(i, 1) = range("e4")
REFP(i, 1) = LOADVAR(i, 1) * REFN(i, 1)
ElseIf a = 4 Then
LOADVAR(i, 1) = 1.2
REFN(i, 1) = range("f4")
REFP(i, 1) = LOADVAR(i, 1) * REFN(i, 1)
End If
REFN(i, 1).NumberFormat = "0.000"
REFP(i, 1).NumberFormat = "0.000"
Next i
End Sub
```

D.1.2 MODULAR

```
Sub MODULAR()

Sheets("Calculations").Delete

Application.ScreenUpdating = False
ActiveWorkbook.Sheets.Add after:=Worksheets(Worksheets.Count)
ActiveSheet.Name = "Calculations"
Dim temp1, temp2
PE1 = range("expander1").Value
VRE1OPT = range("vre1opt").Value
PE2 = range("expander2").Value
VRE2OPT = range("vre2opt").Value
temp1 = PE2
temp2 = VRE2OPT

If PE2 > PE1 Then
PE2 = PE1
VRE2OPT = VRE1OPT
PE1 = temp1
```

```
VRE1OPT = temp2
End If
Dim i, j
i = 1
For VR = 0.5 To 1.25 Step 0.05
For VE1 = 0.5 To 1.25 Step 0.05
j = j + 1
VRE1 = VRE1OPT * VE1        'VRE1 = VRE1OPT*VE1
VRE2 = VR - VRE1 'VR = VRE1 + VRE2
VE2 = VRE2 / VRE2OPT 'VRE2 = VRE2OPT*VE2
Cells(1, i).FormulaR1C1 = "VR"
Cells(1, i + 1).FormulaR1C1 = "VE1"
Cells(1, i + 2).FormulaR1C1 = "VE2"
Cells(1, i + 3).FormulaR1C1 = "Power"
Cells(j + 1, i) = VR 'column VR
Cells(j + 1, i + 1) = VE1 'column VE1
Cells(j + 1, i + 2) = VE2 'column VE2
range(Cells(j + 1, i + 1), Cells(j + 1, i + 2)).Select
Call CONDFORMAT1
If VE2 > 1.2 Or VE2 < 0.5 Then 'E2 is turned off
If VRE1 < VR * 0.95 Or VRE1 > VR * 1.05 Then 'VFR of E1 must be +/- 5Cells(j +
1, i + 1).Select
Selection.Style = "Neutral"
Else
Cells(j + 1, i + 3) = VRE1 * EFF1(VE1, PE1)
End If
Else
Dim temp
temp = Round(VE2, 3)
Cells(j + 1, i + 3) = VRE1 * EFF1(VE1, PE1) + VRE2 * EFF1(VE2, PE2) 'GetN2(GetVpos(temp))
End If
Next VE1
Cells(j + 2, i + 2).FormulaR1C1 = "BEST"
Cells(j + 2, i + 3) = WorksheetFunction.Max(range(Cells(2, i + 3), Cells(j + 1, i + 3)))
range(Cells(2, i + 2), Cells(j + 2, i + 3)).NumberFormat = "0.000"
i = i + 4
j = 0
Next VR
'inserts the best results from the specified VFR values (0.5, 0.8, 1, 1.2) into "control"
sheet, then add them and place the result to the right of the variation columns
Sheets("control").Activate
start = Sheets("control").range("d11").Address
cycles = 1095
r = range(start).Row
c = range(start).Column
Set POWER = Cells(r, c + 3)
```

Q

```
Set LOADVAR = Cells(r, c)
For i = 1 To cycles
If LOADVAR(i, 1) = 0.5 Then
POWER(i, 1) = Sheets("calculations").range("d17")
ElseIf LOADVAR(i, 1) = 0.8 Then
POWER(i, 1) = Sheets("calculations").range("ab17")
ElseIf LOADVAR(i, 1) = 1 Then
POWER(i, 1) = Sheets("calculations").range("ar17")
ElseIf LOADVAR(i, 1) = 1.2 Then
POWER(i, 1) = Sheets("calculations").range("bh17")
End If
POWER(i, 1).NumberFormat = "0.000"
Next i
End Sub
```

D.1.3   CalcAll

```
Sub calcAll()
' Calculates all the different configurations by inserting the power output values (1 to 8
MW) into "inputs" and running MODULAR
' Put all the results in the worksheet "results"
Application.DisplayAlerts = False
'Sheets("results").Delete
ActiveWorkbook.Sheets.Add after:=Worksheets(Worksheets.Count)
ActiveSheet.Name = "results"
Dim i, j
For i = 1 To 8
range("expander1").Value = i
For j = 1 To 8
range("expander2").Value = j
Call MODULAR
Sheets("results").Cells(i, j) = range("power").Value
Next
Next
Application.DisplayAlerts = True
End Sub
```

D.1.4   EFF1

```
Function EFF1(V, P)
' Calculates the efficiency for a given flow rate and power rating according to the created
expander efficiency chart.
If P = 1 Then
```
EFF1 = -0.418 * V^2 + 0.8063 * V + 0.3617

ElseIf P = 2 Then
EFF1 = -0.4323 * V^2 + 0.8339 * V + 0.3741
ElseIf P = 3 Then
EFF1 = -0.4467 * V^2 + 0.8616 * V + 0.3866
ElseIf P = 4 Then
EFF1 = -0.461 * V^2 + 0.8893 * V + 0.399
ElseIf P = 5 Then
EFF1 = -0.4754 * V^2 + 0.917 * V + 0.4114
ElseIf P = 6 Then
EFF1 = -0.4785 * V^2 + 0.923 * V + 0.4141
ElseIf P = 7 Then
EFF1 = -0.5041 * V^2 + 0.9723 * V + 0.4362
ElseIf P = 8 Then
EFF1 = -0.5184 * V^2 + 1 * V + 0.4487
End If
End Function

E Source of the linear k-value
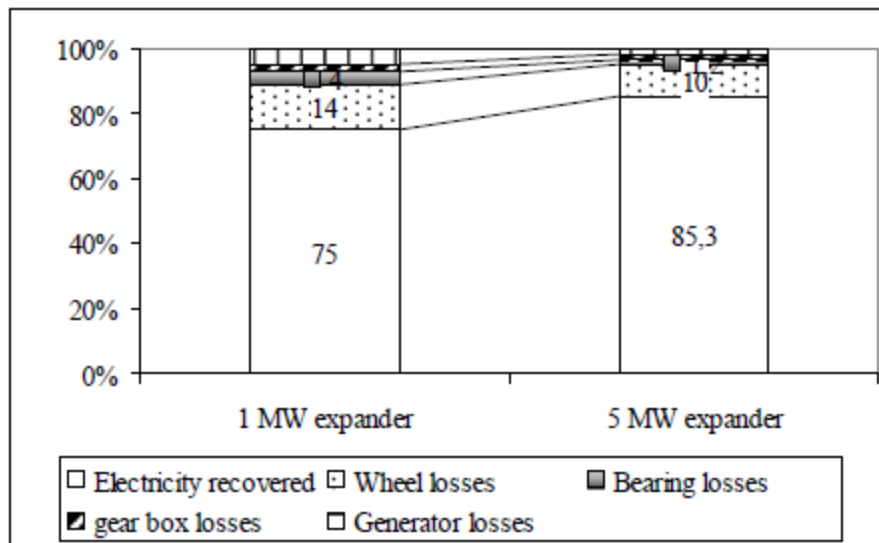
Figure 8: Typical percentage of electricity recovered and losses of a turbogenerator (basis 100% = isentropic enthalpy drop through the expander)

Source of the linear sizing factor, k [41]

water	Tavg,H	186.3366	205.6841	217.4679	225.9685	232.5966	238.0019	242.5404	246.429	249.8101	252.7828	255.4183	257.7699	259.8789	261.7772	263.4905
	Tavg,L	20	20	20	20	20	20	20	20	20	20	20	20	20	20	20
toluene	Tavg,H	243.9193	253.9279	259.1613	262.3686	264.4402	265.7849	266.6281	267.1097	267.3239	267.3392	267.2091	266.9785	266.6868	266.3681	266.05
	Tavg,L	105.1714	98.27819	93.99836	90.76797	88.10484	85.79991	83.74546	81.87938	80.16497	78.57831	77.10551	75.73926	74.4773	73.31845	72.26127
co2	Tavg,H	104.8154	124.3614	137.334	147.4023	155.7921	163.0636	169.3751	174.9117	179.8422	184.2847	188.3252	192.0285	195.4444	198.6126	201.5647
	Tavg,L	240.5953	207.3574	188.9886	176.4066	166.8923	159.2707	152.9294	147.5101	142.7848	138.6005	134.8491	131.452	128.3498	125.4968	122.8573
water	s3	7.871315	7.542599	7.346532	7.204698	7.092525	6.999064	6.918475	6.847272	6.783205	6.724739	6.670776	6.620507	6.573317	6.528728	6.48636
	h4s	2304.476	2208.113	2150.636	2109.057	2076.174	2048.776	2025.151	2004.278	1985.497	1968.357	1952.538	1937.802	1923.968	1910.897	1898.476
	hg @ PL	2537.433	2537.433	2537.433	2537.433	2537.433	2537.433	2537.433	2537.433	2537.433	2537.433	2537.433	2537.433	2537.433	2537.433	2537.433
	hf @ PL	83.91414	83.91414	83.91414	83.91414	83.91414	83.91414	83.91414	83.91414	83.91414	83.91414	83.91414	83.91414	83.91414	83.91414	83.91414
	vapor fraction	0.905052	0.865776	0.84235	0.825403	0.812001	0.800834	0.791205	0.782698	0.775043	0.768057	0.76161	0.755603	0.749965	0.74638	0.739575
	h3	3564.032	3554.53	3544.915	3535.188	3525.347	3515.39	3505.317	3495.127	3484.818	3474.39	3463.842	3453.172	3442.38	3431.465	3420.426
$\eta_{is} = 0.8$	h4	2556.387	2477.396	2429.492	2394.283	2366.008	2342.098	2321.184	2302.448	2285.361	2269.564	2254.799	2240.876	2227.65	2215.01	2202.866
	0.8 vapor fraction	1.007725	0.97553	0.956005	0.941655	0.930131	0.920386	0.911862	0.904225	0.897261	0.890822	0.884804	0.87913	0.873739	0.868587	0.863638
$\eta_{is} = 0.9$	h4	2430.432	2342.755	2290.064	2251.67	2221.091	2195.437	2173.168	2153.363	2135.429	2118.961	2103.668	2089.339	2075.809	2062.953	2050.671
	0.9 vapor fraction	0.956388	0.920653	0.899178	0.883529	0.871066	0.86061	0.851533	0.843461	0.836152	0.82944	0.823207	0.817367	0.811852	0.806612	0.801607
toluene	s3	2.248129	2.178098	2.133743	2.099772	2.071433	2.046648	2.024343	2.003904	1.984962	1.967291	1.950763	1.935318	1.920949	1.907667	1.895478
co2	s3	3.315891	3.183469	3.105411	3.04962	3.006035	2.970177	2.939655	2.913042	2.889418	2.868155	2.848804	2.831034	2.814595	2.799291	2.784966

T

Table 4: Calculations of the required states to get the efficiency. "Tavg" are calculated with the "Tavg" function

T (°C)	q (kW)	Tex (°C)	qex acc (kW)	Tw at qex (°C)	DT (°C)	qex (kW)	Exergy lost in WHRU (kW)	Exergy in by heat (kW)
20.45	75.09	150.00	125.65	23.08	126.92	125.65	37.69	41.57
22.03	150.58	151.33	251.20	25.71	125.61	125.55	37.15	41.80
23.61	226.47	152.66	376.65	28.34	124.31	125.45	36.62	42.03
25.21	302.78	153.98	502.00	30.97	123.01	125.35	36.10	42.26
26.81	379.49	155.31	627.25	33.60	121.71	125.25	35.58	42.48
28.42	456.62	156.63	752.42	36.22	120.41	125.17	35.07	42.70
30.05	534.16	157.95	877.49	38.84	119.11	125.07	34.56	42.93
31.68	612.12	159.27	1002.48	41.46	117.81	124.99	34.05	43.15
33.31	690.49	160.59	1127.38	44.08	116.51	124.90	33.55	43.37
34.96	769.29	161.91	1252.21	46.69	115.22	124.82	33.06	43.59

Table 7: Sample from the calculation of the exergy loss and exergy transfer in the WHRU for water, the temperature range in the leftmost column goes down to 539°C

U

		DT_H	8				10				12				°C
		T_3	541				539				537				°C
		epsilon	0.984877				0.981096				0.977316				-
Tg, out (°C)	q by Tg, out (kW)		Cmin (W/K)	Cr	NTU	UA (W/K)	Cmin (W/K)	Cr	NTU	UA (W/K)	Cmin (W/K)	Cr	NTU	UA (W/K)	
40	48226		94932	0.98	39.78	3776621	95298	0.98	35.97	3428284	95667	0.98	33.01	3158160	
50	47295		93067	0.96	31.30	2913149	93426	0.96	28.51	2663475	93787	0.97	26.32	2468283	
60	46368		91202	0.94	26.20	2389828	91554	0.94	23.98	2195719	91908	0.95	22.23	2043154	
70	45444		89337	0.92	22.73	2030875	89681	0.92	20.88	1872765	90028	0.93	19.42	1748014	
80	44522		87472	0.90	20.19	1765864	87809	0.90	18.60	1633113	88149	0.91	17.33	1528057	
90	43604		85607	0.88	18.23	1560360	85937	0.88	16.83	1446498	86269	0.89	15.72	1356175	
100	42688		83742	0.86	16.66	1395286	84064	0.87	15.42	1296070	84390	0.87	14.42	1217211	
110	41774		81877	0.84	15.38	1259116	82192	0.85	14.25	1171609	82510	0.85	13.36	1101939	
120	40863		80012	0.82	14.30	1144431	80320	0.83	13.28	1066508	80631	0.83	12.46	1004380	
130	39953		78147	0.80	13.39	1046215	78448	0.81	12.45	976288	78751	0.81	11.69	920466	
140	39045		76281	0.79	12.60	960938.5	76575	0.79	11.72	897789	76872	0.79	11.02	847323	
150	38138		74416	0.77	11.91	886041.2	74703	0.77	11.09	828713	74992	0.77	10.44	782854	

Table 9: Heat transfer values at given approach point and exhaust temperature exiting the WHRU

V

W

D	L 2					L 2.5					L 3					L 3.5				
	#	A	hA	Width	"height"	#	A	hA	Width	"height"	#	A	hA	Width	"height"	#	A	hA	Width	"height"
0.001	1315000	5257.64	2323586	1.621727	1621	1504000	7514.109	2839868	1.734359	1733	1680000	10074.33	3306822	1.83303	1832	1845000	12908.7	3718540	1.920937	1920
0.0011	1007000	4427.195	2135328	1.56107	1418	1151000	6325.35	2649852	1.668958	1516	1285000	8475.065	3135623	1.763434	1602	1410000	10848.69	3558546	1.847214	1678
0.0012	790000	3789.042	1953602	1.508377	1256	903000	5414.472	2447945	1.61265	1343	1007000	7244.501	2925441	1.702986	1418	1104000	9267.771	3384979	1.783121	1485
0.0013	633000	3288.187	1786381	1.462717	1124	722000	4690.401	2253676	1.562165	1201	805000	6274.755	2711748	1.649515	1268	883000	8029.802	3159101	1.727582	1328
0.0014	515000	2881.473	1636849	1.420845	1014	588000	4110.552	2072948	1.518209	1083	655000	5499.345	2508513	1.602373	1144	718000	7028.578	2934909	1.677665	1197
0.0015	426000	2553.124	1503740	1.384558	922	486000	3641.67	1912029	1.478851	985	541000	4863.419	2319213	1.560288	1039	593000	6220.575	2725358	1.633554	1088
0.0016	356000	2276.237	1385987	1.350081	843	406000	3243.998	1766032	1.441777	900	452000	4335.599	2149228	1.521263	950	495000	5538.498	2531338	1.59198	994
0.0017	302000	2050.497	1281565	1.321196	776	344000	2918.861	1635971	1.410078	828	382000	3891.626	1994507	1.485921	873	419000	4978.347	2354002	1.55622	914
0.0018	258000	1854.157	1188640	1.292997	717	294000	2643.2	1521452	1.380261	766	327000	3528.531	1857601	1.455665	808	358000	4504.574	2194967	1.523102	845
0.0019	222000	1683.824	1105839	1.266033	665	253000	2398.983	1416365	1.35154	710	281000	3200.552	1732505	1.424367	749	308000	4091.929	2050852	1.491228	784
0.002	193000	1540.797	1032476	1.242578	620	220000	2195.606	1323740	1.32665	662	244000	2925.611	1620722	1.39714	698	267000	3734.148	1919982	1.461506	730
0.0021	169000	1416.236	966559.8	1.220893	580	192000	2013.796	1240935	1.301322	619	214000	2691.384	1519033	1.373856	653	234000	3434.243	1801572	1.436621	683
0.0022	149000	1309.053	908312.4	1.200966	545	169000	1854.595	1164185	1.279031	580	188000	2476.791	1427263	1.349014	612	206000	3168.089	1695142	1.412119	641
0.0023	132000	1212.487	854979	1.181761	513	150000	1722.724	1097927	1.259762	547	167000	2300.902	1346024	1.329233	577	182000	2923.769	1596018	1.387645	602
0.0024	117000	1121.492	805840.2	1.160965	483	134000	1605.866	1036955	1.242449	517	148000	2127.052	1269367	1.305741	543	162000	2715.815	1507772	1.366104	568
0.0025	105000	1047.119	761462	1.145644	457	119000	1484.901	978825.1	1.219631	487	133000	1992.092	1202742	1.28938	515	145000	2535.066	1428988	1.346291	538
0.0026	94000	976.2705	721812.7	1.127333	433	107000	1389.192	928158.2	1.202763	462	119000	1853.156	1138847	1.268416	487	130000	2361.815	1353400	1.325745	509
0.0027	85000	915.0821	684240.6	1.113239	411	97000	1305.176	880390.1	1.189227	439	108000	1746.746	1083071	1.254847	464	118000	2226.535	1287495	1.311655	485
0.0028	77000	859.2611	650397.5	1.098799	391	88000	1230.463	839415.2	1.174666	419	97000	1624.219	1026817	1.233272	439	107000	2094.474	1225913	1.295284	462
0.0029	70000	809.4702	619893.5	1.085081	373	80000	1157.1	798771.5	1.16	399	89000	1545.295	981626.3	1.223511	421	97000	1962.598	1165443	1.27318	439
0.003	64000	766.3452	592345.5	1.073313	357	73000	1091.849	762031.1	1.146298	381	81000	1452.594	934967.8	1.207477	401	88000	1845.694	1113512	1.258571	419

Table 12: WHRU heat transfer parameters at given lengths and hot side channel diameter

Diameter	WHRU Length															
	1.5	1.6	1.7	1.8	1.9	2	2.1	2.2	2.3	2.4	2.5	2.6	2.7	2.8	2.9	3
0.0015	4.44975	4.931091858	5.421506	5.933359	6.466652	7.021385	7.580242344	8.158891	8.75733	9.3755608	10.01358	10.64996	11.30447	11.97713	12.66793	13.37688
0.0016	3.986116	4.421476622	4.863023	5.324008	5.80443	6.286621	6.805035758	7.323452	7.85954	8.4132996	8.962643	9.550862	10.1329	10.73084	11.34468	11.97443
0.0017	3.609564	4.001296237	4.395864	4.82443	5.253943	5.700456	6.144137016	6.623707	7.098556	7.611184	8.117202	8.638332	9.174575	9.699485	10.26501	10.81731
0.0018	3.291168	3.639506497	4.021086	4.384537	4.781229	5.194039	5.601814732	6.023694	6.482845	6.9339397	7.399138	7.85225	8.344649	8.851153	9.342547	9.876252
0.0019	3.020925	3.342399294	3.678885	4.030382	4.396892	4.75697	5.152432318	5.539318	5.939072	6.3516941	6.777184	7.215543	7.666769	8.100841	8.576733	9.033324
0.002	2.799503	3.095482172	3.405131	3.72845	4.043797	4.393317	4.756508457	5.10831	5.471504	5.8734294	6.260548	6.659058	7.068962	7.490258	7.922948	8.332854
0.0021	2.588456	2.876976116	3.159459	3.454022	3.760666	4.079391	4.410197321	4.753085	5.08027	5.4461119	5.793835	6.182633	6.550895	6.928822	7.351449	7.749916
0.0022	2.414381	2.67763856	2.953686	3.219504	3.519852	3.807413	4.105205359	4.41323	4.731487	5.0599764	5.398698	5.747652	6.106839	6.476258	6.8591	7.207427
0.0023	2.268237	2.505954471	2.754486	3.013832	3.283993	3.564968	3.856758796	4.129627	4.441696	4.7321385	5.064487	5.372504	5.725132	6.050725	6.38443	6.766801
0.0024	2.13721	2.348158964	2.591917	2.847089	3.08657	3.334612	3.621171927	3.887761	4.162912	4.4466223	4.774559	5.076819	5.387639	5.70702	5.993589	6.328666
0.0025	2.004413	2.234247423	2.450555	2.675883	2.910232	3.153603	3.405995662	3.66741	3.937846	4.2173037	4.468197	4.764196	5.069216	5.383259	5.662723	5.993307
0.0026	1.896048	2.098389035	2.310224	2.531553	2.762377	2.971052	3.219282364	3.47008	3.707836	3.9829694	4.22804	4.520581	4.779895	5.089845	5.363402	5.643289
0.0027	1.793461	1.992841186	2.2022	2.391606	2.61926	2.823635	3.06958568	3.28893	3.514927	3.7874909	4.028458	4.276079	4.530353	4.79128	5.107094	5.382993
0.0028	1.725757	1.896666956	2.074561	2.290861	2.484469	2.68506	2.892636429	3.145605	3.368897	3.5991726	3.836433	4.080679	4.33191	4.590125	4.855326	5.075131
0.0029	1.644938	1.813172273	1.98873	2.17161	2.361814	2.559342	2.764192467	2.976367	3.195866	3.4226883	3.656835	3.898306	4.097671	4.351959	4.613572	4.88251
0.003	1.579224	1.745853867	1.920154	2.067614	2.255337	2.450731	2.653795508	2.864531	3.038838	3.2629979	3.49483	3.734333	3.929735	4.182663	4.387654	4.654008

Table 13: WHRU volume with varying length and hot side channel diameter

X

Offshore Rankine cycles

Jo Brandsar

Heat and Energy Processes, Energy and Environmental Engineering

Norwegian University of Science and Technology, NTNU

Trondheim, Norway

June 25, 2012

Abstract

This paper summarizes my master thesis during the spring semester 2012 at the Institute of Energy and Process Engineering, NTNU, Norway. The project was given to me as a collaboration with an ongoing project at SINTEF Energy Research. The focus represent electricity production offshore by applying a Rankine cycle with surplus heat as the energy source. Investigations concern foremost a comparison between steam and organic cycles and the effect the waste heat recovery unit (WHRU) has on the cycle as a whole, in addition to an investigation regarding the effect a modular expander setup has on power output wrt large and frequent variations in heat load.

Introduction

The title of the thesis - "Offshore Rankine Cycles" - is very general and cover a large range of engineering fields, e.g. thermodynamic cycles (Rankine, ORC, Brayton, Kalina, etc.), mechanical equipment (gas/steam turbine, heat exchangers and additional equipment) and safety concerns (flammable and/or toxic fluids, high temperature and pressures), to name the most important. The thesis try to give a brief overview of all critical points and alternatives, concerning employment of a waste heat recovery machine on offshore facilities, although focus has been on three more specified cases, namely:

- Comparison of a steam cycle vs. an organic Rankine cycle for high temperature operating conditions.

- Study of heat exchanger parameters on total cycle performance.

- Investigation of a modular expander setup versus a single expander.

To compare a steam cycle to an organic cycle, a choice of working fluid for the organic cycle had to be made. After some investigation, toluene was chosen as it is a "common" fluid with known properties and was found to be a viable option for high temperature heat sources, both for subcritical and supercritical operation. Due to water being constricted to subcritical operation a CO_2 cycle was implemented as a comparison to the supercritical toluene cycle. The main focus of the comparison was exergy losses during heat transfer and

power output.

The heat exchanger parameter study was conducted with a printed circuit heat exchanger as an example. The study of overall cycle performance has close connections to the heat exchanger size, since it is an important parameter concerning offshore employment due to costly "footprint". The cycle's dependency on the heat exchanger is mainly by the heat transfer rate, or heat load, which the heat exchanger applies to the cycle. The heat transfer rate is given by the heat exchanger's ability to reduce the temperature of the exhaust gases. This ability depends on the two fluids involved and the geometry of the heat exchanger. While the choice in working fluid and pinch points sets the amount of heat transferred, the remaining analysis rest on the overall heat transfer coefficient (UA) to balance the heat load. When fluid properties are determined, the UA - value is again dependent on heat exchanger geometry and further variation of these parameters will in turn reveal the size of the heat exchanger. When imposing a working fluid to the cold side of the heat exchanger an optimization in heat exchanger volume could be found at specified heat load.

A VBA macro has been made where expander parameters (rated power and efficiency vs. volumetric flow rate values) could be used as inputs to calculate the power output of two expanders in a modular setup relative to a single expander as reference.

Cycle comparison

Higher fuel prices and elevated environmental concerns promotes the need for waste heat recovery as a mean to increase efficiency of power producing devices, or more general, to produce power where any heat source is readily available. Offshore installations are prone to these methods, first of all since connection to the land based power grid could be difficult and/or cost inefficient. Secondly, heat sources suitable for recovery are readily available, a few sources to be mentioned are: gas turbine and ICE exhaust heat, gas compression intercool-ing/aftercooling, well stream energy and gas expansion. The evaluation will focus on high temperature heat sources, which leaves gas turbine and ICE exhaust heat as a base for discussion.

Gas turbine exhaust heat has the greatest potential and will be used as the working example, more specifically the General Electric's LM2500+ G4 (Table 1) exhaust heat as a load on the Rankine cycle's WHRU. The LM2500+ G4 is chosen because it has wide usage and can be utilized both on marine vessels and offshore structures.

General Electric LM2500+ G4	
Power output	35,3 MW
Exhaust flow	93 kg/s
Exhaust temperature	549°C

Table 1: Exhauxt data from LM2500+ G4 (60Hz, 15C, sea level, 60% rel. humidity)

Working fluid

An ORC (organic Rankine cycle) could be used with a large range of different organic fluids and several studies has been done to try locating the best ones. In general, the fluids with the best efficiency is chosen by their saturation curve and their latent heat at low pressure. That is, isentropic (i.e. vertical saturation curve) [1], low liquid specific heat and high latent heat together with high density [2] for the best performance. These criteria promotes the use of R-123 for lower temperatures and p-Xylene for higher temperatures [3]. CO_2 has also been tested as a working fluid with heat exchange occurring in the supercritical region [4].

Several studies has been performed with a multitude of working fluids. The fluid in this study is chosen to be toluene [5], [6]. The relative high critical values of toluene are more suitable for high temperature heat recovery [7], [2]. Toluene has a low GWP of 2.7 (ipcc.ch), low toxicity, low price and very good availability. The negative side is toluene being highly flammable (flash point of 4°C and auto-ignition point of 508°C) and should not be directly

heated by the exhaust gases as it could auto-ignite at a temperature below the exhaust temperature when mixed with sufficient amounts of oxygen. Supplementary firing could reduce this risk and the fact that safety procedures for highly flammable fluids should already be well implemented on offshore facilities reduces the impact of this hazard to a certain degree. CO_2 is chosen as well, as a comparison to the toluene supercritical cycle [8].

Important parameters for evaluation

Important parameters to be evaluated in this comparison is listed below together with a short description:

Power output High relevance. High power output reduces the need for additional power producing equipment.

System size/Weight High relevance, especially in an offshore context which have costly "footprint".

Efficiency, 1st and 2nd law Decreases fuel costs and emissions per kW output.

Complexity and reliability More complex system often mean less reliability and equipment failure could become critical in the offshore environment.

Environmental and personnel safety Has to be well above certain criteria. Added risks means added costs.

By doing a comparison between cycles where all can be modified in a multitude of different conformations there has to be some "ground rules", i.e.: same heat source load with no variation, expander of either radial inflow or axial single-stage turboexpander (no reheating or multi-pressure HRSG/WHRU) and same environmental reference properties and condensing water temperature.

WHRU

The waste heat recovery unit (WHRU) could either be of a HRSG-type (Heat Recovery Steam Generator) or a CHE (Compact Heat Exchanger). The main differences is size (HRSG is much larger than a CHE) and exhaust pressure drop (larger pressure drop in a CHE).

HRSG

Among the different HRSG types (vertical-, horizontal- and once-through steam generators) the OTSG (Figure 1) looks most promising especially in terms of compactness and low maintenance. As for now the constraint of a single-pressure leaves the OTSG as the best option.

Once-Through properties

- Requires no drum, risers, downcomers, blowdown system, etc.

- No distinct economizer, evaporator or superhaeting section, i.e. a single bank.

- Vertical design, approximately half the size of a vertical HRSG although only a slight decrease in footprint.

- Made of Inconel, not steel.

- Lower installation time.

- More expensive largely due to the use of Inconel.

The main difference in size is the absence of the steam drum in OTSG versus the other types. Water enters at one end of the tube bundle and as the fluid exits fully evaporated at the other end there is no need for circulation and water/steam separation in a steam drum. The lack of steam drum decreases startup time and reduces weight substantially, on the other hand, the water contamination has to be at a minimum prior to injection to the boiler since the OTSG lack the blowdown system where contaminants can be rejected. The water treatment in a OTSG is done by all-volatile treatment (AVT) or oxygenated treatment (OT). AVT introduces chemicals to the stream that increases the pH-value thus provides better corrosion protection for steel. OT increases the electrochemical potential which reduces the

iron oxide in the feedwater. Both methods could be combined with successful results [9].
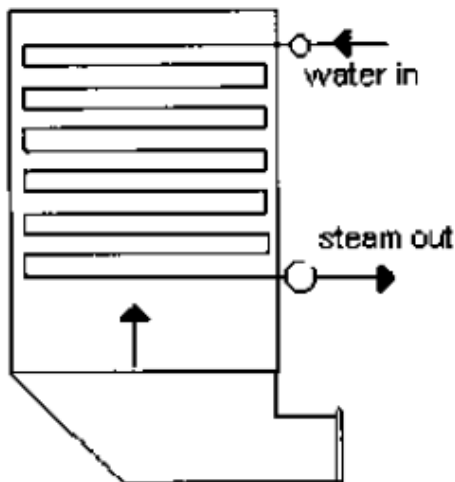

Figure 1: Once-through Steam Generator

CHE

Due to a wide range of usage there exist an equally wide range of heat exchangers available as well. To filter out the possible types some criteria has to be met, i.e. size, capacity and temperature and pressure requirements; secondly, reliability, durability, low maintenance and operation safety. Three main types remains which is: welded plate heat exchanger (preferably of the circular type), plate-fin heat exchanger and printed-circuit heat exchanger (PCHE). The latter is chosen for further investigation.

PCHE

The printed-circuit heat exchanger (Figure 2) has the highest temperature and pressure limits of all types of heat exchangers and can operate in excess of 600 bar and 900°C (Heatric). The reason is the manufacturing method which has some similarities with the manufacturing of circuit boards (thus the name printed circuit HE). The process starts with chemical etching of the flow paths onto sheets of metal. The metal sheets are then stacked and fusion bonded together. The fusion bonding of the plates makes the joining points between the plates as strong as the parental metal. Channel diameter can be made very small (down to

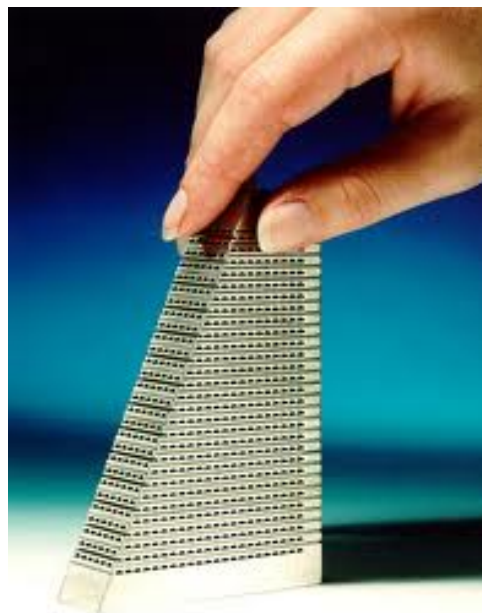0.1 mm) resulting in very high heat exchange surface to volume ratio.

Figure 2: Printed-circuit heat exchanger

Thermodynamic analysis

The 4 different cycles under investigation is described in Table 2 together with the expander inlet pressure.

Water	Subcritical	6 MPa
CO_2	Supercritical	15 MPa
Toluene	Subcritical	3,5 MPa
	Supercritical	15 MPa

Table 2: Selected pressure for each cycle

The procedure in setting the states are shown below.

State 1 - Pump inlet

$$T_1 = T_C + \Delta T_L$$

where ΔT_L is the temperature difference between the cooling water temperature T_C and the working fluid temperature at state 1.

$$P_1 = f(T_{1,sat\ liquid})$$

State 2 - WHRU inlet

$$h_2 = h_1 + \frac{h_{2,is} - h_1}{\eta_p}$$

where

$$h_{2,is} = f(p_3, s_1)$$

$$T_2 = f(p_3, h_2)$$

State 3 - Expander inlet

$$T_3 = T_H - \Delta T_H$$

where ΔT_H is the temperature difference between the heat source temperature T_H and the working fluid temperature at state 3.

$$p_3 \quad \text{Table 2}$$

State 4 - Condenser inlet

$$p_4 = p_1 + \Delta p_L$$

where Δp_L is the pressure drop in the condenser.

$$h_4 = h_3 - \eta_e(h_3 - h_{4,is})$$

where

$$h_{4,\,is} = f(p_4, s_3)$$

Assumptions and environmetal data: The pressure drop in the WHRU is assumed to be negligible wrt the fluid pressure, cooling water temperature (10°C), gas turbine exhaust temperature (549°C), approach points (ΔT_L and ΔT_H) condenser and WHRU (10°C) and pump/expander isentropic efficiencies of 0.8. The pressure drop in the condenser is set to 50 kPa.

Energy transfers

The heat transfer to the subcritical cycles is calculated according to Figure 3 where the total heat transfer is the sum of the heat transfer in section 1 and section 2.
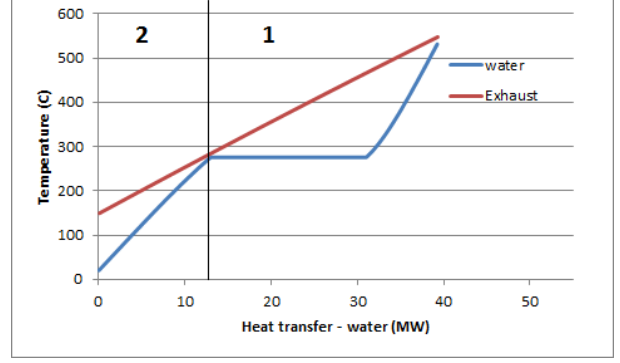

Figure 3: Division of the two heat transfer rates from the heat source

Exergy considerations

The exergy lost during heat transfer is calculated with,

$$\dot{W}_{lost} = \sum_{i=1}^{n} \left(1 - \frac{T_{L,\,i}}{T_{H,\,i}}\right) \dot{Q}_i \qquad (1)$$

where T_L is the working fluid temperature and T_H the heat source temperature. The total exergy transferred to the cycle by,

$$\dot{E}_Q = \sum_{i=1}^{n} \left(1 - \frac{T_C}{T_{H,\,i}}\right) \dot{Q}_i \qquad (2)$$

and the net exergy transferred to the cycle,

$$\dot{E}_{Q,\,net} = \dot{E}_Q - \dot{W}_{lost} = \sum_{i=1}^{n} \left(\frac{T_{L,\,i} - T_C}{T_{H,\,i}}\right) \dot{Q}_i \qquad (3)$$

Exergy lost during non-isentropic pump work,

$$\dot{W}_{p,\,lost} = T_C \dot{m}(s_2 - s_1) \qquad (4)$$

Exergy lost during non-isentropic expansion,

$$\dot{W}_{t,\,lost} = T_C \dot{m}(s_4 - s_3) \qquad (5)$$

The exergy lost in the condenser is readily available as

$$\dot{W}_{c,\,lost} = \dot{E}_{Q,\,net} - \dot{W}_{p,\,lost} - \dot{W}_{e,\,lost} - \dot{W}_{cycle} \qquad (6)$$

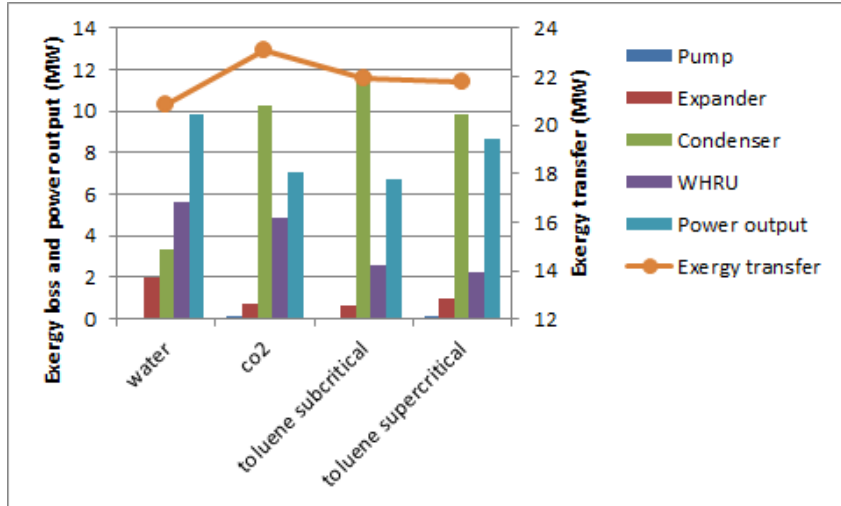Results are shown in Figure 4 and Table 3

5

Figure 4: Exergy losses in each component for all cycles plotted together with work output and exergy transferred to each cycle

	Water	Toluene subcritical	Toluene supercritical	CO2
Heat transfer (kW)	39225	42898	42569	49237
Mass flowrate (kg/s)	11.46	30.81	33.16	65.21
Pinch point (°C)	10	15	90	10
Exhaust temperature (°C)	150	110	115	44
Exergy transfer via heat transfer (kW)	20823	21939	21814	23096
Exergy lost, WHRU (kW)	5617	2629	2217	4844
Exergy lost wrt transferred	27.0%	12.0%	10.2%	21.0%

Table 3: Cycle values given by exhaust properties and set approach and pinch point

Figure 4 shows water to produce the highest power output followed by the supercritical toluene cycle. The high exergy losses in the condenser for the organic cycles is a result of high temperatures at the expander outlet, leaving a high load and temperature difference on the condenser.
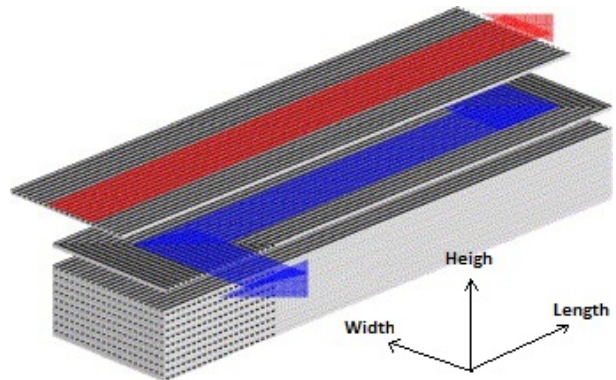

Figure 5: The flow path of a printed circuit heat exchanger (heatric.com)

WHRU parameter study

The study concerns a PCHE, as previously discussed, shown in Figure 5 used as a WHRU in the subcritical steam cycle used in the cycle comparison.

Geometry relations, WHRU

The WHRU is a rectangular shaped box with overall height, H, width, W, and length L as shown in Figure 5. The relation between channel numbers are

$$\# = N_H N_W$$

where $\#$ are the total number of channels in one stream and N_H/N_W are the number of channels in the vertical and horizontal direction respectively. By setting $N_W = 2N_H$ (the overall number of channels are equal in both directions) the channel numbers in each direction can be represented by the total number of channels for one stream, i.e.

$$N_W = \sqrt{2\#}$$

and

$$N_H = \frac{\sqrt{2\#}}{2}$$

The height and width are further reduced to the height with the wall separating the channels subtracted H':

$$H' = N_H(D_h + D_c)$$

where D_h and D_c are the hot side and cold side channel diameter. The width with the wall thickness subtracted is

$$W' = (N_W D)_x$$

where x denotes either the cold or the hot side parameters.
The heat transfer area is thus

$$A = W' * L * (2N_H - 1) \tag{7}$$

where all parameters are independent of the choice of hot or cold side stream. The heat transfer area can thus be seen as a plate heat exchanger (no wall thickness between channels) with $(2N_H - 1)$ being the number of "plates".

Heat transfer coefficient analysis

The heat transfer rate (q) and overall heat transfer coefficient (UA) could be found by the ϵ-NTU method or from the previous mentioned cycle study. The total heat transfer area is calculated with eq. (7). If the goal is to reduce the heat transfer area but keep the overall heat transfer coefficient constant it implies that the "U-value" has to be increased. By setting the heat transfer area on the hot and cold side to be of equal size as the overall area, the overall heat transfer coefficient could be written in terms of the convective heat transfer coefficient on both sides of the WHRU (for unfinned surfaces, no fouling and negligible conduction resistance)

$$U = \frac{h_h h_c}{h_h + h_c} \tag{8}$$

which clearly shows that to increase the U value both h_c and h_h need to be as large as possible. Another criteria seen from eq. (8) is that both convection heat transfer coefficients has to be larger than the overall heat transfer coefficient, i.e.

$$h_h, h_c > U$$

As the convective heat transfer coefficient on the exhaust side has to be higher than the U value but assumed to be lower than the cold side convection coefficient (higher densities on the cold side due to higher pressures enhances the heat transfer), it is regarded the main variable in deciding the overall size of the WHRU. Another important fact is the strong effect h_h has on the needed magnitude of the cold side coefficient h_c. If the smaller convective heat transfer coefficient (hot side) goes below about 1.15 times the overall heat transfer coefficient the needed relative magnitude of the convective heat transfer coefficient on the other side increases rapidly towards infinity when $h_h \to U$. If $h_h/U = 1.2$, h_c has to be 5 times larger than h_h, for $h_h/U = 1.4$, h_c/h_h equals 2.5. Thus, the goal is to enhance the assumed lowest heat transfer coefficient as much as possible.

Reduction of variables

To reduce the convective heat transfer coefficient on the hot side, h_h, several methods can be utilized. The most apparent are listed below with positive and negative properties.

1. Increasing exhaust pressure

- Positive: Increases the allowable pressure drop in the WHRU thus smaller tube diameter and longer tube lengths can be used.
- Negative: Reduction in gas turbine output.

2. Increasing the number of tubes

- Positive: Increases the total heat transfer surface. Decreases the pressure drop by decreasing the massflow through each tube.
- Negative: Proportionally increase in WHRU size. Decreases heat transfer due to lower Reynolds number.

3. Decrease the tube diameter

- Positive: Increases h while decreasing the overall WHRU size.
- Negative: Increases pressure drop.

4. Increase WHRU length

- Positive: Increases the total heat transfer surface.
- Negative: Proportionally increase in WHRU size and pressure drop. h will remain approximately constant throughout the tube length.

Point 4 - Increasing the WHRU length - does not affect the convective heat transfer coefficient in any noticeable degree (ref [10]) and calculations can be made per unit length with proportional increase in both heat transfer area and pressure drop. Since the gas turbine is very sensitive to back pressure increase, a limitation is set to a pressure drop of 0.2 MPa in the WHRU and the effective back pressure at the gas turbine exit will be 0.3 MPa assuming the ambient pressure to be 0.1 MPa. This restriction removes point 1 from the list above. By implementing the pressure limit, parameter 2 and 3 (tube diameter and number of tubes) can be grouped together since for each tube diameter there corresponds a certain amount of tubes to reduce the pressure loss down to sufficient

levels. Thus, two remaining independent variables (length and the group, number of channels/channel diameter) are left and results can be produced with respect to heat transfer area versus heat recovery.

Overall WHRU size

To estimate the overall dimensions of the WHRU a description of the cold side of the heat exchanger is needed as well, mainly to find the cold side channel diameter, D_c. Before the evaluation begins, it is necessary to mention the low precision in the following calculations due to the use of constant fluid properties, in reality these properties will change drastically when evaporating a liquid and further superheating it into the gas region. To get a "reasonable" estimate of the properties an Excel function is created, which is described in the appendix. A more precise method can be applied by looking into the *three-zone flow boiling*-model described by Thome et al. [11]

The cold side channel diameter, D_c

By implementing the results from the exhaust side of the WHRU and results from Table 3 the required $(hA)_c$ value on the cold side can be found. To produce the (hA) values for both sides the ratio $(hA)_h/\mathrm{UA}$ need to be selected. As a starting point this value is chosen to be 1.4 which is then used in equation (8) (solved here for $(hA)_c$)

$$(hA)_c = \frac{h_h/U}{h_h/U - 1}\mathrm{UA} = 3.5\mathrm{UA}$$

The UA-value in the equation above is the needed value to bring the exhaust gas temperature down to $150°\mathrm{C}$ which is the case for water. With both heat transfer conductances set, all parameters on the hot side is readily available (given the pressure restriction), except the channel (WHRU) length. Given the assumption that the convective heat transfer coefficient (h) being constant throughout the length of the heat exchanger it implies that the heat transfer area remains constant as well

$((hA)_c$ is set by $(hA)_h$ and T_{ex}). **Note:** An investigation considering the change in convective heat transfer coefficient reveals a decrease of approximately 6% when the channel length is increased from 2m to 3.5m.

With the heat transfer area set by the hot side the cold side convective heat transfer coefficient is determined by

$$h_c = \frac{(hA)_c}{A}$$

and the Nusselt number on the cold side is found (independent of WHRU length as well). With the Nusselt number and the heat transfer area set by the hot side, the cold side channel diameter is determined. For a $(hA)_h/\text{UA}$ value of 1.4 the cold side channel diameter is found to be 0.8mm.

WHRU Volume

The volume of the WHRU equals

$$V = HWL$$

where L is the length and H is the height in meter and calculated by

$$H = N_H \left[D_h + D_c + w_H \right]$$

where w_H is the wall thickness in the vertical direction.

The width, W, is calculated by

$$W = \sqrt{2\#} \left[D_h + w_W \right] = N_{W,\,h} \left[D_h + w_W \right]$$

or; number of channels in a horizontal row times the size of a channel diameter/wall thickness pair.

An overview of the terms constituting the volume equation reveals that the only independent variables for a given $(hA)_h/\text{UA}$ value is the hot side channel diameter, D_h, and channel length, L, remembering that the total number of channels on the hot side is dependent only on the same two variables. 3D plots can then be made for a given $(hA)_h/\text{UA}$ value. The plot for $(hA)_h/\text{UA} = 1.4$ is shown in Figure 6 where $w_H = w_W = 1mm$
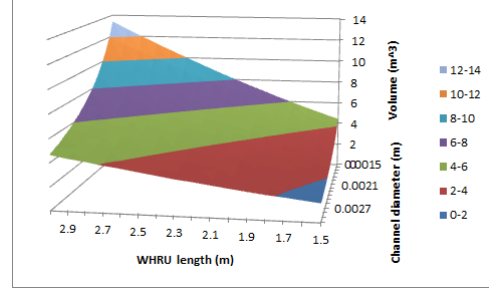

Figure 6: WHRU volume by variation in hot side channel diameter and channel length for $(hA)_h/\text{UA} = 1.4$

There is a clear linear dependency on the volume by the variation in length. Further inspection show that the total volume decreases with a decrease in length and increase in hot side channel diameter. An important fact is the restriction in the hot side channel diameter (at a specific length) given by the set heat transfer area, e.g. for a length of 2m the channel diameter cannot be larger than 1.8mm and for a length of 3m the channel diameter is restricted to 2.6mm. Thus, the variation in length and channel diameter is potentially prone to optimization at the set heat transfer area. With reference to eq. (7) the heat transfer area can be written as

$$A(L,\,D_H) = LD_H\sqrt{2\#_h}(\sqrt{2\#_h}-1) \approx LD_H 2\#_h \tag{9}$$

remembering $\#_h$ being a function of length and hot side channel diameter. Equation (9) needs iteration to be solved. The result is shown in Figure 7.
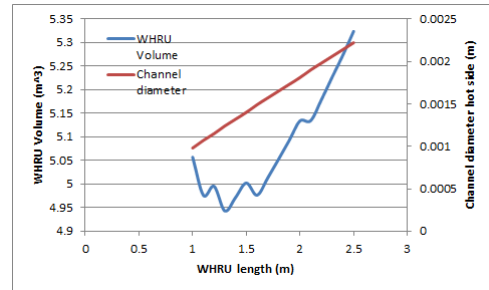

Figure 7: WHRU volume by variation in hot side channel diameter and channel length for $(hA)_h/\text{UA} = 1.4$

Evaluation of single versus modular expander setup

Reliable expander data needed to get conclusive results has not been procured due to corporate secrecy. Thus, a program has been made in Microsoft Excel which could be used when data are available.

Analytical model

The reference case is described by

$$W_R' = VFR_R * N_R$$

where W_R' is the "specific" reference work output, i.e. divided by density and enthalpy drop which is assumed to be the same for the reference case and all modular configurations regarding the states on both inlet and outlet to be constant. VFR_R and N_R are the reference volumetric flow rate and efficiency respectively. The same goes for Expander 1

$$W_{E1}' = VFR_{E1} * N_{E1}$$

and Expander 2

$$W_{E2}' = VFR_{E2} * N_{E2}$$

By summing these two we get the modular work output, W_M'

$$\begin{aligned} W_M' &= W_{E1}' + W_{E2}' = VFR_{E1}N_{E1} + VFR_{E2}N_{E2} \\ &= xVFR_R * k_1N_R + (1-x)VFR_R * k_2N_R \\ &= W_R'[xk_1 + (1-x)k_2] \end{aligned} \quad (10)$$

The second equation is balanced by the use of the sizing factor $k_n = P_{En}/P_R$ and $x = VFR_{E1}/VFR_R$ which leaves $(1-x) = VFR_{E2}/VFR_R$. The last expression on the right side of eq. (10) shows that if a modular set-up to be a viable option it has to reach the following criteria.

$$xk_1 + (1-x)k_2 > 1$$

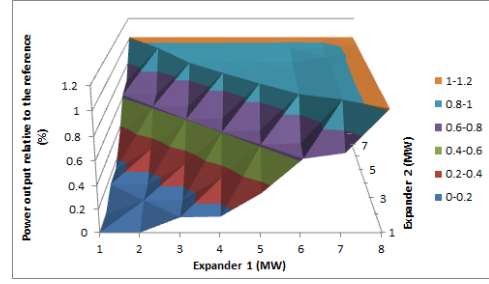The output of the program is a plot as shown in Figure 8

Figure 8: Calculated power from a modular setup (2 expanders) with respect to a reference case (8 MW expander)

This plot is created based on the efficiency chart of a 6 MW expander, where the data of the whole expander range (1 to 8 MW) is created by a constant sizing factor, k.

References

[1] T.C. Hung, T.Y. Shai, and S.K. Wang. A review of organic rankine cycles (orcs) for the recovery of low-grade waste heat. 1996.

[2] Huijuan Chen, D. Yogi Goswami, and Elias K. Stefanakos. A review of thermodynamic cycles and working fluids for the conversion of low-grade heat. *Renewable and sustainable energy reviews*, 14, 2010.

[3] T.C. Hung. Waste heat recovery of organic rankine cycle using dry fluids. *Energy conversion and management*, 42, 2001.

[4] Harald Taxt Walnum, Yves Ladam, Petter Nekså, and Trond Andresen. Off-design operation of orc and co2 power production cycles for lower temperature surplus heat recovery. *9th International conference on sustainable energy technologies; Shanghai, China*, 2010.

[5] T.J. Marciniak, J.L. Krazinski, J.C. Bratis, H.M. Bushby, and E.H. Buycot. Comparison of rankine-cycle power systems: effects of seven working fluids. 1981.

[6] G. Schmidt, P. Schmid, H. Zewen, and S. Moustafa. Development of a point focusing collector farm system. *Solar Energy*, 31, 1993.

[7] Bertrand F. Tchanche, Gr. Lambrinos, A. Frangoudakis, and G. Papadakis. Low-grade heat conversion into power using organic rankine cycles a review of various applications. *Renewable and Sustainable Energy Reviews*, 15, 2011.

[8] Tony Ho, Samuel S. Mao, and Ralph Greif. Comparison of the organic flash cycle (ofc) to other advanced vapor cycles for intermediate and high temperature waste heat reclamation and solar thermal energy. *Energy*, 40, 2012.

[9] Frank Gabrielli and Horst Schwevers. Design factors and water chemistry practices - supercritical power cycles. *Chemical Engineering*, 2008.

[10] F.P. Incropera, D.P. DeWitt, T.L. Bergman, and A.S. Lavine. *Fundamentals of Heat and Mass Transfer*. John Wiley & Sons, Inc., 111 River Street, Hoboken, NJ, 6th edition, 2007.

[11] J.R. Thome, V. Dupont, and A.M. Jacobi. Heat transfer model for evaporation in microchannels. part 1: presentation of the model. *International Journal of Heat and Mass Transfer*, 47, 2004.